

**Neural correlates of conscious  
and unconscious somatosensory  
processing**

Martin Grund



# **Neural correlates of conscious and unconscious somatosensory processing**

Von der Fakultät für Lebenswissenschaften  
der Universität Leipzig  
genehmigte

**DISSERTATION**

zur Erlangung des akademischen Grades

doctor rerum naturalium

Dr. rer. nat.

vorgelegt von

Diplom-Psychologe Martin Grund

geboren am 25.09.1989 in Hoyerswerda

Dekan:	Prof. Dr. Marc Schönwiesner
Gutachter*innen:	Prof. Dr. Erich Schröger Prof. Dr. Simone Schütz-Bosbach
Tag der Verteidigung:	18. August 2022



*In memory of Holger Schild who supported and celebrated the start of this research endeavor, but sadly, passed away before it was completed.*



## Bibliographic Details

Martin Grund

### **Neural correlates of conscious and unconscious somatosensory processing**

Fakultät für Lebenswissenschaften

Universität Leipzig

*Dissertation*

136 pages, 103 references, 2 figures

Every day there are somatosensory stimuli on our skin that we perceive one moment and the next not, despite their unchanged physical presence (e.g., insects, wind, clothing). Yet, which are the physiological determinants and neural correlates that accompany external stimuli to enter consciousness or not? To address this question and inform theories of consciousness, this dissertation presents three empirical studies that used weak electrical finger-nerve stimulation which led - despite being physically identical - to subjective experiences of stimulus presence and absence. The first two studies investigated the interaction of tactile conscious perception with two dominant body rhythms: the cardiac and respiratory cycle. The third study investigated the configuration of neural networks being involved in this near-threshold phenomenon. Tactile conscious perception changed over the course of the cardiac cycle (increased detection during diastole) and respiration was tuned such that stimuli occurred more likely during late inspiration / early expiration, resulting in increased detection during early expiration. On the neural level, conscious perception was accompanied by global broadcasting of sensory content across the brain without substantial reconfiguration of the whole-brain functional network in terms of graph metrics. The cardiac cycle effect on conscious tactile perception is a result of cognitive processes which model and predict our body's internal state to inform

## Bibliographic Details

perception and guide behavior (e.g., tuning respiration). This perceptual integration of interoceptive and exteroceptive "beliefs" is also an explanation for widely distributed brain activity differences without whole-brain functional network changes when a tactile stimulus is perceived.



# Contents

<b>Contents</b>	<b>9</b>
<b>Acknowledgements</b>	<b>11</b>
<b>Summary</b>	<b>13</b>
<b>Deutsche Zusammenfassung</b>	<b>19</b>
<b>1 General Introduction</b>	<b>27</b>
1.1 Previous research on pre-to-post-stimulus determinants for conscious tactile perception	28
1.2 Bodily signals - An integral part of conscious tactile perception	34
1.3 Theories based on neural correlates of consciousness	36
1.4 Research questions and approach	40
1.5 Hypotheses	41
<b>2 Study 1: Interactions between cardiac activity and conscious somatosensory perception</b>	<b>43</b>
<b>3 Study 2: Respiration, heartbeat, and conscious tactile perception</b>	<b>67</b>
<b>4 Study 3: Neural correlates of conscious tactile perception: An analysis of BOLD activation patterns and graph metrics</b>	<b>83</b>
<b>5 General Discussion</b>	<b>99</b>
5.1 Does conscious tactile perception vary across the cardiac cycle?	99
5.2 Does conscious tactile perception vary across the respiration cycle?	101
5.3 Do brain network topologies in terms of graph metrics change with conscious tactile perception?	101
5.4 Interaction of bodily signals with conscious tactile perception and its neural correlates	102
5.5 Outlook and future research	105
<b>Curriculum Vitae</b>	<b>109</b>

## Contents

<b>Research Publications</b>	<b>111</b>
<b>Selbstständigkeitserklärung</b>	<b>113</b>
<b>Nachweise über Anteile der Co-Autor*innen</b>	<b>115</b>
<b>References</b>	<b>123</b>

## Acknowledgements

First, I want to thank my supervisor Arno Villringer who gave me the opportunity to do my doctoral research and the freedom to develop personally as a researcher within the Department of Neurology at the Max Planck Institute for Human Cognitive and Brain Sciences (MPI CBS) in Leipzig.

A great companion to find my way in the beginning of my doctoral studies was Norman Forschack. Thank you for the very long discussions about neural correlates of perception, experimental designs, and statistical analyses. Research is a team effort and so I want to thank particularly the members of the Somatosensory Group: Till Nierhaus, Esra Al, Tilman Stephani, Alice Dabbagh, Michael Gaebler, Carina Forster, Eleni Panagoulas, Marc Pabst, Anahit Babayan, Jonas Witt, Birol Taskin, and Paweł Motyka; and my office colleagues: Elena Cesnaite, Maike Hoff, Isabel García García, Nora Mehl, Deniz Kumral, Eóin Molloy, Benjamin Kalloch, and Şeyma Bayrak. Many more colleagues at the MPI CBS could be named here. Thanks for endless discussions along the corridors of the MPI or in our lovely canteen. The Max Planck Society provided an excellent environment to pursue my research. This also includes many persons behind the scenes that keep a research institute running, e.g., our former head of administration Ingrid Schmude and our former in-house technician Berndt Junghanns, and of course our office managers in the department: Cornelia Ketscher and Birgit Mittag. My extensive empirical research would also have been impossible without many helping hands during data acquisition (Sylvia Stash, Ramona Menger, Anke Kummer, Mandy Jochemko, and Nicole Pampus), technical advice (Bettina Johst, Hendrik Grunert, and Jöran Lepsien), or graphic and proof-reading support (Heike Schmidt-Duderstedt, Kerstin Flake; Joshua Grant). Also, thanks to many science-policy friends, particularly in the Max Planck PhDnet, N<sup>2</sup>, and SPDWissPol, who helped to keep the big picture and the vision that a more diverse academia is possible.

## Acknowledgements

Finally, thanks to my family and friends who never had any doubts that I will not be up for this challenge despite life being not always as linear as one would wish.

## Summary

In our environment, there are weak somatosensory stimuli which are sometimes perceived and sometimes not. This can be for instance our clothing whose presence on our skin will fluctuate between felt and not felt, while its physical presence does not change. Why is this feeling sometimes present and sometimes not, even though our attention is solely focused on our skin and there seems to be no change in the environment? This is not only a central question for psychology but also has clinical relevance at the bedside when physicians must decide whether a patient is conscious or not. In the laboratory, so called near-threshold detection paradigms, which use stimulus intensities at perceptual threshold, can keep the environment constant and allow to study what is physiologically different when humans consciously perceive external stimuli. Subsequently, these empirical observations are used to test theoretical assumptions about the neural correlates of human consciousness, and how internal bodily states and external signals are integrated into a unified percept.

For the studies of determinants for tactile conscious perception in this dissertation, electrical finger-nerve stimulation was used. Steel ring-electrodes were attached to the left index finger and very short rectangular electrical pulses of 0.2 milliseconds were applied at an intensity that was perceived in half of the cases and in the other half not (resulting in a detection rate of 50 percent). Participants had to report each trial whether they perceived the stimulus (*Study 1-3*), and additionally in *Study 2* and *3* whether they were confident or unconfident about their yes/no-decision. While participants performed the task, physiological signals were acquired: electrocardiography (*Study 1* and *2*), finger photoplethysmography (*Study 2*), respiration belt activity (*Study 2*), and functional magnetic resonance imaging (*Study 3*). The purpose of these studies was to address the following main research questions:

## Summary

- Does conscious tactile perception vary across the cardiac cycle? (*Study 1*)
- Does conscious tactile perception vary across the respiration cycle? (*Study 2*)
- Do brain network topologies in terms of graph metrics change with conscious tactile perception? (*Study 3*)

These studies were published in peer-reviewed journals:

1. Motyka, P., **Grund, M.**, Forschack, N., Al, E., Villringer, A., & Gaebler, M. (2019). Interactions between cardiac activity and conscious somatosensory perception. *Psychophysiology*, 56(10), 469–13. <https://doi.org/10.1111/psyp.13424>
2. **Grund, M.**, Al, E., Pabst, M., Dabbagh, A., Stephani, T., Nierhaus, T., Gaebler, M., & Villringer, A. (2022). Respiration, heartbeat, and conscious tactile perception. *Journal of Neuroscience*, 42(4), 643-656. <https://doi.org/10.1523/JNEUROSCI.0592-21.2021>
3. **Grund, M.**, Forschack, N., Nierhaus, T., & Villringer, A. (2021). Neural correlates of conscious tactile perception: An analysis of BOLD activation patterns and graph metrics. *NeuroImage*, 224, 117384. <https://doi.org/10.1016/j.neuroimage.2020.117384>

### **Study 1: Interactions between cardiac activity and conscious somatosensory perception**

Bodily signals generated by cardiac activity were shown to affect cognition and behavior (Critchley & Harrison, 2013). But are they also decisive whether tactile stimuli enter consciousness or not? And does cardiac activity reflect stimulus detection? To examine whether conscious tactile perception varies across the cardiac cycle, near-threshold stimulus onsets were located within the cardiac cycle in degrees (time to preceding R-peak

divided by time of preceding R-peak to subsequent R-peak). Across participants detected near-threshold stimulus onsets showed a unimodal distribution in the last quadrant of the cardiac cycle (diastole), indicating an increased likelihood to perceive an electrical pulse towards the end of the cardiac cycle. Furthermore, the duration of interbeat intervals increased after somatosensory stimulation. This heart slowing was greater for detected compared to undetected near-threshold stimuli. Thus, cardiac activity determined and interacted with conscious tactile perception.

### **Study 2: Respiration, heartbeat, and conscious tactile perception**

Next to the main research question whether another predominant body rhythm (respiration) determines conscious tactile perception, the results of *Study 1* left two follow-up questions that were addressed in *Study 2*: (a) Was increased detection in diastole accompanied by increased decision uncertainty? (b) Did peripheral changes in the finger associated with the pulse wave result in the cardiac cycle effect on conscious tactile perception? That is why in *Study 2*, participants had to report next to their stimulus detection (yes/no) their decision confidence (confident/unconfident) and finger photoplethysmography was acquired. For investigating decision confidence across the cardiac cycle, trials were assigned to four intervals based on the time from the preceding R-peak to stimulus onset (0-200 ms, 200-400 ms, 400-600 ms, 600-800 ms). The dependent probabilities of near-threshold trial outcomes in these intervals revealed that only confident hits were more likely at the end of diastole (600-800 ms). Furthermore, finger photoplethysmography showed that tactile detection was lowest at pulse wave arrival (250-300 ms after the R-peak) indicating that the cardiac cycle effect on conscious tactile perception preceded maximal peripheral cardiac-related movements in the finger pad. Taken together with the recently reported unchanged early cortical somatosensory-evoked potentials (Al et al., 2020), we interpret this as further evidence that the cardiac cycle effect on

## Summary

conscious tactile perception is a result of cognitive processes integrating exteroceptive and interoceptive signals.

Circular statistics of (expected) stimulus onsets within the respiration cycle revealed a unimodal distribution for each participant during late inspiration or early expiration similarly for correct rejections of trials without stimulation, as well as for undetected and detected near-threshold trials. This adaption of the respiration cycle to the paradigm mirrored the distribution of heart frequency across the respiration cycle (sinus arrhythmia), such that stimuli occurred preferentially during phases of highest heart frequency and presumably alertness and neural excitability. Also, near-threshold detection was higher after expiration onset in the first quadrant of the respiration cycle. Additionally, stronger respiratory phase-locking was associated with higher near-threshold detection across participants. This indicates that tuning the respiration rhythm indeed optimizes tactile detection task performance.

### **Study 3: Neural correlates of conscious tactile perception: An analysis of BOLD activation patterns and graph metrics**

What is different in the brain when a stimulus enters consciousness compared to the same stimuli not entering consciousness? Which brain areas are involved and how do they interact? The spatial extent of brain activation and the interaction of brain areas are central criteria for local or global theoretical accounts of perceptual consciousness. With functional magnetic resonance imaging (fMRI) we investigated the brain activity changes that accompany near-threshold somatosensory stimulation and its conscious perception, and particularly addressed the question whether the whole-brain functional network topology changes in terms of graph metrics. For confidently detected (hits) compared to confidently undetected near-threshold trials (misses), we observed greater activation in domain-general brain areas: intraparietal sulcus, precuneus, posterior cingulate cortex, and



anterior insula. For confident misses compared to confident correct rejections of trials without stimulation, bilateral secondary somatosensory cortex (S2) showed a greater activation. When we compared the post-stimulus whole-brain functional network topologies based on graph metrics (modularity, participation, clustering, and path length) between confident correct rejections, misses, and hits, there were no significant differences, which was also supported by Bayes factor statistics.

Taken together contrary to a study with visual stimulation (Godwin et al., 2015), graph metrics of the whole-brain functional network did not change for the used somatosensory stimuli. Yet, activity of domain-general brain areas (precuneus, insula) next to somatosensory cortex correlated strongly with conscious tactile perception. Perceivable yet undetected somatosensory stimuli lead to an activation of S2, in contrast to previously reported deactivations in the primary somatosensory cortex (S1) and S2 for imperceptible stimuli (Blankenburg et al., 2003). These observations support global accounts of perceptual consciousness which require the involvement of domain-general brain areas for conscious perception.

### **Summary Studies 1-3**

The empirical evidence suggests that the cardiac cycle effect on conscious tactile perception is a result of cognitive processes as updating of exteroceptive and interoceptive models to generate predictions. These same processes might also explain the modulation of the respiration rhythm to optimize detection task performance. Furthermore, the perceptual "negotiation" of internal and external signals might be the reason for fMRI showing global broadcasting of sensory content across the brain without substantial reconfiguration of the whole-brain functional network resulting in an integrative conscious experience. The subjective tactile sensation does not just require a "ping" in the somatosensory cortex but involves many processes

## Summary

across the brain to result in the decision: "Yes, I confidently perceived an external tactile stimulus."

## References

- Al, E., Iliopoulos, F., Forschack, N., Nierhaus, T., Grund, M., Motyka, P., Gaebler, M., Nikulin, V. V., & Villringer, A. (2020). Heart-brain interactions shape somatosensory perception and evoked potentials. *Proceedings of the National Academy of Sciences of the United States of America*, 7, 201915629. <https://doi.org/10.1073/pnas.1915629117>
- Blankenburg, F., Taskin, B., Ruben, J., Moosmann, M., Ritter, P., Curio, G., & Villringer, A. (2003). Imperceptible stimuli and sensory processing impediment. *Science*, 299(5614), 1864–1864. <https://doi.org/10.1126/science.1080806>
- Critchley, H. D., & Harrison, N. A. (2013). Visceral influences on brain and behavior. *Neuron*, 77(4), 624–638. <https://doi.org/10.1016/j.neuron.2013.02.008>
- Godwin, D., Barry, R. L., & Marois, R. (2015). Breakdown of the brain's functional network modularity with awareness. *Proceedings of the National Academy of Sciences of the United States of America*, 112(12), 3799–3804. <https://doi.org/10.1073/pnas.1414466112>

## Deutsche Zusammenfassung

In unserer Umgebung gibt es schwache somatosensorische Reize, die manchmal wahrgenommen werden und manchmal nicht. Das kann zum Beispiel unsere Kleidung sein, deren Präsenz auf unserer Haut zwischen gefühlt und nicht gefühlt fluktuiert, während sich ihre physische Präsenz nicht verändert. Warum ist dieses Gefühl manchmal präsent und manchmal nicht, obwohl unsere Aufmerksamkeit allein auf unsere Haut fokussiert ist und es scheint, als gäbe es keine Veränderungen in der Umgebung? Das ist nicht nur eine zentrale Frage für die Psychologie, sondern hat auch klinische Relevanz, wenn Ärzt\*innen entscheiden müssen, ob ein\*e Patient\*in bewusst oder nicht ist. Im Labor erlauben sogenannte schwelennahe Detektionsparadigmen, die Reizintensitäten an der Wahrnehmungsschwelle nutzen, die Umgebung konstant zu halten und zu untersuchen, was physiologisch different ist, wenn Menschen externe Reize bewusst wahrnehmen. Anschließend werden diese empirischen Beobachtungen genutzt, um theoretische Annahmen über neuronale Korrelate des menschlichen Bewusstseins zu testen, und wie interne Körperzustände und externe Signale zu einer einheitlichen Empfindung integriert werden.

Für die Studien von Determinanten bewusster taktiler Wahrnehmung in dieser Dissertation wurde elektrische Fingernervenstimulation eingesetzt. Ringlektroden aus Stahl wurden am linken Zeigefinger angebracht und sehr kurze rechteckige elektrische Pulse von 0,2 Millisekunden wurden mit einer Intensität appliziert, die in der Hälfte der Fälle gespürt wurde und in der anderen Hälfte nicht (Detektionsrate von 50 Prozent). Versuchspersonen mussten in jedem Durchgang berichten, ob sie den Reiz wahrgenommen haben (*Studie 1-3*), und zusätzlich in *Studie 2* und *3*, ob sie sich ihrer Ja/Nein-Entscheidung sicher oder unsicher waren. Während Versuchspersonen die Aufgabe durchführten, wurden physiologische Signale

## Deutsche Zusammenfassung

gemessen: Elektrokardiographie (*Studie 1* und *2*), Finger Photoplethysmographie (*Studie 2*), Atembrustgurt (*Studie 2*), und funktionale Magnetresonanztomographie (*Studie 3*). Der Zweck dieser Studien war es, die folgenden Hauptforschungsfragen zu adressieren:

- Variiert bewusste taktile Wahrnehmung über den Herzzyklus? (*Studie 1*)
- Variiert bewusste taktile Wahrnehmung über den Atemzyklus? (*Studie 2*)
- Verändern sich Netzwerktopologien im Gehirn anhand von Graphmetriken mit bewusster taktiler Wahrnehmung? (*Studie 3*)

Diese Studien wurden in begutachteten Fachzeitschriften veröffentlicht:

1. Motyka, P., **Grund, M.**, Forschack, N., Al, E., Villringer, A., & Gaebler, M. (2019). Interactions between cardiac activity and conscious somatosensory perception. *Psychophysiology*, 56(10), 469–13. <https://doi.org/10.1111/psyp.13424>
2. **Grund, M.**, Al, E., Pabst, M., Dabbagh, A., Stephani, T., Nierhaus, T., Gaebler, M., & Villringer, A. (2022). Respiration, heartbeat, and conscious tactile perception. *Journal of Neuroscience*, 42(4), 643-656. <https://doi.org/10.1523/JNEUROSCI.0592-21.2021>
3. **Grund, M.**, Forschack, N., Nierhaus, T., & Villringer, A. (2021). Neural correlates of conscious tactile perception: An analysis of BOLD activation patterns and graph metrics. *NeuroImage*, 224, 117384. <https://doi.org/10.1016/j.neuroimage.2020.117384>

### **Studie 1: Interaktionen zwischen Herzaktivität und bewusster somatosensorischer Wahrnehmung**

Für durch Herzaktivität generierte körperliche Signale wurde gezeigt, dass sie Kognition und Verhalten beeinflussen (Critchley & Harrison, 2013).

Aber sind sie auch entscheidend, ob ein taktiler Reiz ins Bewusstsein eindringt oder nicht? Und spiegelt sich die Reizdetektion in der Herzaktivität wider? Um zu untersuchen, ob bewusste taktile Wahrnehmung über den Herzzyklus variiert, wurde der Zeitpunkt der schwelennahen Reize im Herzzyklus in Grad bestimmt (Zeit zur vorhegenden R-Zacke geteilt durch die Zeit von der vorhergehenden R-Zacke bis zur darauffolgenden R-Zacke). Über Versuchspersonen zeigte sich für detektierte schwelennahe Reize eine unimodale Verteilung im letzten Quadranten des Herzzyklus (Diastole). Demnach ist die Wahrscheinlichkeit, einen elektrischen Puls wahrzunehmen, zum Ende des Herzzyklus erhöht. Darüber hinaus erhöhte sich die Intervalldauer zwischen Herzschlägen nach somatosensorischer Stimulation. Diese Herzverlangsamung war größer für detektierte Reize im Vergleich zu nicht-detektierten schwelennahen Reizen. Das heißt, Herzaktivität determinierte und interagierte mit bewusster taktiler Wahrnehmung.

### **Studie 2: Atmung, Herzschlag, und bewusste taktile Wahrnehmung**

Neben der Hauptforschungsfrage, ob ein anderer vorherrschender Körperhythmus (Atmung) bewusste taktile Wahrnehmung beeinflusst, hinterließen die Ergebnisse der *Studie 1* zwei Anschlussfragen, die in *Studie 2* adressiert wurden: (a) Ging die höhere Detektion in der Diastole einher mit einer erhöhten Entscheidungsunsicherheit? (b) Führten periphere Unterschiede im Finger einhergehend mit der Pulswelle zum Herzzykluseffekt auf bewusste taktile Wahrnehmung? Daher mussten in *Studie 2* Versuchspersonen neben der Reizdetektion (ja/nein) auch ihre Entscheidungssicherheit berichten (sicher/unsicher), und Finger Photoplethysmographie wurde erhoben. Um Entscheidungssicherheit über den Herzzyklus zu untersuchen, wurden die Durchgänge basierend auf der Zeit von der vorhergehenden R-Zacke bis zum Stimulationszeitpunkt vier Intervallen zugeordnet (0-200 ms, 200-400 ms, 400-600 ms, 600-800 ms). Die abhängigen

## Deutsche Zusammenfassung

Wahrscheinlichkeiten für Reaktionen auf schwelennahe Reize in diesen Intervallen ergaben, dass nur sichere Detektionen wahrscheinlicher zum Ende der Diastole waren (600-800 ms). Außerdem zeigte die Finger Photoplethysmographie, dass taktile Detektion am niedrigsten zur Pulswellenankunft war (250-300 ms nach der R-Zacke). Das zeigt, dass der Herzzykluseffekt auf bewusste taktile Wahrnehmung der maximalen peripheren Herz-bezogenen Bewegung in der Fingerbeere vorausging. Zusammen mit den kürzlich berichteten unveränderten frühen kortikalen somatosensorisch evozierten Potentialen (Al et al., 2020) interpretieren wir das als weitere Evidenz, dass der Herzzykluseffekt auf bewusste taktile Wahrnehmung ein Resultat von kognitiven Prozessen ist, die interozeptive und exterozeptive Signale integrieren.

Zirkuläre Statistiken von (erwarteten) Stimulationszeitpunkten innerhalb des Atemzyklus ergaben eine unimodale Verteilung für jede Versuchsperson während der späten Einatmung und frühen Ausatmung für korrekt zurückgewiesene Durchgänge ohne Stimulation, sowie nicht detektierte und detektierte Schwellenreize. Diese Anpassung des Atemzyklus an das Paradigma spiegelte die Verteilung der Herzfrequenz über den Atemzyklus (Sinusarrhythmie) wider, sodass Reize bevorzugt auftraten in Phasen mit der höchsten Herzfrequenz und vermutlich Wachsamkeit und neuronalen Erregbarkeit. Auch war die schwelennahe Detektion höher nach dem Beginn der Ausatmung im ersten Quadranten des Atemzyklus. Zusätzlich zeigte eine stärkere Atemphasenanpassung eine Korrelation mit höherer schwelennaher Detektion über Versuchspersonen. Das zeigt, dass das Abstimmen des Atemrhythmus tatsächlich die Leistung in einer taktilen Detektionsaufgabe optimiert.

### **Studie 3: Neuronale Korrelate bewusster Wahrnehmung: Eine Analyse von BOLD-Aktivierungsmustern und Graphmetriken**

Was ist im Gehirn anders, wenn ein Reiz ins Bewusstsein eintritt im Vergleich zu, wenn der gleiche Reiz nicht ins Bewusstsein eintritt? Welche Gehirnareale sind involviert und wie interagieren sie? Die räumliche Ausdehnung von Gehirnaktivierung und die Interaktion von der Gehirnarealen sind zentrale Kriterien für lokale oder globale theoretische Ansätze zum perzeptuellen Bewusstsein. Mit funktionaler Magnetresonanztomographie (fMRT) haben wir die Gehirnaktivitätsunterschiede untersucht, die mit schwellennaher somatosensorischer Stimulation und ihrer bewussten Wahrnehmung einhergehen. Insbesondere wurde die Frage adressiert, ob sich funktionale Netzwerktopologien des ganzen Gehirns hinsichtlich Graphmetriken ändern. Für sicher detektierte im Vergleich zu sicher nicht-detektierten schwellennahen Reizen wurde eine stärkere Aktivierung in Domain-generellen Gehirnarealen beobachtet: intraparietaler Sulcus, Precuneus, posteriorer cingulärer Kortex, und anteriore Insula. Für sicher nicht-detektierte im Vergleich zu sicher korrekt zurückgewiesenen Durchgängen ohne Stimulation zeigte der sekundäre somatosensorische Kortex (S2) bilateral eine starke Aktivierung. Wenn nach der Stimulation die funktionalen Netzwerktopologien für das ganze Gehirn anhand von Graphmetriken (Modularität, Partizipation, Clusterbildung, und Pfadlänge) zwischen sicher korrekt zurückgewiesenen Durchgängen ohne Stimulation, sowie nicht-detektierten und detektierten schwellennahen Reizen verglichen wurden, dann ergaben sich keine signifikanten Unterschiede, was auch von Bayes-Faktoren unterstützt wurde.

Zusammengefasst lässt sich im Gegensatz zu einer Studie mit visueller Stimulation sagen (Godwin et al., 2015), dass sich Graphmetriken des funktionalen Gehirnnetzwerks für die verwendeten somatosensorischen Reize nicht veränderten. Jedoch zeigten Domain-generelle Gehirnareale (Precuneus, Insula) neben dem somatosensorischen Kortex eine starke

## Deutsche Zusammenfassung

Korrelation mit bewusster taktiler Wahrnehmung. Wahrnehmbare, aber nicht-detektierte somatosensorische Reize führten zu einer Aktivierung von S2, im Gegensatz zu früher berichteten Deaktivierungen im primären somatosensorischen Kortex (S1) und S2 für nicht-wahrnehmbare Reize (Blankenburg et al., 2003). Diese Beobachtungen unterstützen globale Theorien über perzeptuelles Bewusstsein, die die Beteiligung von Domain-generellen Gehirnaralen für bewusste Wahrnehmung voraussetzen.

### **Zusammenfassung Studien 1-3**

Die empirische Evidenz spricht dafür, dass der Herzzykluseffekt auf bewusste taktile Wahrnehmung ein Ergebnis von kognitiven Prozessen ist, wie das Aktualisieren von exterozeptiven und interozeptiven Modellen, um Vorhersagen zu generieren. Diese gleichen Prozesse könnten auch die Modulation des Atemrhythmus für die Leistungsoptimierung in der Detektionsaufgabe erklären. Darüber hinaus kann die perzeptuelle Aushandlung von internen und externen Signalen der Grund dafür sein, dass sich mit fMRT eine globale Übertragung von sensorischen Inhalten über das Gehirn zeigt, die ohne eine substanzielle Rekonfiguration des funktionalen Gehirnetzwerks in einem integrativen bewussten Erlebnis resultiert. Die subjektive taktile Sinnesempfindung benötigt nicht nur ein "Anpingen" im somatosensorischen Kortex, sondern involviert viele Prozesse über das Gehirn, die in der Entscheidung resultieren: "Ja, ich habe mit Sicherheit einen externen taktilen Reiz wahrgenommen."

### **Literatur**

Al, E., Iliopoulos, F., Forschack, N., Nierhaus, T., Grund, M., Motyka, P., Gaebler, M., Nikulin, V. V., & Villringer, A. (2020). Heart-brain interactions shape somatosensory perception and evoked potentials. *Proceedings of the National Academy of Sciences of the United States of America*, 7, 201915629. <https://doi.org/10.1073/pnas.1915629117>



- Blankenburg, F., Taskin, B., Ruben, J., Moosmann, M., Ritter, P., Curio, G., & Villringer, A. (2003). Imperceptible stimuli and sensory processing impediment. *Science*, *299*(5614), 1864–1864. <https://doi.org/10.1126/science.1080806>
- Critchley, H. D., & Harrison, N. A. (2013). Visceral influences on brain and behavior. *Neuron*, *77*(4), 624–638. <https://doi.org/10.1016/j.neuron.2013.02.008>
- Godwin, D., Barry, R. L., & Marois, R. (2015). Breakdown of the brain's functional network modularity with awareness. *Proceedings of the National Academy of Sciences of the United States of America*, *112*(12), 3799–3804. <https://doi.org/10.1073/pnas.1414466112>

## General Introduction

## Chapter 1

### 1 General Introduction

Try to imagine a situation where you feel something faintly on your skin. A feeling which might be already gone in the next moment. This could be the top you are wearing or an insect that stepped on you. It might be even a slight itching that comes and goes despite there is nothing touching your skin. Why we sometimes experience an external stimulus on our skin and the other moment not, despite its physical properties did not change, is the central question of my dissertation. In three empirical studies, very weak electrical pulses (as an experimental model for these everyday sensations) were applied at the left index finger of healthy human volunteers to investigate the body and brain determinants for conscious somatosensory experiences.

Why is this important to be addressed? Despite all our technical advances, we do not know yet the neural underpinnings that give rise to subjective sensations. Particularly the complex interplay of body and brain processes is unknown and was under-investigated so far while searching for the neural correlates of consciousness (Critchley & Harrison, 2013; Park & Blanke, 2019b; Seth & Friston, 2016). However, knowing the mechanisms for sensory awareness is of high relevance for clinicians who must decide at the bedside whether a patient is conscious or not (Arzi et al., 2020; Faugeras et al., 2011; Owen et al., 2006; Raimondo et al., 2017). This knowledge enables the development of appropriate tests which assess whether the mechanisms of consciousness are still intact (Kondziella et al., 2020).

One approach to study the underpinnings of consciousness is the "contrastive analysis" which given the same level of vigilance/consciousness (alert participants) subtracts from the stimulus presence report the absence report (content of consciousness) to highlight what is different in

## General Introduction

the organism when the presence of a stimulus is reported (Aru et al., 2012). In the laboratory, this is combined with multiple measures of physiological activity, e.g., heart and brain activity during visual conscious perception (Park et al., 2014). In the analysis, this allows to map out the determinants on a continuous time scale from before to after stimulus onset (pre-to-post-stimulus continuum). For instance, heart evoked brain potentials indicated before the stimulation, whether a stimulus will be perceived or not, and whether post-stimulus the neural processing will be attenuated or not (Al et al., 2020; Park et al., 2014). Approaching conscious perception experimentally with the contrastive analysis requires to keep everything - which can be controlled - stable, while only the conscious percept fluctuates between stimulus presence and absence. An in this sense very promising category of experiments is called near-threshold paradigms. For these experiments, the stimulus intensity is assessed individually for each participant in such a way that half of the stimuli are perceived and the other half not (50% detection rate) while all presented stimuli are physically identical. Running near-threshold paradigms in the somatosensory domain has the advantage of very fine-grained technical stimulation abilities (e.g., electrical finger-nerve stimulation with direct current stimulators) in comparison to the visual domain which mostly relies on standard office monitors at 60 Hz with a minimum presentation duration of 17 milliseconds (Sperdin et al., 2013). Furthermore, electrical finger-nerve stimulation does not require masking in comparison to visual stimulation, which often makes it necessary due to afterimages or visible persistence (Lollo et al., 1988).

### **1.1 Previous research on pre-to-post-stimulus determinants for conscious tactile perception**

The determinants of tactile conscious perception which have been addressed by previous research can be grouped by their physiological source (brain or body) and by their timing relative to the stimulation (before or

after; Figure 1). Additionally, pre-stimulus determinants for conscious tactile perception can also affect post-stimulus determinants, e.g., neural oscillations preceding a stimulus will affect its evoked neural responses thereafter (Forschack et al., 2017; Weisz et al., 2014).

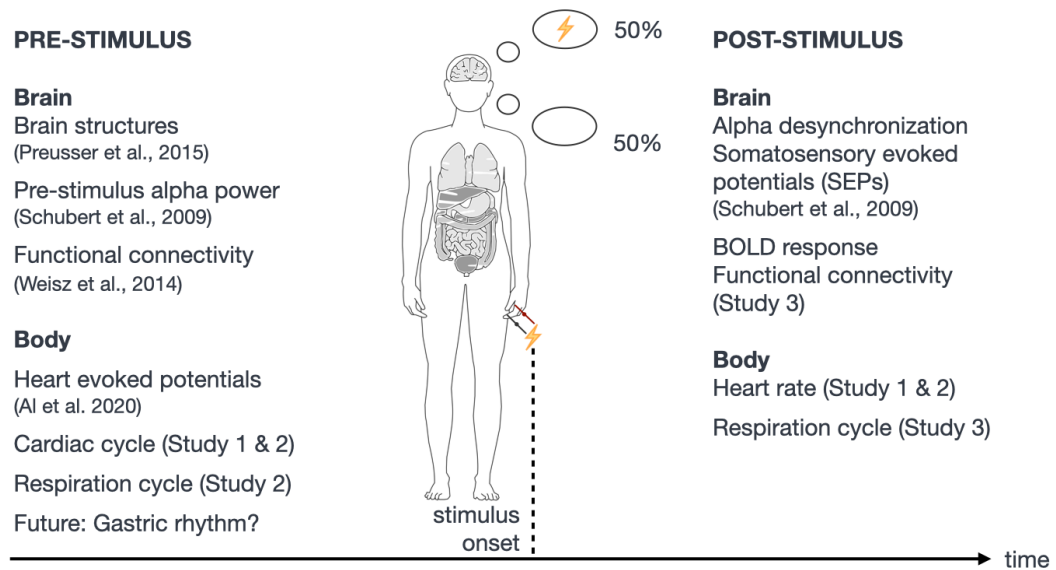


**Figure 1.** Pre-to-post-stimulus continuum of determinants for conscious tactile perception. On the left site, relevant pre-stimulus brain and body conditions for detecting a stimulus are listed. In the center, a body is shown with internal organs (brain, lungs, heart, gut, etc.) and electrical nerve stimulation attached to the left index finger which is perceived or not (50:50). On the right site, the consequences in the brain or body are listed which have been associated with conscious tactile perception.

In the brain, somatosensory processing of electrical pulses is driven via input at nerve endings in the finger, first arriving in the dorsal root ganglion adjacent to the spinal cord, transmitted (because no specific receptors are stimulated) via the dorsal column medial lemniscal system (touch) or the anterolateral system (pain, temperature) in the spinal cord, the medulla, the pons to the thalamus and the primary somatosensory cortex (Figure 2) which is organized somatotopically (reflecting the body surface) (Gardner

## General Introduction

et al., 2012; Gardner & Johnson, 2012). However, there are also necessary brain structures for conscious tactile perception beyond the primary somatosensory cortex (S1) as impaired touch perception has been demonstrated in stroke patients - despite intact S1 - for lesions in the secondary somatosensory cortex (along with the anterior and posterior insula, the putamen, and subcortical white matter connections to prefrontal structures) (Preusser et al., 2015).

A great extent of the previous literature on determinants of conscious tactile perception investigated pre-stimulus neural oscillations with electroencephalography (EEG) and magnetoencephalography (MEG) as a proxy for neural excitability and attention (Baumgarten et al., 2016; Craddock et al., 2017; Forschack et al., 2017; Jones et al., 2010; Linkenkaer-Hansen et al., 2004; Nierhaus et al., 2015; Palva et al., 2005; Schubert et al., 2009; Stephani et al., 2021; Weisz et al., 2014). Decreased pre-stimulus power of frequencies between 8 and 14 Hz (alpha power) in the somatosensory cortex (also called mu rhythm) have been associated with facilitating conscious tactile perception (Craddock et al., 2017; Forschack et al., 2020; Schubert et al., 2009). Additionally, differences in pre-stimulus alpha power predicted divergence in post-stimulus somatosensory evoked potentials (SEPs), for amplitudes of early components as N20 and P50 (Forschack et al., 2017; Stephani et al., 2021) and of late components as N140 and P260 (Reinacher et al., 2009). Late components have been also shown to be the first components (N140) to distinguish between perceived and not perceived stimuli (Auksztulewicz et al., 2012; Forschack et al., 2020; Nierhaus et al., 2015; Schröder et al., 2021; Schubert et al., 2006).

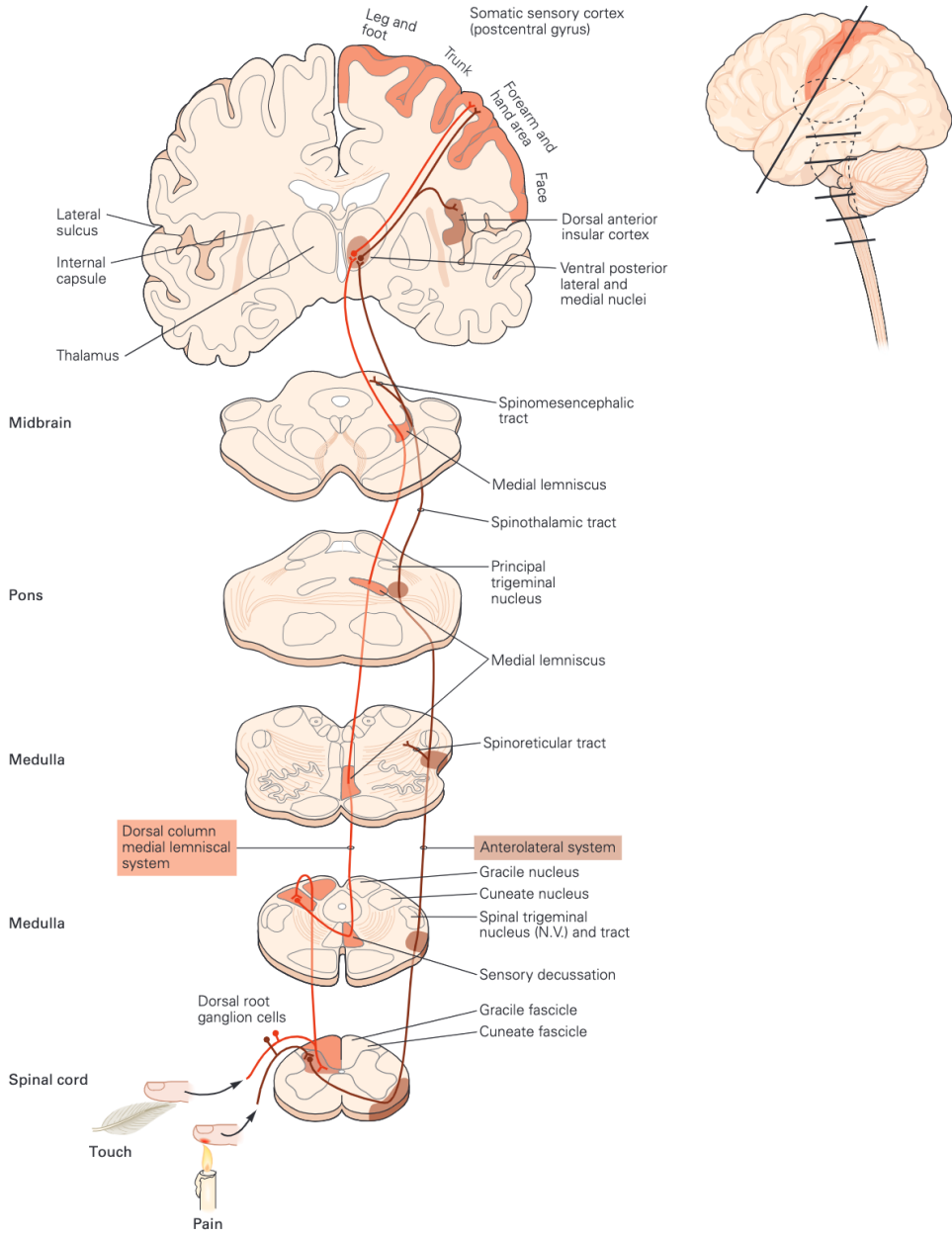


**Figure 2.** Somatosensory processing pathways for touch and pain/temperature in the dorsal column medial lemniscal system and the anterolateral systems from fingertip via the dorsal root ganglion, the spinal cord, the medulla, the pons, and the thalamus to the primary somatosensory cortex. Copy of Figure 22-11 (Gardner et al., 2012).

## General Introduction

Diverging late components and their fronto-parietal topographies suggest that processing in S1 is not sufficient for conscious tactile perception. Next to recurrent processing between S1 and S2 in EEG (Auksztulewicz et al., 2012), greater brain activity has been shown in bilateral S2, the anterior insula, and the superior temporal gyrus with functional magnetic resonance imaging (fMRI) (Moore et al., 2013), and with MEG, S2 has been reported to be more integrated pre-stimulus in the whole-brain functional network for stimulus detection (Weisz et al., 2014). Determining the spatial extent of brain activity accompanying conscious tactile perception is of high relevance for the development of consciousness theories which widely differ from local to global accounts (Baars, 1988; Dehaene et al., 2006; Koch et al., 2016; Lamme, 2006; Lau & Rosenthal, 2011). Lately, fronto-parietal activities have been challenged as serving the tactile detection task (reporting successful perception) but not the subjective experience of the stimulus itself (Schröder et al., 2019). So far, a whole-brain analysis of the post-stimulus functional network configurations in terms of graph metrics while also acquiring decision confidence and correct rejections of trials without stimulation has not been done and is addressed in *Study 3* (Grund et al., 2021).

The investigation of determinants for conscious tactile perception has been very brain focused. Body dynamics have been rarely recognized and if so, mainly heart activity has been monitored. The only study of somatosensation and bodily signals - we are aware of - investigated tactile detection thresholds at three time points in the cardiac cycle: 0, 300, and 600 milliseconds after the R-peak - the maximum depolarization of the heart muscle (contraction) and hence outflow of blood into the body (Edwards et al., 2009). The authors reported a lower detection threshold for electrical pulse trains applied 300 ms after the R-peak (Edwards et al., 2009). This was contrary to their initial visceral afferent feedback hypothesis that baroreceptor firing during systole (due to pulse pressure wave) is accompa-



nied by cortical inhibition and hence decreased perceptual sensitivity compared to diastole (Edwards et al., 2009). The authors discussed alternative explanations, e.g., a modified visceral afferent feedback hypothesis that argues in case of tactile stimuli baroreceptor-related cortical inhibition reduces the inhibition of afferent somatosensory transmission (Edwards et al., 2009). However, conscious tactile perception has been never sampled uniformly with high temporal resolution across the cardiac cycle. In *Study 1*, we pioneered this by combining a near-threshold tactile detection paradigm with measuring electrocardiography and applying circular statistics (Motyka et al., 2019). The neural correlates of the cardiac cycle effect on conscious tactile perception were investigated subsequently and published by our group (Al et al., 2020). *Study 2* added to this line of research by investigating conscious tactile perception in relation to another predominant body rhythm (the respiratory cycle) and cardiac-related movements in the finger (photoplethysmography) caused by the blood pulse wave (Grund et al., 2022). *Study 2* also pioneered the investigation of near-threshold detection in context of respiration.

## **1.2 Bodily signals - An integral part of conscious tactile perception**

Humans are obviously not a brain in the vat. After decades of brain-focused research programs more and more data are published showing the influence of bodily signals on cognition and perception (Azzalini et al., 2019; Garfinkel & Critchley, 2016). Mapping out the bodily determinants for conscious perception also helps to understand the underpinnings of consciousness, because our body is always an integral part of our subjective experience (Park & Blanke, 2019b). Particularly for tactile conscious perception, our body perception must be combined with the percept of an external stimulus on our skin (Martuzzi et al., 2015). Some convincing theories of

## General Introduction

consciousness even discuss our self as a prerequisite for subjective experiences (Graziano et al., 2019; Graziano & Kastner, 2011; Park & Tallon-Baudry, 2014; Prinz, 2017).

Cardiac activity is inherently coupled with somatosensation. For instance, our body pulsates with the blood wave which results in cardiac modulation of receptors in our skin (Macefield, 2003). Heartbeat sensations were mainly localized on the chest (Hassanpour et al., 2016; Khalsa et al., 2009). Furthermore, heart-evoked potentials (HEPs) in the brain were demonstrated to originate in the anterior cingulate cortex, the insula, the prefrontal cortex, and the somatosensory cortices (Kern et al., 2013; Park et al., 2017; Pollatos et al., 2005). HEPs showed an attentional modulation between exteroceptive and interoceptive focus (Petzschner et al., 2019) and differed between imagining oneself or a friend (Babo-Rebelo et al., 2019). In sum, over the course of the cardiac cycle, cardiac activity might interfere at different stages of somatosensory processing (from receptor via cortex to perception). Additionally, heart activity does not only determine but in turn is also affected by somatosensory perception, e.g., clearly perceivable (supra-threshold) electrical skin stimuli caused increased blood pressure when applied early in the cardiac cycle (systole) (Gray et al., 2009). Thus, studying conscious tactile perception requires to measure bodily signals as cardiac activity, because only with understanding the integration of internal and external signals we will get closer to the mechanisms which give rise to conscious sensory experiences. One possible theoretical and computational framework to capture these processes lies in interoceptive predictive coding models (Allen et al., 2019; Seth, 2013). The idea is that such models make predictions about upcoming bodily states while minimizing their prediction error when updated with the actual bodily state. Decision confidence in a perceptual detection task would be in this line of thinking not only a readout of sensory precision (prediction errors by an exteroceptive model) but also of prediction errors about internal

states, namely unexpected internal arousal (e.g., increased heart rate) would lead to less confidence (Allen et al., 2016, 2019). Furthermore, interoceptive predictive coding models would also allow to form predictions on how to act to reduce prediction errors by internal bodily states on external sensory signals (Allen et al., 2019; Corcoran et al., 2018).

While the timing of the cardiac cycle seems to be less accessible for control (you can hold your breath, but you cannot stop your heart), the modulation of the respiration rhythm has been shown to optimize memory and visual task performance (Huijbers et al., 2014; Perl et al., 2019; Zelano et al., 2016). In a visuospatial perception task, inspiration onsets locked to task onsets which increased task-related brain activity and task performance accuracy (Perl et al., 2019). Thus, tasked-locked inspiration was interpreted as tuning the sensory system for incoming information (Perl et al., 2019). Furthermore, it has been argued that respiration-entrained oscillations in rodents are supporting long-range communication in the brain (Tort et al., 2018). In humans, voluntary deep compared to involuntary normal breathing showed greater corticomuscular coherence (CMC) in the beta range over sensorimotor cortex, a marker for efficient long-range brain-muscle interactions (Kluger & Gross, 2020). This modulation of neural excitability as a function of respiratory phase (Kluger & Gross, 2020) and the behavioral results of phase-locked respiration to task onsets (Huijbers et al., 2014; Perl et al., 2019; Zelano et al., 2016) suggest that this relationship is used for timing the sampling of sensory information. In terms of predictive coding accounts, this is called *active sensing* (Corcoran et al., 2018). Particularly for near-threshold paradigms, the organism must be in an optimal state to detect very faint stimuli. Recently, in a visual detection paradigm, posterior alpha power, an inverse correlate of neural excitability, has been shown to be modulated by respiration, preceding the concomitant respiratory modulation on perceptual sensitivity, resulting in a decreased sensory threshold in the beginning of the second half of the inspiration interval

(Kluger et al., 2021). When inhaling deeply, the immanent connection between respiration and somatosensory perception (due to thorax expansion) can be experienced very vividly. Yet, we do not know how respiration relates to tactile detection and shapes our subjective experience jointly with other bodily signals as cardiac activity.

### **1.3 Theories based on neural correlates of consciousness**

The scientific study of neural correlates of consciousness (NCC) was facilitated by the development of new brain imaging techniques which allowed to dissociate levels and contents of consciousness (Crick & Koch, 1990; Laureys, 2005). Particularly, the study of exteroceptive contents of consciousness in detection studies benefited from fMRI and its possibility to spatially separate brain activity between perceived and unperceived stimuli (contrastive analysis) (Aru et al., 2012). Consecutively, also theoretical developments of stimulus awareness were related to the spatial extent of brain activity associated with conscious stimulus perception (Koch et al., 2016). While some authors proposed local accounts of perceptual awareness limited to sensory cortices of the corresponding stimulus modality, e.g., recurrent processing in somatosensory cortex (Auksztulewicz et al., 2012; Schröder et al., 2019). Others proposed a temporo-parietal-occipital hot zone (Boly et al., 2017; Koch et al., 2016), a fronto-parietal network (Naghavi & Nyberg, 2005; Rees et al., 2002), or frontal areas (Lau & Rosenthal, 2011) to give rise to conscious sensory experiences. The community did not converge to one of the spatial accounts yet. There is also no consensus in sight, as the debate between proponents for parietal or frontal cortical accounts shows (Boly et al., 2017; Odegaard et al., 2017).

The Recurrent Processing Theory (RPT) follows the idea that the feedforward sweep of sensory input along the sensory cortical processing hierarchies is not sufficient for conscious perception (Lamme, 2006), but

that it takes - in context of somatosensory processing - feedback loops between S1 and S2 which sufficiently amplify sensory processing to generate perceptual awareness (Auksztulewicz et al., 2012; Schröder et al., 2019). This is labeled a local theory, because it describes sensory cortices as sufficient neural structures for conscious sensory experiences (*phenomenal consciousness*). Frontoparietal activations, visible when contrasting detected and undetected trials, are in this framework a result of task requirements, e.g., reporting stimulus presence (Lamme, 2006; Schröder et al., 2019). In contrast, the Global Workspace Theory (GWT) requires global broadcasting of sensory information to distant brain areas to generate conscious percepts by making sensory information accessible for various cognitive functions (*access consciousness*) (Baars, 1988; Dehaene et al., 2006). In terms of the GWT, recurrent processing in sensory areas would be a pre-conscious state, and hence not sufficient for consciousness (Dehaene et al., 2003). Another class of theories, e.g., the higher-order thought (HOT) theory, argues that a necessary condition for perceptual awareness is the formation of a meta representation of being in a particular mental state (Lau & Rosenthal, 2011). This representation, reflected in sensory metacognition, is associated with activation in the frontal cortex (Lau & Rosenthal, 2011). While the HOT theory does not require self-referential thinking as a necessary condition for perceptual awareness (Lau & Rosenthal, 2011), others have argued that metacognition, e.g., confidence, is the result of integrating internal and external signals (Allen et al., 2016, 2019). Particularly near-threshold detection paradigms with very weak stimulus intensities face the organism with the challenge to decide whether the origin was of internal or external nature. Thus, it is very likely - independent of phenomenal or access consciousness - that also brain areas beyond sensory areas must be involved to generate a coherent conscious percept, e.g., to decide whether a pulse in the finger was generated internally or externally.

## General Introduction

Next to the spatial extent of increased or decreased brain activity, a further open question is how the involved brain areas interact with each other. The RPT suggests the amount of recurrent processing is crucial for a stable percept and awareness (Lamme, 2006). This has been tested in the somatosensory domain between S1 and S2 (Auksztulewicz et al., 2012), but very few studies investigated whole-brain functional connectivity accompanying conscious perception (Godwin et al., 2015; Nierhaus et al., 2015; Sadaghiani et al., 2015; Weisz et al., 2014), despite the general assumption that only neural interactions can give rise to consciousness. There are among many two mathematical tools with substantial advantages to assess and quantify whole-brain functional connectivity in tactile detection tasks: First, the generalized psychophysiological interaction (gPPI, a linear regression model) which allows to disentangle (a) task-associated brain activity and (b) baseline functional connectivity from (c) the condition-dependent functional connectivity (McLaren et al., 2012). And second, graph theory which has the power to aggregate large networks into single metrics for comparison between experimental conditions (Rubinov & Sporns, 2010). Even when condensing the brain to a limited number of brain areas or network nodes, the number of possible network connections (edges) is still very high, e.g., 264 nodes have 69,432 potential edges. The condition-dependent functional connectivity (c) describes the correlation of brain activity between two network nodes given a condition (e.g., detected near-threshold trial) and controlled for (a) evoked-brain activity by the stimulus within the nodes and (b) baseline correlation of brain activity between the two network nodes independent of the present condition. Graph metrics, as for instance modularity which measures the organization of nodes in sub-networks, provide then single values each for perceived and unperceived near-threshold trials that can be statistically compared across participants. A lower modularity as reported for visual awareness was interpreted as an

indicator for increased global integration, and hence broadcasting for access to consciousness as suggested by the GWT (Godwin et al., 2015).

For somatosensory perception, a similar approach using graph metrics (but without gPPI) has been applied to magnetoencephalography (MEG) and fMRI data (Nierhaus et al., 2015; Weisz et al., 2014). For MEG data and tactile stimulus detection, it has been shown that the contralateral secondary somatosensory cortex (S2) was in the pre-stimulus phase more integrated locally and globally (increased clustering and efficiency) to a widespread brain network (Weisz et al., 2014). This pre-stimulus functional brain network topology was interpreted as forming a window to consciousness (Weisz et al., 2014). For imperceptible electrical finger nerve stimulation, fMRI data showed decreased eigenvector centrality of the primary somatosensory cortex (S1), primarily driven by reduced functional connectivity to fronto-parietal areas (Nierhaus et al., 2015). Taken together, both observations of conscious and unconscious somatosensory processing provide evidence for the global workspace theory (GWT) of consciousness (Baars, 1988; Dehaene et al., 2006), which defines the global broadcasting of sensory information to domain-general areas as the necessary condition for access to consciousness. The only study we know that combined graph metrics with gPPI in a perceptual detection task is the work by Godwin and colleagues (2015). These authors showed that with visual conscious perception the whole-brain functional network modularity breaks down to a more globally integrated state (increased participation), in line with the GWT (Godwin et al., 2015). Due to the convincing methodological advantages of combining gPPI with graph metrics, we followed the example by Godwin et al. (2015) and investigated in *Study 3* (Grund et al., 2021) whether this observation extends to somatosensory awareness in a tactile detection paradigm. Present or absent differences in graph metrics would further inform neural theories of consciousness.

## 1.4 Research questions and approach

The thesis had the goal to improve our understanding of (a) interactions between bodily signals and conscious tactile perception, and (b) neural correlates accompanying conscious tactile perception. The overarching motivation was to shed light on determinants and consequences of perceptual awareness as a core component of human consciousness, and hence inform with empirical work the theory development. For reaching these goals, the following three main research questions were addressed:

1. Does conscious tactile perception vary across the cardiac cycle?  
(*Study 1*)
2. Does conscious tactile perception vary across the respiration cycle?  
(*Study 2*)
3. Do brain network topologies in terms of graph metrics change with conscious tactile perception? (*Study 3*)

For generating empirical answers to these questions, we used a tactile detection paradigm which asked participants to report whether they perceived a weak electrical pulse applied to their left index finger while physiological activity was recorded. In *Study 1* (Motyka et al., 2019), electrocardiography (ECG) was acquired during the detection task (a) to locate stimulus onsets relative to the cardiac cycle and (b) to analyze the heart rate before and after stimulus onset. In *Study 2* (Grund et al., 2022), participants had to report - next to stimulus detection - their decision confidence, and additionally to ECG, respiration activity and photoplethysmography were acquired. This allowed us to investigate stimulus detection relative to (a) respiratory cycle and (b) cardiac-related movement in the finger pad (pulse wave arrival). In *Study 3* (Grund et al., 2021), participants reported stimulus detection and decision confidence during fMRI data acquisition to investigate post-stimulus whole-brain functional networks in terms of graph metrics.



## 1.5 Hypotheses

*Hypothesis 1: Conscious tactile perception does not vary across the cardiac cycle.*

When uniformly sampled across the cardiac cycle, the detection of near-threshold stimuli should not vary with cardiac phase. Even given an interference with somatosensory processing, the brain should account for it to secure a stable percept of the world. This hypothesis is in contrast with the report of increased tactile sensitivity 300 ms after the R-peak (Edwards et al., 2009). However, the reported sensitivity effect was small (circa 0.02 mA) and contrary to their initial hypothesis (decreased sensitivity during systole) (Edwards et al., 2009). Our study differed in two main aspects: Instead of measuring somatosensory thresholds (multiple intensities) for pulse trains (60 ms) at three time intervals relative to the R-peak, we measured conscious perception of single pulses (0.2 ms) with fixed near-threshold intensities uniformly across the cardiac cycle.

*Hypothesis 2: Respiration rhythm is locked to the paradigm to optimize task performance.*

While in contrast to cardiac activity respiration can be modulated - as shown in natural tasks which require a high attentional focus and an optimal state of the organism (e.g., rifle shooting in biathlon), we also expected that respiration might be tuned to optimize tactile detection task performance.

*Hypothesis 3: Conscious tactile perception does change the whole-brain functional network configuration in terms of graph metrics (increased global integration).*

Based on previous reports for visual conscious perception (Godwin et al., 2015), we expected that conscious perception of near-threshold somatosensory stimuli is accompanied by a change of the whole-brain functional

## General Introduction

network topology. Particularly the pre-stimulus attentional focus on somatosensory input should be resolved in a less modular configuration which creates an integrative global workspace for conscious tactile perception (Baars, 1988; Dehaene et al., 2006).

## **Chapter 2**



### 2 Study 1: Interactions between cardiac activity and conscious somatosensory perception

Paweł Motyka, **Martin Grund**, Norman Forschack, Esra Al, Arno Villringer, and Michael Gaebler

Published in *Psychophysiology* in 2019.



# Interactions between cardiac activity and conscious somatosensory perception

Paweł Motyka<sup>1,2</sup>  | Martin Grund<sup>2</sup> | Norman Forschack<sup>2,3</sup> | Esra Al<sup>2,4</sup> | Arno Villringer<sup>2,4</sup> | Michael Gaebler<sup>2,4,5</sup> 

<sup>1</sup>Faculty of Psychology, University of Warsaw, Warsaw, Poland

<sup>2</sup>Department of Neurology, Max Planck Institute for Human Cognitive and Brain Sciences, Leipzig, Germany

<sup>3</sup>Experimental Psychology and Methods, Faculty of Life Sciences, University of Leipzig, Leipzig, Germany

<sup>4</sup>MindBrainBody Institute at the Berlin School of Mind and Brain, Humboldt-Universität zu Berlin, Berlin, Germany

<sup>5</sup>Leipzig Research Centre for Civilization Diseases (LIFE), University of Leipzig, Leipzig, Germany

## Correspondence

Paweł Motyka, Faculty of Psychology, University of Warsaw, Stawki 5/7, 00-183 Warsaw, Poland.  
Email: pawel.motyka@psych.uw.edu.pl

## Funding information

National Science Centre, Poland, grant (2016/23/N/HS6/02920) (to P.M.); Federal Ministry of Education and Research, Germany, grant (13GW0206B) (to M.Ga.)

## Abstract

Fluctuations in the heart's activity can modulate the access of external stimuli to consciousness. The link between perceptual awareness and cardiac signals has been investigated mainly in the visual and auditory domain. Here, we investigated whether the phase of the cardiac cycle and the prestimulus heart rate influence conscious somatosensory perception. We also tested how conscious detection of somatosensory stimuli affects the heart rate. Electrocardiograms (ECG) of 33 healthy volunteers were recorded while applying near-threshold electrical pulses at a fixed intensity to the left index finger. Conscious detection was not uniformly distributed across the cardiac cycle but significantly higher in diastole than in systole. We found no evidence that the heart rate before a stimulus influenced its detection, but hits (correctly detected somatosensory stimuli) led to a more pronounced cardiac deceleration than misses. Our findings demonstrate interactions between cardiac activity and conscious somatosensory perception, which highlights the importance of internal bodily states for sensory processing beyond the auditory and visual domain.

## KEYWORDS

cardiac cycle, heart rate, interoception, perceptual awareness, somatosensory perception

## 1 | INTRODUCTION

The internal state of the body is continuously monitored by interoceptive regions and networks in the brain (Barrett & Simmons, 2015; Craig, 2009; Kleckner et al., 2017). Besides their well-described role in homeostatic regulation, visceral signals have been argued to contribute to a wide range of psychological phenomena, including emotions (Critchley & Garfinkel, 2017; Wiens, 2005), empathy (Fukushima, Terasawa, & Umeda, 2011; Grynberg & Pollatos, 2015), time perception (Di Lernia et al., 2018; Meissner & Wittmann, 2011), self-consciousness (Craig, 2009; Park & Tallon-Baudry, 2014), and decision making (Gu & Fitzgerald, 2014; Seth, 2014). At the perceptual level, it remains unclear to

what extent signals from visceral organs can modulate the conscious access to exteroceptive (e.g., visual, auditory, somatosensory) input. Here, we examined the interactions between perceptual awareness for somatosensory stimuli and cardiac activity, that is, the phase of the cardiac cycle and the heart rate.

The cardiac cycle from one heartbeat to the next can be divided into two phases: systole, when the heart contracts and ejects blood into the arteries—leading to activation of pressure-sensitive baroreceptors in arterial vessel walls—and diastole, when the cardiac muscle relaxes, the heart refills with blood, and baroreceptors remain quiescent (Landgren, 1952; Mancia & Mark, 2011). Baroreceptor activity signals the strength and timing of each heartbeat to the nuclei in the

lower brain stem, where the signal is relayed to subcortical and cortical brain regions (Dampney, 2016). In studies with noninvasive baroreceptor stimulation, their activity was found to decrease the BOLD signal (Makovac et al., 2015) and ERP amplitudes (Rau & Elbert, 2001; Rau, Pauli, Brody, Elbert, & Birbaumer, 1993) in cortical regions. Baroreceptor firing is thought to underlie cardiac cycle effects on behavior and cognition (Duschek, Werner, & Reyes Del Paso, 2013; Garfinkel & Critchley, 2016), like decreased intensity ratings for acoustic (Cohen, Lieb, & Rist, 1980; Schulz et al., 2009) or painful stimulation (Wilkinson, McIntyre, & Edwards, 2013) as well as higher reaction times to stimuli (Birren, Cardon, & Phillips, 1963; Edwards, Ring, McIntyre, Carroll, & Martin, 2007; McIntyre, Ring, Edwards, & Carroll, 2008) during early (i.e., at systole) compared to later phases (i.e., at diastole) of the cardiac cycle.

There are conflicting findings as to what extent the cardiac cycle modulates the access of exteroceptive information to perceptual awareness. Earlier studies reported that the detection of visual (Réquin & Brouchon, 1964; Sandman, McCanne, Kaiser, & Diamond, 1977) and auditory signals (Saxon, 1970) vary for different points of the cardiac cycle. However, other studies in the visual (Elliott & Graf, 1972) and auditory domain (Delfini & Campos, 1972; Velden & Juris, 1975) did not find such variations. More recently, an enhanced detection selectively for fearful faces was observed during cardiac systole (Garfinkel et al., 2014). As almost all studies in that field involved visual or auditory stimuli, it remains unclear whether cardiac phase-related fluctuations occur in other sensory modalities. The only previous study in the somatosensory domain with a behavioral measure of perception reported lower detection thresholds for electrical stimulation at systole compared to diastole (Edwards, Ring, McIntyre, Winer, & Martin, 2009). As in most studies of cardiac phase effects, the detection performance was sampled only at fixed time points (R+0, R+300, and R+600 ms), which may have missed perceptual changes at other parts of the cardiac cycle.

In the present study, we examined fluctuations in conscious somatosensory perception across the entire cardiac cycle. Given the variations in cortical excitability over the cardiac cycle, we hypothesized that detection of near-threshold electrical stimuli is not equally distributed but varies over the interval between one heartbeat and the next. We also aimed to explore associations between conscious somatosensory perception and the heart rate. The bidirectional information flow between the heart and the brain (Faes et al., 2017; Lin, Liu, Bartsch, & Ivanov, 2016; Valenza, Toschi, & Barbieri, 2016) implies that cardiac activity may not only impact perception but is also influenced by it. Therefore, we tested whether the prestimulus heart rate influences conscious perception and, in turn, whether perception changes the (poststimulus) heart rate.

Regarding the relation between the heart rate and perception, an early theory suggested that a decreased heart rate increases sensitivity to sensory stimulation by directing attention to external rather than internal signals (Graham & Clifton, 1966; Lacey, 1967; Lacey, Kagan, Lacey, & Moss, 1963; Sandman, 1986). The evidence for this hypothesis is mixed and comes only from studies in the auditory and visual domain: For auditory thresholds, there were no differences between transient periods of low and high heart rate (Edwards & Alsip, 1969) unless the procedure involved exercise-induced changes in heart rate (Saxon & Dahle, 1971). In addition to such heart rate variations over longer periods of time, quick changes from one heartbeat to the next were suggested to modulate perception (Lacey & Lacey, 1974; Sandman et al., 1977). In general, cardiac deceleration (i.e., a lengthening of the period between consecutive heartbeats) is known to occur in anticipation of a (cued) stimulus or in reaction to a salient stimulus (Lacey & Lacey, 1970, 1977; Simons, 1988), and it is typically followed by cardiac acceleration after the behavioral response (e.g., Börger & van Meere, 2000; Park, Correia, Ducorps, & Tallon-Baudry, 2014). While both spontaneous (Sandman et al., 1977) and conditioned (McCanne & Sandman, 1974) cardiac deceleration coincident with a visual stimulus was found to increase its detection, other—more recent—studies did not show a modulation of visual awareness by heart rate changes prior to and coincident with a near-threshold stimulus (Cobos, Guerra, Vila, & Chica, 2018; Park et al., 2014).

For heart rate changes after stimulus presentation, earlier studies found a cardiac deceleration in response to suprathreshold visual (Davis & Buchwald, 1957), auditory (Davis, Buchwald, & Frankmann, 1955; Uno & Grings, 1965; Wilson, 1964), tactile (Davis et al., 1955), and olfactory stimuli (Gray & Crowell, 1968). Additionally, cardiac deceleration was found to be more pronounced after viewing unpleasant compared to pleasant or neutral scenes (Bradley, Cuthbert, & Lang, 1990; Greenwald, Cook, & Lang, 1989; Hare, 1973; Libby, Lacey, & Lacey, 1973; Walker & Sandman, 1977). Most importantly in the context of this work, recent studies using near-threshold visual stimuli showed that hits resulted in increased cardiac deceleration compared to misses (Cobos et al., 2018; Park et al., 2014). This suggests that not only the physical characteristics of a stimulus determine the cardiac response but also the level of its processing (i.e., conscious vs. nonconscious).

The association between cardiac activity and perception was also related to cardiac-phase independent variations in arterial pressure after changes in heart rate (Sandman et al., 1977). In this view, the late phase of the cardiac cycle (i.e., diastole) and cardiac deceleration result in—similar but not identical—transient decreases in blood pressure, thus facilitating the access of external stimuli to consciousness by decreasing the inhibitory effects of baroreceptor activity on the

brain (Sandman, 1986; Sandman et al., 1977). Notably, even though higher mean arterial blood pressure has been associated with higher resting heart rate (Christofaro, Casonatto, Vanderlei, Cucato, & Dias, 2017; Mancia et al., 1983), increases in blood pressure after cardiac deceleration (i.e., decreases in heart rate) were observed during experimental tasks (Otten, Gaillard, & Wientjes, 1995; Wölk, Velden, Zimmermann, & Krug, 1989). In addition, animal studies showed that, also with constant mean arterial pressure, the heart rate elevation leads to an increased discharge of arterial baroreceptors (Abboud & Chappleau, 1988; Barrett & Bolter, 2006). Taken together, these findings suggest that the heart rate contributes to cortical excitability through a transient modulation of baroreceptor activity.

Furthermore, we aimed to test whether the influence of cardiac signals on perception varies with interindividual differences in interoceptive accuracy, that is, the ability to consciously perceive signals originating from the body (Garfinkel, Seth, Barrett, Suzuki, & Critchley, 2015). Given that the capacity to detect one's own heartbeat has been repeatedly shown to modulate (usually strengthen) cardiac effects on perception and behavior (Critchley & Garfinkel, 2018; Dunn et al., 2010; Suzuki, Garfinkel, Critchley, & Seth, 2013), we hypothesized that the link between conscious somatosensory perception and cardiac activity would be stronger for participants with higher interoceptive accuracy (measured with the heartbeat counting task; Schandry, 1981).

In sum, given that baroreceptor activity, which is thought to suppress the processing of external input, varies both across the cardiac cycle and with the heart rate, we hypothesized that perceptual awareness for somatosensory stimuli increases at the later phases of the cardiac cycle (at diastole) and with greater cardiac deceleration. Also, we explored whether a consciously detected somatosensory stimulus affects the heart rate differently compared to a nondetected stimulus and whether cardiac effects on conscious somatosensory perception vary with the capacity to consciously perceive one's heartbeat.

## 2 | METHOD

### 2.1 | Participants

Thirty-three healthy volunteers (17 female, mean age = 25.9,  $SD = 4.1$ , range: 19–36 years, right-handed) were recruited from the database of the Max Planck Institute for Human Cognitive and Brain Sciences in Leipzig, Germany. The procedure was approved by the ethics committee of the Medical Faculty at the University of Leipzig. All participants gave written informed consent before taking part in the study and were financially compensated for their participation.

### 2.2 | Apparatus

Electrocardiography (ECG) was measured while near-threshold electrical finger nerve stimulation was applied. ECG was recorded at a sampling frequency of 1,000 Hz with BrainAmp (Brain Products GmbH, Gilching, Germany). Electrodes were placed on the wrists and the left ankle (ground) according to Einthoven's triangle. Electrical finger nerve stimulation was performed with a constant-current stimulator (DS5; Digitimer) applying single rectangular pulses with a length of 200  $\mu$ S. A pair of steel wire ring electrodes was attached to the middle (anode) and the proximal (cathode) phalanx of the left index finger. The experiment was programmed, and behavioral data were recorded with MATLAB 8.5.1 (Psychtoolbox 3.0.11, Brainard, 1997; Kleiner et al., 2007; Pelli, 1997).

### 2.3 | Procedure

Each participant was tested individually in a dimly lit experimental chamber seated in a comfortable chair and facing a computer screen. After a brief explanation of the experimental procedure and the attachment of ECG electrodes, the steel wire ring electrodes were attached to the left index finger. The response button box was placed under the right hand. The computer screen indicated when to expect a stimulus and when to respond (Figure 1). Participants responded with *yes* if they felt an electrical stimulus and *no* if not. The left/right button-response mapping (yes-no or no-yes) was pseudorandomized across participants. The experimental session consisted of 360 trials divided into three blocks. Each block included 100 trials with near-threshold stimulation and 20 catch trials without stimulation in pseudorandomized order. The intensity of electrical stimulation was fixed throughout a block. Before each block, the somatosensory perceptual threshold was assessed using an automated staircase procedure to estimate a stimulus intensity that would be equally likely to be felt or not (the 50% detectability level). The applied method combines a coarser staircase procedure (up/down method) and a more fine-grained Bayesian procedure (psi method) of the Palamedes Toolbox (Kingdom & Prins, 2010). The automated threshold assessment resembled the actual experimental design, except for the shorter (500 ms) intertrial interval and the time window in which stimulation could occur (1,000 ms). Thus, before each block, the experimenter made a data-driven decision of the individual sensory threshold ( $M = 2.24$ ,  $SD = 0.81$ , range = 1–5 milliamperes). At the end of the experimental session and after a short break of approximately 3 min, interindividual differences in interoceptive accuracy (Garfinkel et al., 2015) were assessed with a heartbeat counting task (Schandry, 1981), in which participants were asked to estimate the number of their heartbeats in five intervals of different duration (detailed in the online supporting information, Appendix S1).

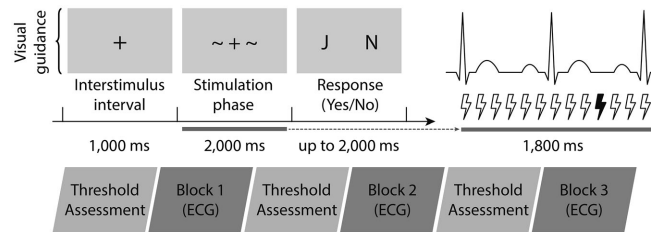


**FIGURE 1** Near-threshold somatosensory signal detection task. Upper: Each trial started with a 1,000-ms central fixation cross, followed by the 2,000-ms time window during which the stimulus could occur (except for the first and the last 100 ms of this interval). The stimulation onset was pseudorandomized within this 1,800-ms time window, aiming for a uniform distribution of stimuli over the entire cardiac cycle. Next, the response phase began (cued by displaying *JN*—corresponding to *yes* and *no*, respectively) and lasted until participants gave a response within the maximum time of 2,000 ms. After the button press, the fixation cross was visible for the rest of the 2,000-ms interval so that the total duration of each trial was kept constant at 5,000 ms. The next trial followed immediately so that the duration of each block was fixed (10 min). Lower: An experimental session consisted of three such blocks, which were each preceded by a threshold assessment to estimate stimulus intensities with 50% detection probability

## 2.4 | Statistical analysis

All statistical analyses were conducted using R version 3.5.1 (R Core Team, 2016) with RStudio version 1.1.453 (RStudio Team, 2016) and the Circular package version 0.4.93 (Agostinelli & Lund, 2013). Kubios 2.2 (Tavainen, Niskanen, Lipponen, Ranta-aho, & Karjalainen, 2014; Biosignal Analysis and Medical Imaging Group, Department of Applied Physics, University of Eastern Finland, Kuopio, <http://kubios.uef.fi/>) was used to automatically detect and visually inspect R peaks in the ECG. Falsely detected or missed R peaks (<0.2%) were manually corrected. A two-sided alpha level of 0.05 was used in all statistical analyses. All preprocessed data and the codes used for the main and supplementary analyses are available on GitHub at <<https://github.com/Pawel-Motyka/CCSomato>>.

### 2.4.1 | Behavior

Prior to the analysis, the following data were excluded: 191 trials (from 26 participants) with no response within 2 s (1.7% of all trials), 15 trials where the stimulation failed, two trials with the unassigned button pressed, and two trials with physiologically implausible interbeat interval (IBI) lengths (>1,500 ms). Also, one block of one participant was excluded due to data recording failure. Thus, the total number of trials retained for analysis was 11,550 (from 33 participants): 4,530 hits (correctly detected near-threshold stimuli), 5,104 misses (not detected near-threshold stimuli), 81 false alarms (wrongly detected nonstimulation), and 1,835 correct rejections (correctly detected nonstimulation).

### 2.4.2 | ECG data

To investigate cardiac phase-related variations in perceptual awareness for somatosensory stimuli while accounting for both the oscillatory and the biphasic nature of cardiac activity, the distribution of hits and misses were examined (a) over the whole cardiac cycle by means of circular statistics (Pewsey, Neuhauser, & Ruxton, 2013), and (b) by testing differences in hit rates between the two cardiac phases (systole and diastole), respectively. Furthermore, it was analyzed (c) whether pre- and poststimulus changes in heart period differed between hits and misses.

1. Circular statistics allowed us to analyze the distribution of hits and misses along the entire cardiac cycle (from one R peak to the next). For each participant, the mean phase angle, at which hits or misses occurred on average, was calculated in degrees (see Section 2.5 Determination of stimulus onset distribution across the cardiac cycle). At the group level, it was tested with Rayleigh tests (Pewsey et al., 2013) whether the distributions of hits and misses deviated from the uniform distribution. The Rayleigh test is based on the mean vector length out of a sample of circular data points and specifies the average concentration of these phase values around the circle—ranging from 0 to 1 indicating no to perfect (angular) concentration, respectively. A statistically significant Rayleigh test result indicates that the data are unlikely to be uniformly distributed around the circle (in this case, the cardiac cycle).
2. Binary analysis, based on the segmentation of the cardiac cycle into the two cardiac phases, allowed us to compare our results to previous studies of cardiac effects on perception.



To divide the cardiac cycle into systole and diastole, the trial-specific cardiac phases were computed based on cardio-mechanical events related to the ECG signal (for a description of the applied t-wave end detection algorithm, see Section 2.6 Determination of individual cardiac phases). Given the between-subjects variation of cardiac phase lengths arising, for example, from differences in heart rate (Herzog et al., 2002; Lewis, Rittgers, Froester, & Boudoulas, 1977; Wallace, Mitchell, Skinner, & Sarnoff, 1963), an individualized approach was used—instead of rather arbitrary and fixed systole and diastole intervals (e.g., defining systole as the 300 ms following an R peak). Stimulus onsets were assigned to the corresponding cardiac phase (i.e., systole or diastole) for each trial. Then, for each participant, hit rates were calculated separately for systole and diastole. A paired *t* test was used to determine whether hit rates differed between cardiac phases.

- To analyze the pre- and poststimulus heart rate for hits and misses, the mean lengths of six consecutive IBIs were computed (with an average IBI of 827 ms,  $SD = 119$  ms; these aimed to cover the full trial length of 5,000 ms): two before the stimulation (S-2, S-1), one at which the stimulus occurred (stimulus), and three after the stimulation (S+1, S+2, S+3). To test whether the (changes in) heart period differed between hits and misses, a two-way repeated measures analysis of variance (ANOVA) was used—with perceptual awareness (hits/misses) and time (six IBIs, S-2 to S+3, per trial) as factors—followed by post hoc Bonferroni-corrected paired *t* tests. Furthermore, an association between the extent of cardiac deceleration and the conscious access to somatosensory stimuli was investigated. For each trial, cardiac deceleration was calculated (and *z* scored within participants) as the difference between the lengths of the IBI at which the stimulus occurred (stimulus) and the IBI prior to it (S-1). A paired *t* test was used to examine whether the extent of cardiac deceleration differed between hits and misses.

### 2.4.3 | Interoceptive accuracy

A score of interoceptive accuracy was calculated for each participant. The closer the estimated number to the number of heartbeats measured by the ECG over five intervals, the higher the interoceptive accuracy score (cf. supporting information, Appendix S1). The sample was then median-split into groups of high and low interoceptive accuracy, which were compared using analyses described in Section 2.4.2.

### 2.5 | Determination of stimulus onset distribution across the cardiac cycle

In each trial, stimulus onset was pseudorandomized within a 1,800-ms time window. Stimulation at different points of IBI aimed to cover the entire cardiac cycle for each subject. For each stimulus, the time of the previous and the subsequent R peak were extracted from the ECG to calculate the stimulus onset's relative position within the IBI using the following formula:  $[(\text{onset time} - \text{previous R peak time}) / (\text{subsequent R peak time} - \text{previous R peak time})] \times 360$ , assigning the values from 0 to 360 degrees (with 0 indicating the R peak before the stimulus). The distribution of stimulus onsets was tested separately for each participant with a Rayleigh test for uniformity. One participant was excluded from further circular analyses due to nonuniformly distributed stimulation onsets across the cardiac cycle,  $\bar{R} = 0.11$ ,  $p = 0.009$ . For the rest of the participants, the assumption of uniform onset distributions was fulfilled (all  $ps > 0.091$ ).

### 2.6 | Determination of individual cardiac phases

To account for the biphasic nature of cardiac activity, we encoded the length of individual cardiac phases using the t-wave end detection method (Vázquez-Seisdedos, Neto, Marañón Reyes, Klautau, & Limão de Oliveira, 2011): First, the peak of the t wave was located as a local maximum within a physiologically plausible interval (up to 350 ms after the R peak). Subsequently, a series of trapezes were calculated along the descending part of the t-wave signal, defining the point at which the trapezium's area gets maximal as the t-wave end. Detection performance was visually controlled by overlaying the t-wave ends and the ECG trace from each trial. Twenty-seven trials with extreme systole lengths (more than 4 *SDs* above or below the participant-specific mean) were excluded.

Although mechanical systole cannot be fully equated with the duration of electrical systole in the ECG (Fridericia, 1920), both are closely tied under normal conditions (Boudoulas, Geleris, Lewis, & Rittgers, 1981; Coblentz, Harvey, Ferrer, Cournand, & Richards, 1949; Fridericia, 1920; Gill & Hoffmann, 2010). Systolic contraction of the ventricles follows from their depolarization (marked in the ECG by the QRS complex), whereas the closure of the aortic valve, terminating the systolic blood outflow, corresponds to ventricular repolarization (around the end of the t wave; Gill & Hoffmann, 2010). In our study, the ventricular systolic phase (further referred to as systole) was defined as the time between the R peak of the QRS complex and the t-wave end, while diastole was defined as the remaining part of the RR interval.

### 3 | RESULTS

#### 3.1 | Detection rate for near-threshold somatosensory stimuli

On average, 46.7% of the near-threshold somatosensory stimuli were detected ( $SD = 16.2\%$ , range: 15.1%–79.3%). The false alarm rate was 4.2% ( $SD = 5.7\%$ , range: 0%–16.6%).

#### 3.2 | Hits concentrated in the late phase of the cardiac cycle

Rayleigh tests were applied to analyze the distribution of hits and misses across the cardiac cycle. Hits were not uniformly distributed across the cardiac cycle,  $\bar{R} = 0.32$ ,  $p = 0.034$  (Figure 2a), with their mean angle directing to the later phase of the cardiac cycle (i.e., diastole). Misses showed a non-significant tendency to deviate from uniformity,  $\bar{R} = 0.30$ ,  $p = 0.060$  (Figure 2b), with their mean angle directing to the earlier phase of the cardiac cycle (i.e., systole). For 14 out of 32 participants, the individual mean angles for hits fell into the last quarter of the cardiac cycle. The individual mean angles for misses accumulated in the second quarter of the cardiac cycle for 13 participants. Distributions of hits or misses across the cardiac cycle did not differ significantly between participants with high or low interoceptive accuracy (see supporting information, Figure S1).

#### 3.3 | Higher hit rates in diastole than in systole

Accounting for the biphasic nature of cardiac activity, differences in hit rates between systole and diastole were examined. Hit rates for near-threshold somatosensory stimuli were

significantly higher during diastole ( $M = 47.9\%$ ,  $SD = 16.5\%$ ) than during systole ( $M = 45.1\%$ ,  $SD = 16.3\%$ ),  $t(32) = -2.76$ ,  $p = 0.009$ , Cohen's  $d = 0.48$ . Increased hit rate during diastole was observed for 25 out of 33 participants (Figure 3). This mirrors the concentration of hits in the later phase of the cardiac cycle (see circular statistics, Figure 2). Hit rates at different cardiac phases did not differ significantly between the groups with high and low interoceptive accuracy (see Figure S2). Further, to allow a more direct comparison with the previous study by Edwards et al. (2009), hit rates were analyzed across the three 100-ms intervals of the cardiac cycle centered around the time points used therein: R+0 ms; R+300 ms, R+600 ms. Hit rates were significantly higher during the R+600 ms (at diastole) than during the R+300 ms interval (at systole), with no other significant differences between intervals (see supporting information, Appendix S1, for details and Figure S3).

#### 3.4 | Pre- and poststimulus heart rate (changes) for hits and misses

To investigate how the heart rate interacts with conscious somatosensory perception, pre- and poststimulus IBIs (factor: time) were analyzed separately for hits and misses (factor: detection). The analysis showed significant main effects of time (Greenhouse-Geisser corrected;  $F(5, 160) = 57.9$ ,  $p < 0.001$ ,  $\epsilon = 0.299$ ,  $\eta^2_G = 0.008$ ) and detection,  $F(1, 32) = 6.37$ ,  $p = 0.020$ ,  $\eta^2_G = 0.0004$ , as well as their significant interaction (Greenhouse-Geisser corrected;  $F(5, 160) = 13.5$ ,  $p < 0.001$ ,  $\epsilon = 0.399$ ,  $\eta^2_G = 0.0003$ ; Figure 4a). IBIs prior to the stimulus (S-1, S-2) did not differ significantly between hits and misses. IBIs concurrent with the stimulus were significantly longer for hits than for misses (stimulus:  $t(32) = 4.21$ ,

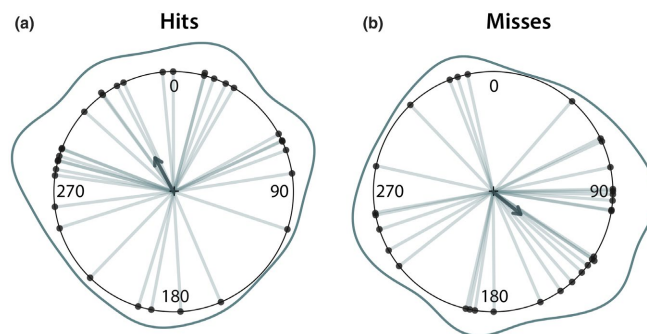


**FIGURE 2** Distribution of (a) hits, and (b) misses across the cardiac cycle (i.e., the interval between two R peaks; at 0/360°). Rayleigh tests showed a significant deviation from a uniform distribution for hits ( $\bar{R} = 0.32$ ,  $p = 0.034$ ) and a nonsignificant trend for misses ( $\bar{R} = 0.30$ ,  $p = 0.060$ ). Each dot (and line) indicates one participant's mean phase angle. The annular line depicts the distribution of individual means. The darker arrows represent the directions of the group means for hits (331°) and misses (129°), with their length indicating the concentration of individual means across the cardiac cycle (hits: 0.32; misses: 0.30—with 1 indicating perfect angular concentration)

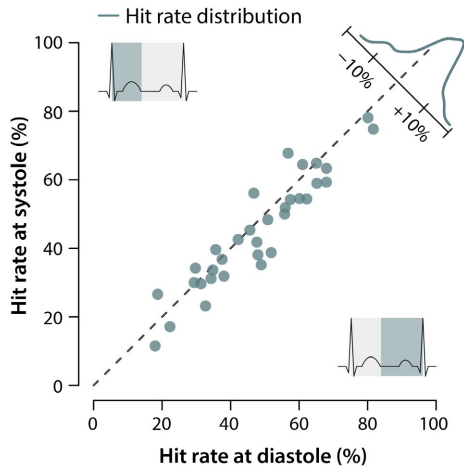


**FIGURE 3** Significantly higher hit rates in diastole than in systole. Coordinates of each dot represent a participant's mean hit rate at systole ( $x$  axis) and diastole ( $y$  axis). Dashed lines mark the identity line in hit rate between cardiac phases. The distribution in the upper right corner aggregates the frequency across participants. The probability distribution was shifted toward diastole indicating significantly higher hit rates during the later phase (i.e., diastole) than the earlier phase (i.e., systole) of the cardiac cycle,  $t(32) = -2.76$ ,  $p = 0.009$ , Cohen's  $d = 0.48$

$p = 0.006$ ). This effect was also observed for IBIs right after the stimulus (S+1:  $t(32) = 5.22$ ,  $p < 0.001$ ) but not for subsequent IBIs (S+2, S+3). For both hits and misses, a significant

cardiac deceleration was found between the IBIs before and during the stimulus (from/S to stimulus, hits:  $t(32) = -7.28$ ,  $p < 0.001$ , misses:  $t(32) = -4.96$ ,  $p < 0.001$ ) as well as between the IBIs during and after the stimulus (from stimulus to S+1, hits:  $t(32) = -5.95$ ,  $p < 0.001$ , misses:  $t(32) = -5.00$ ,  $p < 0.001$ ). Cardiac deceleration was followed by an immediate acceleration for hits (from S+1 to S+2:  $t(32) = 4.93$ ,  $p < 0.001$ ), which was not observed for misses (from S+1 to S+2:  $t(32) = 1.28$ ,  $p_{\text{corrected}} = 1.000$ ). In the later phase of the trials (from S+2 to S+3), cardiac acceleration was present after both hits,  $t(32) = 7.50$ ,  $p < 0.001$ , and misses,  $t(32) = 5.67$ ,  $p < 0.001$ .

To further explore the association between cardiac deceleration and conscious somatosensory perception, the "slopes" of the stimulus-induced heartbeat deceleration (stimulus - S-1) were compared between hits and misses. Consciously perceiving the stimulus was accompanied by larger cardiac deceleration ( $M = 0.07$ ,  $SD = 0.08$ ) than missing the stimulus ( $M = -0.08$ ,  $SD = 0.07$ ),  $t(32) = 6.97$ ,  $p < 0.001$ , Cohen's  $d = 1.21$  (Figure 4b).

## 4 | DISCUSSION

In this study, we investigated if conscious somatosensory perception varies across the cardiac cycle and how it interacts with the heart rate. In line with our main hypothesis of an increased somatosensory sensitivity during the later phase of the cardiac cycle, we found that the detection of near-threshold electrical finger nerve stimulation is significantly increased during diastole compared to systole. We also found

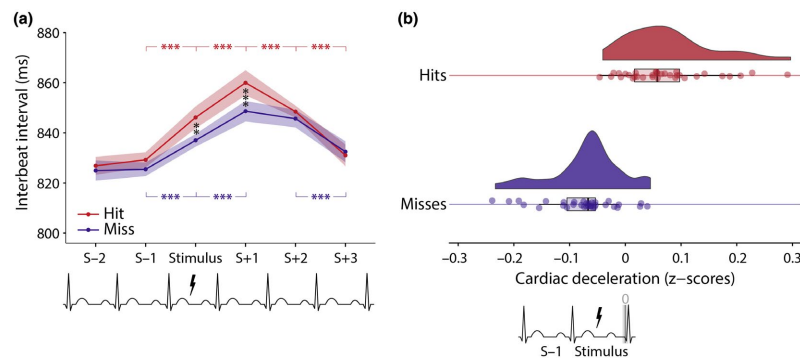


**FIGURE 4** Association between heart rate and perceptual performance over the course of a trial. (a) Mean interbeat intervals (IBIs) for hits and misses: two IBIs before (S-1, S-2) and three IBIs after (S+1, S+2, S+3) the stimulus onset (stimulus). In sum, the previously found deceleration-acceleration pattern was observed during the detection task, with more pronounced cardiac deceleration after hits than after misses. Vertical and horizontal bars with asterisks indicate significant pairwise post hoc comparisons. (b) The extent of cardiac deceleration as a correlate of conscious perception, visualized using raincloud plots (Allen, Poggiali, Whitaker, Marshall, & Kievit, 2019). The standardized slope of cardiac deceleration (i.e., the difference between stimulus and S-1) was greater for hits than for misses. Colored bands indicate 95% within-participant confidence intervals (Morey, 2008). \*\* $p < 0.01$ ; \*\*\* $p < 0.001$



(a) no evidence that the heart rate before a stimulus influenced perceptual performance, (b) that conscious detection was significantly associated with a stronger cardiac deceleration in the IBI during and after a stimulus, and (c) that the heart rate significantly accelerated with a delay after nondetected compared to detected stimuli. Taken together, these results indicate that conscious access to somatosensory signals varies across the cardiac cycle and transiently decreases the heart rate.

The difference between our findings and a previous study, which reported increased somatosensory sensitivity during systole (R+300 ms) compared to diastole (R+600 ms; Edwards et al., 2009), may have several—also methodological—reasons: (a) Edwards et al. (2009) assessed perceptual thresholds at different time points within the cardiac cycle, whereas we used stimuli of constant intensity distributed across the entire cardiac cycle; (b) the stimuli in the previous study consisted of 1-ms square wave pulses at 250 Hz for 60 ms, while we used single rectangular pulses with a length of 200  $\mu$ S; (c) in our analysis of detection across the cardiac cycle, perceptual performance was highest in the last quarter of the cardiac cycle. This period was not necessarily covered in the study by Edwards et al. (2009), in which the latest stimulation after the R peak occurred at R+600 ms. We conducted an additional analysis of our data to facilitate the comparison with Edwards et al. (2009), detailed in the supporting information. It might also be worth pointing out that our findings are in line with the original hypothesis of Edwards et al. (2009) that perceptual sensitivity is higher (and sensory thresholds are lower) at diastole than at systole.

A possible physiological mechanism for the relatively increased detection during diastole is the baroreceptor-driven inhibition of sensory neural systems during systole (Critchley & Garfinkel, 2015; Duschek et al., 2013). This is consistent with previous findings in which baroreceptor activity has been related to lower intensity ratings for acoustic (Cohen et al., 1980; Schulz et al., 2009) and painful stimuli (Wilkinson et al., 2013) as well as longer reaction times (Birren, Cardon, & Phillips, 1963; Edwards et al., 2007; McIntyre et al., 2008) for stimuli presented early (i.e., at systole) compared to late (i.e., at diastole) in the cardiac cycle. However, there is also evidence that specifically threatening visual stimuli are perceived more easily and rated as more intense during systole (Garfinkel et al., 2014). Yet, the faint electrical stimulation in our study does not qualify as a threat signal but is rather an emotionally neutral stimulus, as they are typically used in studies of cardiac effects on conscious perception.

More broadly, it is not clear whether perceptual fluctuations related to rhythmic activity of the body and the brain (such as the heartbeat and respiration and various forms of brain rhythms) come with an overall “functional advantage” or whether they are just an epiphenomenal consequence of physiological and anatomical constraints. For neural oscillations

(e.g., alpha band-related variations in visual perception; Busch, Dubois, & VanRullen, 2009; Dugué, Marque, & VanRullen, 2011), it remains a matter of debate how perception benefits from inherent rhythmicity (VanRullen, 2016). It has been proposed that brain oscillations serve the effective communication between neurons (Fries, 2015) and enable the simultaneous encoding of multiple stimulus features (Lisman, 2005; VanRullen, Guyonneau, & Thorpe, 2005). However, perceptual rhythms in the brain have also been suggested to not have any functional role but result from satisfying biological constraints (VanRullen, 2016). A similar point could be made about the role of cardiac-related fluctuations in perception—especially because both are likely to be linked (Klimesch, 2013, 2018).

The present findings could also be understood as suppressing weak and nonsalient somatosensory signals from reaching consciousness during baroreceptor firing. Given the enhanced processing of threat stimuli (Garfinkel et al., 2014) and pain inhibition during systole (Wilkinson et al., 2013), it has been proposed that baroreceptor signals promote a fight-or-flight mode of behavior (Garfinkel & Critchley, 2016). In line with this interpretation, Pramme, Larra, Schächinger, and Frings (2016) reported enhanced visual selection during systole. Hence, baroreceptor-mediated inhibition of cortical activation might facilitate the allocation of attention to situationally relevant stimuli (Pramme et al., 2016). It could be hypothesized that a stressor-evoked heart rate increase facilitates the processing of situation-relevant information in the external world; by shortening diastole rather than systole (Herzog et al., 2002), this results in proportionally longer periods during which nonsalient stimuli are inhibited. Future studies could explore the functional role of perceptual periodicity, for example, by manipulating the salience of the near-threshold signals through different task requirements or an association with threatening stimuli (e.g., declaring or animating near-threshold somatosensory stimuli as bites from malaria-infected mosquitoes).

Further, accounting for the bidirectional information flow between the heart and the brain (Faes et al., 2017; Lin et al., 2016), we investigated the influence of the (prestimulus) heart rate on perception and, in turn, the influence of perception on (poststimulus) heart rate changes. Even though it was early hypothesized that cardiac deceleration enhances perceptual sensitivity (Graham & Clifton, 1966; Lacey, 1967; Lacey et al., 1963; Sandman, 1986; but see also Elliott, 1972), results are inconsistent in the auditory (Edwards & Alsip, 1969; Saxon & Dahle, 1971) or visual (Cobos et al., 2018; McCanne & Sandman, 1974; Park et al., 2014; Sandman et al., 1977) and outright lacking in the somatosensory modality. Our findings match reports in the visual domain (Cobos et al., 2018; Park et al., 2014) with respect to (a) the lack of evidence for the influence of the prestimulus heart rate on detection, and (b) a more pronounced cardiac deceleration after

detecting (relative to not detecting) near-threshold stimuli. In addition, we found that also the interbeat interval length during the somatosensory stimulation differed between hits and misses and that the extent of cardiac deceleration coincident with the stimulation was higher for detected compared to nondetected stimuli. Moreover, for nondetected stimuli, we observed a delayed cardiac acceleration, which might be a side effect of less pronounced deceleration after misses but has been also reported to occur after an incorrect visual stimuli discrimination (Lukowska, Sznajder, & Wierchoń, 2018) and, more broadly, is thought to reflect the processing of erroneous responses (Crone et al., 2003; Danev & de Winter, 1971; Fiehler, Ullsperger, Grigutsch, & von Cramon, 2004; Hajcak, McDonald, & Simons, 2003).

This lengthening of the IBI reflects the rapid autonomic (i.e., parasympathetic) response to the consciously perceived stimulus (Barry, 2006; Knippenberg, Barry, Kuniecki, & van Luijckelaar, 2012). Due to its speed, it is likely to also affect the duration of the IBI, during which the stimulus is presented (Jennings & van der Molen, 1993; Jennings, van der Molen, Somsen, & Brock, 1991; Lacey & Lacey, 1977; Velden, Barry, & Wölk, 1987; Zimmerman, Velden, & Wölk, 1991; but see also Barry, 1993). It could also be that both cardiac deceleration and enhanced detection are the result of the central processes responsible for attentional preparation, which involve the activity of inhibitory brain circuits (Aron et al., 2007). Particularly subthalamic nuclei have been proposed to regulate the extent of (preparatory) cardiac deceleration (Jennings, van der Molen, & Tanase, 2009), which—as a marker of increased vigilance (Barry, 1988, 1996)—has also been shown to predict accuracy in tasks requiring skilled motor performance (Fahimi & Vaezmousavi, 2011; Tremayne & Barry, 2001). Even though our design minimized the influence of preparation attempts by randomizing stimulus onsets, it cannot be ruled out that the concomitant increases in cardiac deceleration and conscious detection were both caused by coincident peaks of attentional engagement (Fiebelkorn & Kastner, 2018).

The present study has several limitations: First, as baroreceptor or brain activity were not directly measured, we can only speculate about the baroreceptor influences on (central) sensory processing. Peripheral processes like pulse wave-related sensations may equally contribute to changes in perceptual sensitivity. Second, the lack of significant differences in cardiac effects on somatosensory perception between the groups with high and low interoceptive accuracy might be due to the limited sample sizes or the insufficient validity of the heartbeat counting task itself (Brener & Ring, 2016). Third, to apply signal detection theory measures (Green & Swets, 1966), future studies should allow to temporally locate false alarms within the cardiac cycle. In the current design, we used a noncued stimulus onset within a 1,800-ms time window. This precluded determination of the position of false alarms

within the cardiac phases. Visual or acoustic cues for stimulus onsets would suffice for this purpose but may themselves introduce crossmodal interactions (Dionne, Meehan, Legon, & Staines, 2010), for which the influence of the cardiac cycle remains unknown. Future research could also consider including a graded measure of stimulus awareness (Ramsøy & Overgaard, 2004; Sandberg, Timmermans, Overgaard, & Cleeremans, 2010) to parametrically assess the effects of (un)conscious sensory processing on cardiac activity.

In sum, we find that conscious perception of somatosensory stimuli varies across the cardiac cycle and is associated with increased cardiac deceleration. This highlights the importance of activity in the autonomic nervous system for perceptual awareness. Our findings emphasize the irreducible relevance of bodily states for sensory processing and suggest a more holistic picture of an organism's cognition, for which contributions from the brain and from the rest of the body cannot be clearly separated.

## ACKNOWLEDGMENTS

We thank Sylvia Stasch for her assistance in data acquisition as well as Sven Ohl, Till Nierhaus, Birol Taskin, Fivos Iliopoulos, and Stella Kunzendorf for their methodological advice and useful discussions. The authors declare no conflict of interest.

## ORCID

Paweł Motyka  <https://orcid.org/0000-0001-5575-5601>

Michael Gaebler  <https://orcid.org/0000-0002-4442-5778>

## REFERENCES

- Aboud, F. M., & Chapleau, M. W. (1988). Effects of pulse frequency on single-unit baroreceptor activity during sine-wave and natural pulses in dogs. *Journal of Physiology*, *401*, 295–308. <https://doi.org/10.1113/jphysiol.1988.sp017163>
- Agostinelli, C., & Lund, U. (2013). R package Circular: Circular statistics (version 0.4-7). Retrieved from <https://r-forge.r-project.org/projects/circular/>
- Allen, M., Poggiali, D., Whitaker, K., Marshall, T. R., & Kievit, R. A. (2019). Raincloud plots: A multi-platform tool for robust data visualization. *Wellcome Open Research*, *4*, 63. <https://doi.org/10.12688/wellcomeopenres.15191.1>
- Aron, A. R., Durston, S., Eagle, D. M., Logan, G. D., Stinear, C. M., & Stuphorn, V. (2007). Converging evidence for a fronto-basal-ganglia network for inhibitory control of action and cognition. *Journal of Neuroscience*, *27*(44), 11860–11864. <https://doi.org/10.1523/JNEUROSCI.3644-07.2007>
- Barrett, C. J., & Bolter, C. P. (2006). The influence of heart rate on baroreceptor fibre activity in the carotid sinus and aortic depressor nerves of the rabbit. *Experimental Physiology*, *91*(5), 845–852. <https://doi.org/10.1113/expphysiol.2006.033902>

- Barrett, L. F., & Simmons, W. K. (2015). Interoceptive predictions in the brain. *Nature Reviews. Neuroscience*, *16*(7), 419–429. <https://doi.org/10.1038/nrn3950>
- Barry, R. J. (1988). Significance and components of the orienting response: Effects of signal value versus vigilance. *International Journal of Psychophysiology*, *6*(4), 343–346. [https://doi.org/10.1016/0167-8760\(88\)90023-2](https://doi.org/10.1016/0167-8760(88)90023-2)
- Barry, R. J. (1993). Graphical and statistical techniques for cardiac cycle time (phase) dependent changes in interbeat interval: Problems with the Jennings et al. (1991) proposals. *Biological Psychology*, *35*(1), 59–65. [https://doi.org/10.1016/0301-0511\(93\)90092-M](https://doi.org/10.1016/0301-0511(93)90092-M)
- Barry, R. J. (1996). Preliminary process theory: Towards an integrated account of the psychophysiology of cognitive processes. *Acta Neurobiologiae Experimentalis*, *56*(1), 469–484.
- Barry, R. J. (2006). Promise versus reality in relation to the unitary orienting reflex: A case study examining the role of theory in psychophysiology. *International Journal of Psychophysiology*, *62*(3), 353–366. <https://doi.org/10.1016/j.ijpsycho.2006.01.004>
- Birren, J. E., Cardon, P. V., & Phillips, S. L. (1963). Reaction time as a function of the cardiac cycle in young adults. *Science*, *140*(3563), 195–196. <https://doi.org/10.1126/science.140.3563.195-a>
- Börger, N., & van der Meere, J. (2000). Motor control and state regulation in children with ADHD: A cardiac response study. *Biological Psychology*, *51*(2–3), 247–267. [https://doi.org/10.1016/S0301-0511\(99\)00040-X](https://doi.org/10.1016/S0301-0511(99)00040-X)
- Boudoulas, H., Geleris, P., Lewis, R. P., & Rittgers, S. E. (1981). Linear relationship between electrical systole, mechanical systole, and heart rate. *Chest*, *80*(5), 613–617. <https://doi.org/10.1378/chest.80.5.613>
- Bradley, M. M., Cuthbert, B. N., & Lang, P. J. (1990). Startle reflex modification: Emotion or attention? *Psychophysiology*, *27*(5), 513–522. <https://doi.org/10.1111/j.1469-8986.1990.tb01966.x>
- Brainard, D. H. (1997). The psychophysics toolbox. *Spatial Vision*, *10*(4), 433–436. <https://doi.org/10.1163/156856897X00357>
- Brener, J., & Ring, C. (2016). Towards a psychophysics of interoceptive processes: The measurement of heartbeat detection. *Philosophical Transactions of the Royal Society of London. Series B, Biological Sciences*, *371*(1708). <https://doi.org/10.1098/rstb.2016.0015>
- Busch, N. A., Dubois, J., & VanRullen, R. (2009). The phase of ongoing EEG oscillations predicts visual perception. *Journal of Neuroscience*, *29*(24), 7869–7876. <https://doi.org/10.1523/JNEUROSCI.0113-09.2009>
- Christofaro, D. G. D., Casonatto, J., Vanderlei, L. C. M., Cucato, G. G., & Dias, R. M. R. (2017). Relationship between resting heart rate, blood pressure and pulse pressure in adolescents. *Arquivos Brasileiros de Cardiologia*, *108*(5), 405–410. <https://doi.org/10.5935/abc.20170050>
- Coblentz, B., Harvey, R. M., Ferrer, M. I., Courmand, A., & Richards, D. W. (1949). The relationship between electrical and mechanical events in the cardiac cycle of man. *Heart*, *11*(1), 1–22. <https://doi.org/10.1136/hrt.11.1.1>
- Cobos, M. I., Guerra, P. M., Vila, J., & Chica, A. B. (2018). Heart-rate modulations reveal attention and consciousness interactions. *Psychophysiology*, *56*(3), e13295. <https://doi.org/10.1111/psyp.13295>
- Cohen, R., Lieb, H., & Rist, F. (1980). Loudness judgments, evoked potentials, and reaction time to acoustic stimuli early and late in the cardiac cycle in chronic schizophrenics. *Psychiatry Research*, *3*(1), 23–29. [https://doi.org/10.1016/0165-1781\(80\)90044-X](https://doi.org/10.1016/0165-1781(80)90044-X)
- Craig, A. D. B. (2009). How do you feel—Now? The anterior insula and human awareness. *Nature Reviews Neuroscience*, *10*(1), 59–70. <https://doi.org/10.1038/nrn2555>
- Critchley, H. D., & Garfinkel, S. N. (2015). Interactions between visceral afferent signaling and stimulus processing. *Frontiers in Neuroscience*, *9*. <https://doi.org/10.3389/fnins.2015.00286>
- Critchley, H. D., & Garfinkel, S. N. (2017). Interoception and emotion. *Current Opinion in Psychology*, *17*, 7–14. <https://doi.org/10.1016/j.copsyc.2017.04.020>
- Critchley, H. D., & Garfinkel, S. N. (2018). The influence of physiological signals on cognition. *Current Opinion in Behavioral Sciences*, *19*, 13–18. <https://doi.org/10.1016/j.cobeha.2017.08.014>
- Crone, E. A., Van der Veen, F. M., Van der Molen, M. W., Somsen, R. J., Van Beek, B., & Jennings, J. (2003). Cardiac concomitants of feedback processing. *Biological Psychology*, *64*(1–2), 143–156. [https://doi.org/10.1016/S0301-0511\(03\)00106-6](https://doi.org/10.1016/S0301-0511(03)00106-6)
- Dampney, R. A. L. (2016). Central neural control of the cardiovascular system: Current perspectives. *Advances in Physiology Education*, *40*(3), 283–296. <https://doi.org/10.1152/advan.00027.2016>
- Danev, S. G., & de Winter, C. R. (1971). Heart rate deceleration after erroneous responses. *Psychologische Forschung*, *35*(1), 27–34. <https://doi.org/10.1007/BF00424472>
- Davis, R. C., & Buchwald, A. M. (1957). An exploration of somatic response patterns: Stimulus and sex differences. *Journal of Comparative and Physiological Psychology*, *50*(1), 44–52. <https://doi.org/10.1037/h0046428>
- Davis, R. C., Buchwald, A. M., & Frankmann, R. W. (1955). Autonomic and muscular responses, and their relation to simple stimuli. *Psychological Monographs: General and Applied*, *69*(20), 1–71. <https://doi.org/10.1037/h0093734>
- Delfini, L. F., & Campos, J. J. (1972). Signal detection and the “cardiac arousal cycle”. *Psychophysiology*, *9*(5), 484–491. <https://doi.org/10.1111/j.1469-8986.1972.tb01801.x>
- Di Lernia, D., Serino, S., Pezzulo, G., Pedroli, E., Cipresso, P., & Riva, G. (2018). Feel the time. Time perception as a function of interoceptive processing. *Frontiers in Human Neuroscience*, *12*, 74. <https://doi.org/10.3389/fnhum.2018.00074>
- Dionne, J. K., Meehan, S. K., Legon, W., & Staines, W. R. (2010). Crossmodal influences in somatosensory cortex: Interaction of vision and touch. *Human Brain Mapping*, *31*(1), 14–25. <https://doi.org/10.1002/hbm.20841>
- Dugué, L., Marque, P., & VanRullen, R. (2011). The phase of ongoing oscillations mediates the causal relation between brain excitation and visual perception. *Journal of Neuroscience*, *31*(33), 11889–11893. <https://doi.org/10.1523/JNEUROSCI.1161-11.2011>
- Dunn, B. D., Galton, H. C., Morgan, R., Evans, D., Oliver, C., Meyer, M., ... Dalgleish, T. (2010). Listening to your heart: How interoception shapes emotion experience and intuitive decision making. *Psychological Science*, *21*(12), 1835–1844. <https://doi.org/10.1177/0956797610389191>
- Dushek, S., Werner, N. S., & Reyes Del Paso, G. A. (2013). The behavioral impact of baroreflex function: A review. *Psychophysiology*, *50*(12), 1183–1193. <https://doi.org/10.1111/psyp.12136>
- Edwards, D. C., & Alsip, J. E. (1969). Stimulus detection during periods of high and low heart rate. *Psychophysiology*, *5*(4), 431–434. <https://doi.org/10.1111/j.1469-8986.1969.tb02843.x>
- Edwards, L., Ring, C., McIntyre, D., Carroll, D., & Martin, U. (2007). Psychomotor speed in hypertension: Effects of reaction time components, stimulus modality, and phase of the cardiac cycle. *Psychophysiology*, *44*(3), 459–468. <https://doi.org/10.1111/j.1469-8986.2007.00521.x>
- Edwards, L., Ring, C., McIntyre, D., Winer, J. B., & Martin, U. (2009). Sensory detection thresholds are modulated across the cardiac cycle:

- Evidence that cutaneous sensibility is greatest for systolic stimulation. *Psychophysiology*, 46(2), 252–256. <https://doi.org/10.1111/j.1469-8986.2008.00769.x>
- Elliott, R. (1972). The significance of heart rate for behavior: A critique of Lacey's hypothesis. *Journal of Personality and Social Psychology*, 22(3), 398–409. <https://doi.org/10.1037/h0032832>
- Elliott, R., & Graf, V. (1972). Visual sensitivity as a function of phase of cardiac cycle. *Psychophysiology*, 9(3), 357–361. <https://doi.org/10.1111/j.1469-8986.1972.tb03219.x>
- Faes, L., Greco, A., Lanata, A., Barbieri, R., Scilingo, E. P., & Valenza, G. (2017). Causal brain-heart information transfer during visual emotional elicitation in healthy subjects: Preliminary evaluations and future perspectives. *Proceedings of the Annual International Conference of the IEEE Engineering in Medicine and Biology Society*, 1559–1562. <https://doi.org/10.1109/EMBC.2017.8037134>
- Fahimi, F., & Vaezmousavi, M. (2011). Physiological patterning of short badminton serve: A psychophysiological perspective to vigilance and arousal. *World Applied Sciences Journal*, 12, 347–353.
- Fiebelkorn, I. C., & Kastner, S. (2018). A rhythmic theory of attention. *Trends in Cognitive Sciences*, 23(2), 87–101. <https://doi.org/10.1016/j.tics.2018.11.009>
- Fiehler, K., Ullsperger, M., Grigutsch, M., & von Cramon, D. Y. V. (2004). Cardiac responses to error processing and response conflict. In M. Ullsperger & M. Falkenstein (Eds.), *Errors, conflicts, and the brain. Current opinions on performance monitoring* (pp. 135–140). Leipzig, Germany: Max Planck Institute for Human Cognitive and Brain Sciences.
- Fridericia, L. S. (1920). Die Systolendauer im Elektrokardiogramm bei normalen Menschen und bei Herzkranken [The duration of systole in the electrocardiogram of normal subjects and of patients with heart disease]. *Acta Medica Scandinavica*, 54(1), 17–50. <https://doi.org/10.1111/j.0954-6820.1921.tb15167.x>
- Fries, P. (2015). Rhythms for cognition: Communication through coherence. *Neuron*, 88(1), 220–235. <https://doi.org/10.1016/j.neuron.2015.09.034>
- Fukushima, H., Terasawa, Y., & Umeda, S. (2011). Association between interoception and empathy: Evidence from heartbeat-evoked brain potential. *International Journal of Psychophysiology*, 79(2), 259–265. <https://doi.org/10.1016/j.ijpsycho.2010.10.015>
- Garfinkel, S. N., & Critchley, H. D. (2016). Threat and the Body: How the heart supports fear processing. *Trends in Cognitive Sciences*, 20(1), 34–46. <https://doi.org/10.1016/j.tics.2015.10.005>
- Garfinkel, S. N., Minati, L., Gray, M. A., Seth, A. K., Dolan, R. J., & Critchley, H. D. (2014). Fear from the heart: Sensitivity to fear stimuli depends on individual heartbeats. *Journal of Neuroscience*, 34(19), 6573–6582. <https://doi.org/10.1523/JNEUROSCI.3507-13.2014>
- Garfinkel, S. N., Seth, A. K., Barrett, A. B., Suzuki, K., & Critchley, H. D. (2015). Knowing your own heart: Distinguishing interoceptive accuracy from interoceptive awareness. *Biological Psychology*, 104, 65–74. <https://doi.org/10.1016/j.biopsycho.2014.11.004>
- Gill, H., & Hoffmann, A. K. (2010). The timing of onset of mechanical systole and diastole in reference to the QRS-T complex: A study to determine performance criteria for a non-invasive diastolic timed vibration massage system in treatment of potentially unstable cardiac disorders. *Cardiovascular Engineering*, 10(4), 235–245. <https://doi.org/10.1007/s10558-010-9108-x>
- Graham, F. K., & Clifton, R. K. (1966). Heart-rate change as a component of the orienting response. *Psychological Bulletin*, 65(5), 305–320. <https://doi.org/10.1037/h0023258>
- Gray, M. L., & Crowell, D. H. (1968). Heart rate changes to sudden peripheral stimuli in the human during early infancy. *Journal of Pediatrics*, 72(6), 807–814. [https://doi.org/10.1016/S0022-3476\(68\)80433-0](https://doi.org/10.1016/S0022-3476(68)80433-0)
- Green, D. M., & Swets, J. A. (1966). *Signal detection theory and psychophysics*. Oxford, England: John Wiley.
- Greenwald, M. K., Cook, E. W., & Lang, P. J. (1989). Affective judgment and psychophysiological response: Dimensional covariation in the evaluation of pictorial stimuli. *Journal of Psychophysiology*, 3(1), 51–64.
- Grynberg, D., & Pollatos, O. (2015). Perceiving one's body shapes empathy. *Physiology & Behavior*, 140, 54–60. <https://doi.org/10.1016/j.physbeh.2014.12.026>
- Gu, X., & FitzGerald, T. H. B. (2014). Interoceptive inference: Homeostasis and decision-making. *Trends in Cognitive Sciences*, 18(6), 269–270. <https://doi.org/10.1016/j.tics.2014.02.001>
- Hajcak, G., McDonald, N., & Simons, R. F. (2003). To err is autonomic: Error-related brain potentials, ANS activity, and post-error compensatory behavior. *Psychophysiology*, 40(6), 895–903. <https://doi.org/10.1111/1469-8986.00107>
- Hare, R. D. (1973). Orienting and defensive responses to visual stimuli. *Psychophysiology*, 10(5), 453–464. <https://doi.org/10.1111/j.1469-8986.1973.tb00532.x>
- Herzog, C., Abolmaali, N., Balzer, J. O., Baunach, S., Ackermann, H., Doğan, S., ... Vogl, T. J. (2002). Heart-rate-adapted image reconstruction in multidetector-row cardiac CT: Influence of physiological and technical prerequisite on image quality. *European Radiology*, 12, 2670–2678. <https://doi.org/10.1007/s00330-002-1553-5>
- Jennings, J. R., & van der Molen, M. W. (1993). Phase sensitivity: A dead end or a challenge? *Biological Psychology*, 35, 67–71. [https://doi.org/10.1016/0301-0511\(93\)90093-n](https://doi.org/10.1016/0301-0511(93)90093-n)
- Jennings, J. R., van der Molen, M. W., Somsen, R. J., & Brock, K. (1991). Weak sensory stimuli induce a phase sensitive bradycardia. *Psychophysiology*, 28(1), 1–10. <https://doi.org/10.1111/j.1469-8986.1991.tb03380.x>
- Jennings, J. R., van der Molen, M. W., & Tanase, C. (2009). Preparing hearts and minds: Cardiac slowing and a cortical inhibitory network. *Psychophysiology*, 46(6), 1170–1178. <https://doi.org/10.1111/j.1469-8986.2009.00866.x>
- Kingdom, F. A. A., & Prins, N. (2010). *Psychophysics: A practical introduction*. San Diego, CA: Elsevier Academic Press.
- Kleckner, I. R., Zhang, J., Touroutoglou, A., Chanes, L., Xia, C., Simmons, W. K., ... Feldman Barrett, L. (2017). Evidence for a large-scale brain system supporting allostasis and interoception in humans. *Nature Human Behaviour*, 1, 0069. <https://doi.org/10.1038/s41562-017-0069>
- Kleiner, M., Brainard, D., Pelli, D., Ingling, A., Murray, R., & Broussard, C. (2007). What's new in Psychtoolbox-3. *Perception*, 36(14), 1–16. <https://doi.org/10.1068/v070821>
- Klimesch, W. (2013). An algorithm for the EEG frequency architecture of consciousness and brain body coupling. *Frontiers in Human Neuroscience*, 7. <https://doi.org/10.3389/fnhum.2013.00766>
- Klimesch, W. (2018). The frequency architecture of brain and body oscillations: An analysis. *European Journal of Neuroscience*, 48(7), 2431–2453. <https://doi.org/10.1111/ejn.14192>
- Knippenberg, J. M. J., Barry, R. J., Kuniecki, M. J., & van Luijtelaar, G. (2012). Fast, transient cardiac accelerations and decelerations during fear conditioning in rats. *Physiology & Behavior*, 105(3), 607–612. <https://doi.org/10.1016/j.physbeh.2011.09.018>
- Lacey, B. C., & Lacey, J. I. (1977). Change in heart period: A function of sensorimotor event timing within the cardiac cycle. *Physiological Psychology*, 5(3), 383–393. <https://doi.org/10.3758/BF03335349>

- Lacey, J. (1967). Somatic response patterning and stress : Some revisions of activation theory. In M. H. Appley, & R. Trumbull (Eds.), *Psychological stress: Issues in research* (pp. 14–42). New York, NY: Appleton-Century-Crofts.
- Lacey, J. I., Kagan, J., Lacey, B. C., & Moss, H. A. (1963). The visceral level: Situational determinants and behavioral correlates of autonomic response patterns. In P. H. Knapp (Ed.), *Expressions of the emotions in man* (pp. 161–196). New York, NY: International Universities Press.
- Lacey, J. I., & Lacey, B. C. (1970). Some autonomic-central nervous system interrelationships. In P. Black (Ed.), *Physiological correlates of emotion* (pp. 205–227). New York, NY: Academic Press.
- Lacey, J. I., & Lacey, B. C. (1974). On heart rate responses and behavior: A reply to Elliott. *Journal of Personality and Social Psychology*, 30(1), 1–18. <https://doi.org/10.1037/h0036559>
- Landgren, W. (1952). On the excitation mechanism of the carotid baroreceptors. *Acta Physiologica Scandinavica*, 26(1), 1–34. <https://doi.org/10.1111/j.1748-1716.1952.tb00889.x>
- Lewis, R. L., Rittogers, S. E., Froester, W. F., & Boudoulas, H. (1977). A critical review of the systolic time intervals. *Circulation*, 56(2), 146–158. <https://doi.org/10.1161/01.CIR.56.2.146>
- Libby, W. L., Lacey, B. C., & Lacey, J. I. (1973). Pupillary and cardiac activity during visual attention. *Psychophysiology*, 10(3), 270–294. <https://doi.org/10.1111/j.1469-8986.1973.tb00526.x>
- Lin, A., Liu, K., Bartsch, R., & Ivanov, P. (2016). Delay-correlation landscape reveals characteristic time delays of brain rhythms and heart interactions. *Philosophical Transactions of the Royal Society A: Mathematical, Physical and Engineering Sciences*, 374(2067), <https://doi.org/10.1098/rsta.2015.0182>
- Lisman, J. (2005). The theta/gamma discrete phase code occurring during the hippocampal phase precession may be a more general brain coding scheme. *Hippocampus*, 15(7), 913–922. <https://doi.org/10.1002/hipo.20121>
- Lukowska, M., Sznajder, M., & Wierchoń, M. (2018). Error-related cardiac response as information for visibility judgements. *Scientific Reports*, 8(1), 1131. <https://doi.org/10.1038/s41598-018-19144-0>
- Makovac, E., Garfinkel, S. N., Bassi, A., Basile, B., Macaluso, E., Cercignani, M., ... Critchley, H. (2015). Effect of parasympathetic stimulation on brain activity during appraisal of fearful expressions. *Neuropsychopharmacology*, 40(7), 1649–1658. <https://doi.org/10.1038/npp.2015.10>
- Mancia, G., Ferrari, A., Gregorini, L., Parati, G., Pomidossi, G., Bertinieri, G., ... Zanchetti, A. (1983). Blood pressure and heart rate variabilities in normotensive and hypertensive human beings. *Circulation Research*, 53(1), 96–104. <https://doi.org/10.1161/01.RES.53.1.96>
- Mancia, G., & Mark, A. L. (2011). Arterial baroreflexes in humans. In R. Terjung (Ed.), *Comprehensive physiology*. Hoboken, NJ: John Wiley & Sons, Inc. <https://doi.org/10.1002/cphy.cp020320>
- McCanne, T. R., & Sandman, C. A. (1974). Instrumental heart rate responses and visual perception: A preliminary study. *Psychophysiology*, 11(3), 283–287. <https://doi.org/10.1111/j.1469-8986.1974.tb00545.x>
- McIntyre, D., Ring, C., Edwards, L., & Carroll, D. (2008). Simple reaction time as a function of the phase of the cardiac cycle in young adults at risk for hypertension. *Psychophysiology*, 45(2), 333–336. <https://doi.org/10.1111/j.1469-8986.2007.00619.x>
- Meissner, K., & Wittmann, M. (2011). Body signals, cardiac awareness, and the perception of time. *Biological Psychology*, 86(3), 289–297. <https://doi.org/10.1016/j.biopsycho.2011.01.001>
- Morey, R. D. (2008). Confidence Intervals from Normalized Data: A correction to Cousineau (2005). *Tutorials in Quantitative Methods for Psychology*, 4(2), 61–64. <https://doi.org/10.20982/tqmp.04.2.p061>
- Otten, L. J., Gaillard, A. W. K., & Wientjes, C. J. E. (1995). The relation between event-related brain potential, heart rate, and blood pressure responses in an S1–S2 paradigm. *Biological Psychology*, 39(2), 81–102. [https://doi.org/10.1016/0301-0511\(94\)00969-5](https://doi.org/10.1016/0301-0511(94)00969-5)
- Park, H.-D., Correia, S., Ducorps, A., & Tallon-Baudry, C. (2014). Spontaneous fluctuations in neural responses to heartbeats predict visual detection. *Nature Neuroscience*, 17(4), 612–618. <https://doi.org/10.1038/nn.3671>
- Park, H.-D., & Tallon-Baudry, C. (2014). The neural subjective frame: From bodily signals to perceptual consciousness. *Philosophical Transactions of the Royal Society of London. Series B, Biological Sciences*, 369(1641), <https://doi.org/10.1098/rstb.2013.0208>
- Pelli, D. G. (1997). The VideoToolbox software for visual psychophysics: Transforming numbers into movies. *Spatial Vision*, 10(4), 437–442. <https://doi.org/10.1163/156856897X00366>
- Pewsey, A., Neuhäuser, M., & Ruxton, G. D. (2013). *Circular statistics in R*. New York, NY: Oxford University Press.
- Pramme, L., Larra, M. F., Schächinger, H., & Frings, C. (2016). Cardiac cycle time effects on selection efficiency in vision. *Psychophysiology*, 53(11), 1702–1711. <https://doi.org/10.1111/psyp.12728>
- Ramsøy, T. Z., & Overgaard, M. (2004). Introspection and subliminal perception. *Phenomenology and the Cognitive Sciences*, 3(1), 1–23. <https://doi.org/10.1023/B:PHEN.0000041900.30172.e8>
- Rau, H., & Elbert, T. (2001). Psychophysiology of arterial baroreceptors and the etiology of hypertension. *Biological Psychology*, 57(1–3), 179–201. [https://doi.org/10.1016/S0301-0511\(01\)00094-1](https://doi.org/10.1016/S0301-0511(01)00094-1)
- Rau, H., Pauli, P., Brody, S., Elbert, T., & Birbaumer, N. (1993). Baroreceptor stimulation alters cortical activity. *Psychophysiology*, 30(3), 322–325. <https://doi.org/10.1111/j.1469-8986.1993.tb03359.x>
- R Core Team. (2016). *R: A language and environment for statistical computing*. Vienna: R Foundation for Statistical Computing. Retrieved from <https://www.r-project.org>
- Réquin, J., & Brouchon, M. (1964). Mise en évidence chez l'homme d'une fluctuation des seuils perceptifs visuels dans la période cardiaque [Demonstration in man of a fluctuation of visual perceptive thresholds in the cardiac period]. *Comptes Rendus Des Séances de La Société de Biologie et de Ses Filiales*, 158, 1891–1894.
- RStudio Team. (2016). *RStudio: Integrated development environment for R*. Boston, MA: RStudio, Inc. Retrieved from <https://www.rstudio.com>
- Sandberg, K., Timmermans, B., Overgaard, M., & Cleeremans, A. (2010). Measuring consciousness: Is one measure better than the other? *Consciousness and Cognition*, 19(4), 1069–1078. <https://doi.org/10.1016/j.concog.2009.12.013>
- Sandman, C. A. (1986). Cardiac afferent influences on consciousness. In R. J. Davidson, G. E. Schwartz, & D. Shapiro (Eds.), *Consciousness and self-regulation: Advances in research and theory* (Vol. 4, pp. 55–85). Boston, MA: Springer, US. [https://doi.org/10.1007/978-1-4757-0629-1\\_3](https://doi.org/10.1007/978-1-4757-0629-1_3)
- Sandman, C. A., McCanne, T. R., Kaiser, D. N., & Diamond, B. (1977). Heart rate and cardiac phase influences on visual perception. *Journal of Comparative and Physiological Psychology*, 91(1), 189–202. <https://doi.org/10.1037/h0077302>
- Saxon, S. A. (1970). Detection of near threshold signals during four phases of cardiac cycle. *Alabama Journal of Medical Sciences*, 7(4), 427–430.



- Saxon, S. A., & Dahle, A. J. (1971). Auditory threshold variations during periods of induced high and low heart rates. *Psychophysiology*, *8*(1), 23–29. <https://doi.org/10.1111/j.1469-8986.1971.tb00433.x>
- Schandy, R. (1981). Heart beat perception and emotional experience. *Psychophysiology*, *18*, 483–488. <https://doi.org/10.1111/j.1469-8986.1981.tb02486>
- Schulz, A., Reichert, C. F., Richter, S., Lass-Hennemann, J., Blumenthal, T. D., & Schächinger, H. (2009). Cardiac modulation of startle: Effects on eye blink and higher cognitive processing. *Brain and Cognition*, *71*(3), 265–271. <https://doi.org/10.1016/j.bandc.2009.08.00>
- Seth, A. K. (2014). Response to Gu and FitzGerald: Interoceptive inference: From decision-making to organism integrity. *Trends in Cognitive Sciences*, *18*(6), 270–271. <https://doi.org/10.1016/j.tics.2014.03.006>
- Simons, R. F. (1988). Event-related slow brain potentials: A perspective from ANS psychophysiology. In P. K. Ackles, J. R. Jennings, & M. G. H. Coles (Eds.), *Advances in psychophysiology* (Vol. 3, pp. 223–267). Greenwich, England: JAI Press Inc.
- Suzuki, K., Garfinkel, S. N., Critchley, H. D., & Seth, A. K. (2013). Multisensory integration across exteroceptive and interoceptive domains modulates self-experience in the rubber-hand illusion. *Neuropsychologia*, *51*(13), 2909–2917. <https://doi.org/10.1016/j.neuropsychologia.2013.08.014>
- Tarvainen, M. P., Niskanen, J.-P., Lippinen, J. A., Ranta-aho, P. O., & Karjalainen, P. A. (2014). Kubios HR—Heart rate variability analysis software. *Computer Methods and Programs in Biomedicine*, *113*(1), 210–220. <https://doi.org/10.1016/j.cmpb.2013.07.024>
- Tremayne, P., & Barry, R. J. (2001). Elite pistol shooters: Physiological patterning of best vs. worst shots. *International Journal of Psychophysiology*, *41*(1), 19–29. [https://doi.org/10.1016/S0167-8760\(00\)00175-6](https://doi.org/10.1016/S0167-8760(00)00175-6)
- Uno, T., & Grings, W. W. (1965). Autonomic components of orienting behavior. *Psychophysiology*, *1*(4), 311–321. <https://doi.org/10.1111/j.1469-8986.1965.tb03263.x>
- Valenza, G., Toschi, N., & Barbieri, R. (2016). Uncovering brain–heart information through advanced signal and image processing. *Philosophical Transactions. Series A, Mathematical, Physical, and Engineering Sciences*, *374*(2067). <https://doi.org/10.1098/rsta.2016.0020>
- VanRullen, R. (2016). Perceptual cycles. *Trends in Cognitive Sciences*, *20*(10), 723–735. <https://doi.org/10.1016/j.tics.2016.07.006>
- VanRullen, R., Guyonneau, R., & Thorpe, S. J. (2005). Spike times make sense. *Trends in Neurosciences*, *28*(1), 1–4. <https://doi.org/10.1016/j.tins.2004.10.010>
- Vázquez-Seisdedos, C. R., Neto, J. E., Marañón Reyes, E. J., Klautau, A., & Limão de Oliveira, R. C. (2011). New approach for T-wave end detection on electrocardiogram: Performance in noisy conditions. *BioMedical Engineering OnLine*, *10*(1), 77. <https://doi.org/10.1186/1475-925X-10-77>
- Velden, M., Barry, R. J., & Wölk, C. (1987). Time-dependent bradycardia: A new effect? *International Journal of Psychophysiology*, *4*(4), 299–306. [https://doi.org/10.1016/0167-8760\(87\)90042-0](https://doi.org/10.1016/0167-8760(87)90042-0)
- Velden, M., & Juris, M. (1975). Perceptual performance as a function of intra-cycle cardiac activity. *Psychophysiology*, *12*(6), 685–692. <https://doi.org/10.1111/j.1469-8986.1975.tb00075.x>
- Walker, B. B., & Sandman, C. A. (1977). Physiological response patterns in ulcer patients: Phasic and tonic components of the electrogastrogram. *Psychophysiology*, *14*(4), 393–400. <https://doi.org/10.1111/j.1469-8986.1977.tb02971.x>
- Wallace, A. G., Mitchell, J. H., Skinner, S. N., & Sarnoff, S. J. (1963). Duration of the phases of left ventricular systole. *Circulation Research*, *12*(6), 611–619. <https://doi.org/10.1161/01.RES.12.6.611>
- Wiens, S. (2005). Interoception in emotional experience. *Current Opinion in Neurology*, *18*(4), 442–447. <https://doi.org/10.1097/01.wco.0000168079.92106.99>
- Wilkinson, M., McIntyre, D., & Edwards, L. (2013). Electrocutaneous pain thresholds are higher during systole than diastole. *Biological Psychology*, *94*(1), 71–73. <https://doi.org/10.1016/j.biopsycho.2013.05.002>
- Wilson, R. S. (1964). Autonomic changes produced by noxious and innocuous stimulation. *Journal of Comparative and Physiological Psychology*, *58*(2), 290–295. <https://doi.org/10.1037/h0045264>
- Wölk, C., Velden, M., Zimmermann, U., & Krug, S. (1989). The interrelation between phasic blood pressure and heart rate changes in the context of the “baroreceptor hypothesis”. *Journal of Psychophysiology*, *3*(4), 397–402.
- Zimmerman, U., Velden, M., & Wölk, C. (1991). Empirical evidence against the “cycle time dependency” assumption. *International Journal of Psychophysiology*, *11*(2), 125–129. [https://doi.org/10.1016/0167-8760\(91\)90004-H](https://doi.org/10.1016/0167-8760(91)90004-H)

## SUPPORTING INFORMATION

Additional supporting information may be found online in the Supporting Information section at the end of the article.

### Appendix S1

### Figure S1

### Figure S2

### Figure S3

**How to cite this article:** Motyka P, Grund M, Forschack N, Al E, Villringer A, Gaebler M. Interactions between cardiac activity and conscious somatosensory perception. *Psychophysiology*. 2019;56:e13424. <https://doi.org/10.1111/psyp.13424>

## **Supplementary Material**

### **Interactions between cardiac activity and conscious somatosensory perception**

Paweł Motyka<sup>1,2</sup>, Martin Grund<sup>2</sup>, Norman Fuschack<sup>2,3</sup>, Esra Al<sup>2,4</sup>, Arno Villringer<sup>2,4</sup>, and Michael Gaebler<sup>2,4,5</sup>

<sup>1</sup>Faculty of Psychology, University of Warsaw, Warsaw, Poland

<sup>2</sup>Department of Neurology, Max Planck Institute for Human Cognitive and Brain Sciences, Leipzig, Germany

<sup>3</sup>Experimental Psychology and Methods, Faculty of Life Sciences, University of Leipzig, Leipzig, Germany

<sup>4</sup>MindBrainBody Institute at the Berlin School of Mind and Brain, Humboldt-Universität zu Berlin, Berlin, Germany

<sup>5</sup>Leipzig Research Centre for Civilization Diseases (LIFE), University of Leipzig, Leipzig, Germany

Corresponding author: Paweł Motyka, University of Warsaw, Faculty of Psychology, Stawki 5/7, 00-183 Warsaw, Poland. E-mail: pawel.motyka@psych.uw.edu.pl

## 1. SUPPLEMENTARY METHOD

In an exploratory analysis, we tested whether the link between conscious somatosensory perception and cardiac activity is influenced by the capacity to consciously perceive one's heartbeat (i.e., interoceptive accuracy; Garfinkel et al., 2015). After the completion of three blocks of somatosensory perception (after the steel wire ring electrodes had been removed from the left index finger) and a break of approximately 3 minutes, interoceptive accuracy (Garfinkel et al., 2015) was measured using a Heartbeat Counting Task (Schandry, 1981): The participants were asked to count their heartbeats silently during acoustically signaled time intervals of the following lengths (presented in this order): 25, 45, 15, 55, and 35 s. Individual interoceptive accuracy (IA) scores were calculated comparing the objectively measured number of heartbeats and the subjectively reported number of heartbeats from the five intervals with the following formula:  $1/5 \sum (1 - (|recorded\ heartbeats - reported\ heartbeats|)/recorded\ heartbeats)$ . The score varies between 0 and 1, with 1 indicating absolute accuracy of heartbeat perception. One participant was excluded due to not properly reported heartbeats (all zeroes). Also, one participant was excluded from the circular analyses due to non-uniformly distributed stimulation onsets across the cardiac cycle (see section 2.5 in the main text of the paper). In total, the supplementary circular analysis (section 2.2) included data from 31 participants (15 females, mean age = 25.7,  $SD = 4.0$ , range: 19-36 years) whereas the supplementary binary analysis (section 2.3) included data from 32 participants (16 females, mean age = 25.8,  $SD = 4.0$ , range: 19-36 years).

## 2. SUPPLEMENTARY RESULTS

### 2.1 Summary statistics for interoceptive accuracy

The mean IA score of 32 participants was 0.72 ( $SD = 0.15$ , range = 0.38-0.96). For further analyses, participants were median-split ( $Me = 0.75$ ) into a high and a low IA group.

### 2.2. Distribution of hits and misses across the cardiac cycle for high and low interoceptive accuracy groups

A Watson's Two Sample test was used to assess whether the angular directions of hit and miss concentration across the cardiac cycle differed between the groups of high and low IA, (Pewsey et al., 2013, p. 144). No significant group differences were found both for hits ( $U^2 = .09$ ,  $p > .05$ ) or misses ( $U^2 = .07$ ,  $p > .05$ ). Hence, there is no evidence that both groups differ with respect to the position of increased perceptual awareness for near-threshold somatosensory stimuli within the cardiac cycle. Further, Rayleigh tests were used to test the uniformity of hits and misses distribution across the cardiac cycle separately for high and low IA groups. There was no evidence for the non-uniformity of hits distribution both for high IA ( $\bar{R} = .34$ ,  $p = .161$ ) and low IA group ( $\bar{R} = .38$ ,  $p = .114$ ; Fig. S1A). Similarly for misses, the tests did not yield significant results both for high IA ( $\bar{R} = .29$ ,  $p = .257$ ) and low IA group ( $\bar{R} = .42$ ,  $p = .72$ ; Fig. S1B). These results suggest that interoceptive accuracy does not modulate the effects of the cardiac cycle on conscious somatosensory perception. Yet, the small sample sizes in the IA groups limit the statistical power of the used tests. As a side remark, continuous IA were not significantly correlated with the levels of hit ( $r(29) = .04$ ,  $p = .801$ ) or miss concentration ( $r(29) = -.13$ ,  $p = .485$ ).

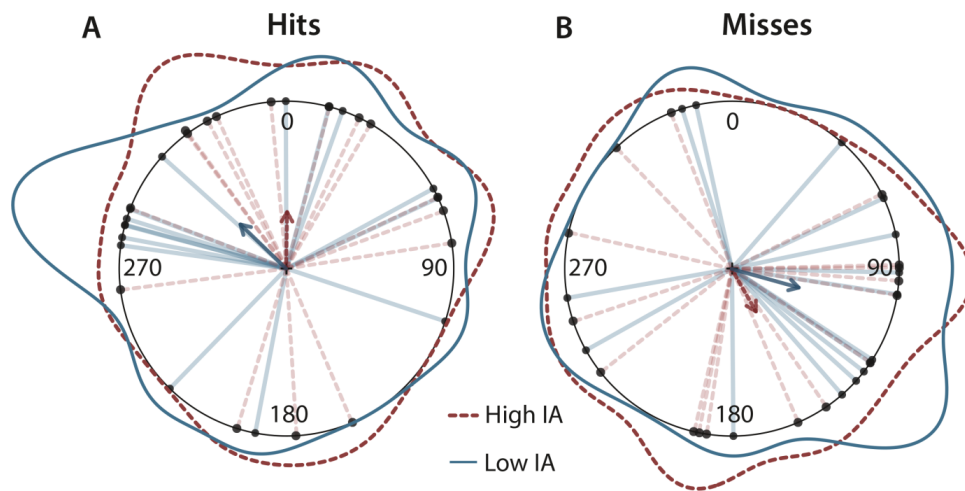


**Figure S1.** Distribution of (A) hits and (B) misses across the cardiac cycle (i.e., the interval between two R peaks; at 0/360°) separately for subjects with high (dashed red lines) or low (solid blue lines) interoceptive accuracy (IA). Each dot (and line) indicates one participant's mean phase angle. The annular line depicts the distribution of individual means. The darker arrows represent the directions of the group means for hits (high IA: 1°, low IA: 314°) and misses (high IA: 150°, low IA: 105°), with their length indicating the concentration of individual means across the cardiac cycle (hits: high IA - .34, low IA - .38; misses: high IA - .29, low IA - .42). Distributions of hits or misses did not differ significantly between the groups with high or low IA.

### 2.3. Differences in hit rates between systole and diastole for high and low interoceptive accuracy groups

A two-way mixed ANOVA of hit rates was conducted, with cardiac phase as a within-subject factor (systole and diastole) and interoceptive accuracy as a between-subject factor (high and low IA). In line with the results reported in the main text of the paper (section 3.3), we found a significant main effect of cardiac phase ( $F(1, 30) = 6.36, p = .017, \eta^2_G = .006$ ; Fig. S2) and neither the main effect of IA ( $F(1, 30) = 2.50, p = .960, \eta^2_G < .001$ ) nor the interaction between IA and

cardiac phase ( $F(1, 30) = 1.23, p = .728, \eta^2_G < .001$ ) were significant. These results are consistent with the outcomes of the circular analyses in not showing a significant influence of interoceptive accuracy on variations of conscious somatosensory perception across the cardiac cycle.

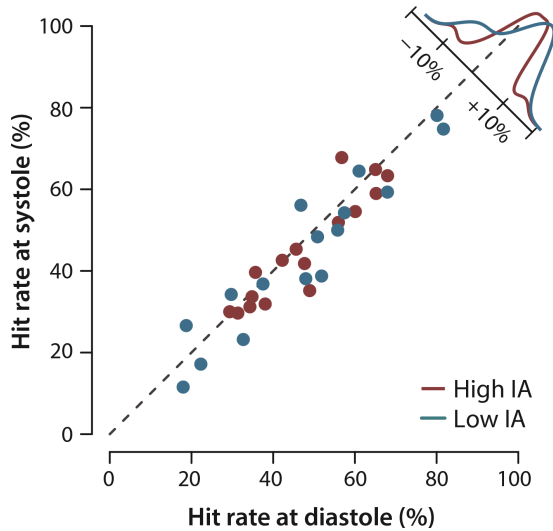


**Figure S2.** Hit rates in diastole and systole for subjects with high (red) or low (blue) interoceptive accuracy (IA). The coordinates of each dot represent a participant's mean hit rate at systole (x-axis) and diastole (y-axis). The dashed lines mark the identity line in hit rate between cardiac phases. The distribution in the upper right corner aggregates the frequencies for high and low IA. Hit rates were significantly higher in diastole than in systole but did not differ between the groups with high or low IA.

#### **2.4. Differences in hit rates between the three intervals of the cardiac cycle (R-50 to R+50 ms, R+250 to R+350 ms, and 550 to R+650 ms).**

In the study by Edwards et al. (2009), perceptual thresholds for somatosensory stimuli were assessed at the three fixed time points R+0 (unclear whether assigned to systole or diastole),

R+300 (systole), and R+600 ms (diastole). To facilitate the comparison with this study, we analyzed the hit rates in three (100-ms) intervals centered on the time points used in Edwards et al. (2009). To ensure that a comparable number of stimuli are aggregated in the three intervals and to exclude the possibility of double assignment (i.e., being assigned to both the R+600 ms and the R+0 ms interval in case of a short IBI and a stimulus onset towards the end of the cardiac cycle), trials with IBIs <700 ms were excluded from this analysis. Data from five participants with more than 30% of such trials and 328 trials from 19 other participants ( $M = 17.2$ ,  $SD = 23.1$ , range: 1-78 trials) were excluded. Hence, this analysis included data from 28 participants (14 females, mean age = 26.5,  $SD = 3.9$ , range: 19-36 years). The numbers of trials per interval did not differ significantly ( $\chi^2(2) = 0.005$ ,  $p = .997$ ; R-50 to R+50 ms:  $M = 32.8$ , range: 22-47; R+250 to R+350 ms:  $M = 32.8$ , range: 21-43; R+550 to R+650 ms:  $M = 32.3$ , range: 15-41 trials).

A repeated-measures analysis of variance (ANOVA) showed that hit rates differed significantly between the intervals ( $F(2, 54) = 5.03$ ,  $p = .010$ ,  $\eta^2_c = .03$ ). Post-hoc Bonferroni-corrected paired  $t$  tests indicated significantly higher hit rates in the R+600 ms (from R+550 to R+650 ms;  $M = 46.9\%$ ) than in the R+300 ms interval (from R+250 to R+350 ms;  $M = 39.8\%$ ;  $t(27) = -3.19$ ,  $p = .009$ ; Fig. S3). The differences in hit rates between the R+0 ms interval (from R-50 to R+50 ms;  $M = 44.4\%$ ) did not differ significantly from hit rates in the R+300 ms interval ( $t(27) = 2.02$ ,  $p = .143$ ) and R+600 ms interval ( $t(27) = -1.10$ ,  $p = .827$ ). This mirrors the results of both circular and binary analysis with respect to increased detection of near-threshold somatosensory stimuli towards the end of the cardiac cycle (diastole).

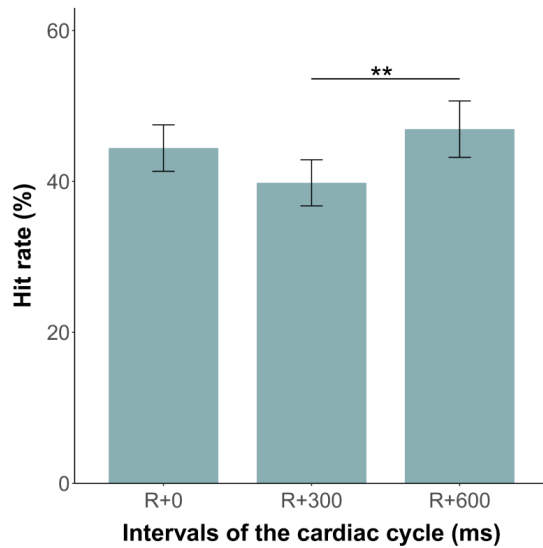


**Figure S3.** Hit rates in three 100-ms intervals centered on the time points at which Edwards et al. (2009) determined perceptual thresholds: R+0 ms (interval: R-50 ms to R+50 ms), R+300 ms (interval: R+250 ms to R+350 ms), and R+600 ms (interval: R+550 ms to R+650 ms). The detection of near-threshold somatosensory stimuli was significantly higher at the later phase of the cardiac cycle (R+550 to R+650 ms; diastole) compared to the earlier phase of the cardiac cycle (R+250 to R+350 ms; systole). Barplots were chosen to maximize comparability to Figure 1 in Edwards et al. (2009). The error bars represent 95% within-participants confidence intervals (Morey, 2008). R = R-peak in the ECG; \*\*  $p < .01$ .



#### REFERENCES CITED IN SUPPLEMENT

- Garfinkel, S.N., Seth, A.K., Barrett, A.B., Suzuki, K., & Critchley, H.D. (2015) Knowing your own heart: distinguishing interoceptive accuracy from interoceptive awareness. *Biological Psychology*, 104, 65–74. <https://doi.org/10.1016/j.biopsycho.2014.11.004>
- Edwards, L., Ring, C., McIntyre, D., Winer, J. B., & Martin, U. (2009). Sensory detection thresholds are modulated across the cardiac cycle: evidence that cutaneous sensibility is greatest for systolic stimulation. *Psychophysiology*, 46(2), 252–256.  
<https://doi.org/10.1111/j.1469-8986.2008.00769.x>
- Morey, R. D. (2008). Confidence Intervals from Normalized Data: A correction to Cousineau (2005). *Tutorials in Quantitative Methods for Psychology*, 4(2), 61–64.  
<https://doi.org/10.20982/tqmp.04.2.p061>
- Pewsey, A., Neuhäuser, M., & Ruxton, G.D. (2013). *Circular statistics in R*. Oxford and New York: Oxford University Press.
- Schandry, R. (1981) Heart Beat Perception and Emotional Experience. *Psychophysiology*, 18, 483–488. <https://doi.org/10.1111/j.1469-8986.1981.tb02486.x>



## **Chapter 3**

### **3 Study 2: Respiration, heartbeat, and conscious tactile perception**

**Martin Grund**, Esra Al, Marc Pabst, Alice Dabbagh, Tilman Stephani, Till Nierhaus, Michael Gaebler, and Arno Villringer

Published in *The Journal of Neuroscience* in 2022.



Behavioral/Cognitive

# Respiration, Heartbeat, and Conscious Tactile Perception

Martin Grund,<sup>1</sup> Esra Al,<sup>1,2,6</sup> Marc Pabst,<sup>1</sup> Alice Dabbagh,<sup>1,3</sup> Tilman Stephani,<sup>1,4</sup> Till Nierhaus,<sup>1,5</sup> Michael Gaebler,<sup>1,2</sup> and Arno Villringer<sup>1,2</sup>

<sup>1</sup>Department of Neurology, Max Planck Institute for Human Cognitive and Brain Sciences, Leipzig 04103, Germany, <sup>2</sup>MindBrainBody Institute, Berlin School of Mind and Brain, Charité – Universitätsmedizin Berlin and Humboldt-Universität zu Berlin, Berlin 10099, Germany, <sup>3</sup>Max Planck Institute for Human Cognitive and Brain Sciences, Pain Perception Group, Leipzig 04103, Germany, <sup>4</sup>International Max Planck Research School NeuroCom, Leipzig 04103, Germany, <sup>5</sup>Neurocomputation and Neuroimaging Unit, Department of Education and Psychology, Freie Universität Berlin, Berlin 14195, Germany, and <sup>6</sup>DFG Research Training Group 2386 Extrospection, Humboldt-Universität zu Berlin, Berlin 10099, Germany

Previous studies have shown that timing of sensory stimulation during the cardiac cycle interacts with perception. Given the natural coupling of respiration and cardiac activity, we investigated here their joint effects on tactile perception. Forty-one healthy female and male human participants reported conscious perception of finger near-threshold electrical pulses (33% null trials) and decision confidence while electrocardiography, respiratory activity, and finger photoplethysmography were recorded. Participants adapted their respiratory cycle to expected stimulus onsets to preferentially occur during late inspiration/early expiration. This closely matched heart rate variation (sinus arrhythmia) across the respiratory cycle such that most frequent stimulation onsets occurred during the period of highest heart rate probably indicating highest alertness and cortical excitability. Tactile detection rate was highest during the first quadrant after expiration onset. Interindividually, stronger respiratory phase-locking to the task was associated with higher detection rates. Regarding the cardiac cycle, we confirmed previous findings that tactile detection rate was higher during diastole than systole and newly specified its minimum at 250–300 ms after the R-peak corresponding to the pulse wave arrival in the finger. Expectation of stimulation induced a transient heart deceleration which was more pronounced for unconfident decision ratings. Interindividually, stronger poststimulus modulations of heart rate were linked to higher detection rates. In summary, we demonstrate how tuning to the respiratory cycle and integration of respiratory-cardiac signals are used to optimize performance of a tactile detection task.

**Key words:** cardiac cycle; electrocardiogram; interoception; photoplethysmography; respiration; tactile perception

## Significance Statement

Mechanistic studies on perception and cognition tend to focus on the brain neglecting contributions of the body. Here, we investigated how respiration and heartbeat influence tactile perception: respiration phase-locking to expected stimulus onsets corresponds to highest heart rate (and presumably alertness/cortical excitability) and correlates with detection performance. Tactile detection varies across the heart cycle with a minimum when the pulse reaches the finger and a maximum in diastole. Taken together with our previous finding of unchanged early event-related potentials across the cardiac cycle, we conclude that these effects are not a peripheral physiological artifact but a result of cognitive processes that model our body's internal state, make predictions to guide behavior, and might also tune respiration to serve the task.

## Introduction

Our body senses signals from the outer world (exteroception), but also visceral signals from inside the body (interoception) and it has

been shown that these two continuous types of perception interact (Critchley and Harrison, 2013; Critchley and Garfinkel, 2015; Babo-Rebelo et al., 2016; Seth and Friston, 2016; Azzalini et al., 2019). For example, we have recently shown that tactile perception interacts with cardiac activity as conscious detection of near-threshold stimuli was more likely toward the end of the cardiac cycle (Motyka et al., 2019; Al et al., 2020) and was followed by a more pronounced deceleration of heart rate as compared with missed stimuli (Motyka et al., 2019). In line with increased detection during diastole, late (P300) cortical somatosensory evoked potentials (SEPs) were also higher during diastole as compared with systole (Al et al., 2020). A similar cardiac phase dependency has also been revealed for visual sampling: microsaccades and saccades were more likely during systole, whereas fixations and blinks during diastole (Ohl et al., 2016; Galvez-Pol et al., 2020). Following an interoceptive predictive

Received Mar. 18, 2021; revised Oct. 26, 2021; accepted Nov. 4, 2021.

Author contributions: M. Grund, E.A., T.N., and A.V. designed research; M. Grund, A.D., and T.S. performed research; M. Grund, E.A., M.P., A.D., T.S., M. Gaebler, and A.V. analyzed data; M.G. wrote the first draft of the paper; M. Grund, E.A., M.P., A.D., T.S., T.N., M. Gaebler, and A.V. edited the paper; M. Grund, M.P., T.S., T.N., M. Gaebler, and A.V. wrote the paper.

This work was supported by the Max Planck Society. We thank Sylvia Stash for her data acquisition support, Mina Jamshidi Idjji and Carina Forster for data analysis advice and support, and Heike Schmidt-Duderstedt and Kerstin Flake for preparing the figures for publication.

The authors declare no competing financial interests.

Correspondence should be addressed to Martin Grund at mgrund@cbs.mpg.de.

<https://doi.org/10.1523/JNEUROSCI.0592-21.2021>

Copyright © 2022 the authors

coding account, the very same brain model that predicts (e.g., cardiac-associated) bodily changes and suppresses their access to consciousness (as unwanted “noise”) might also suppress perception of external stimuli which happen to coincide with those bodily changes (Allen et al., 2019).

Another dominant body rhythm that can even be regulated intentionally in contrast to cardiac activity is the respiration rhythm (Azzalini et al., 2019). Also for respiration, which naturally drives and is driven by cardiac activity (Kralemann et al., 2013; Dick et al., 2014), phase dependency of behavior and perception has been reported. For instance, self-initiated actions were more likely during expiration, whereas externally-triggered actions showed no correlation with the respiration phase (Park et al., 2020). Furthermore, inspiration onsets were reported to be phase-locked to task onsets which resulted in greater task-related brain activity and increased task performance for visuospatial perception, memory encoding and retrieval, and fearful face detection (Huijbers et al., 2014; Zelano et al., 2016; Perl et al., 2019). Respiratory phase locking has also been shown for brain rhythms and cortical excitability offering a neurophysiological basis for modulations of task performance and accordingly, phase locking to respiration has been interpreted as tuning the sensory system for upcoming information (Perl et al., 2019). Thus, for both, the cardiac cycle and the respiratory cycle, certain phases might also be beneficial for conscious perception and could be timed to paradigms instead of modeled as noise within an interoceptive predictive coding framework. While cardiac activity and respiration are closely interdependent, it remains unclear how they jointly shape perceptual processes.

Our present study combined the observation of cardiac and respiratory activity with a paradigm that asked participants to report (1) detection of weak electrical pulses applied to their left index finger and (2) their decision confidence. Decision confidence was assessed to identify the link between metacognition and cardiorespiratory cycle effects on somatosensation. As we have previously shown that greater tactile detection during diastole corresponded to increased perceptual sensitivity and not to a more liberal response criterion (Al et al., 2020), we expected the cardiac cycle effect not to be a side-effect of unconfident perceptual decisions. Afferent fibers in the finger have been reported to be modulated by cardiac pressure changes which the brain has to ignore or filter out (Macefield, 2003). Thus, we measured photoplethysmography to investigate whether cardiac related movements in the finger caused by the blood pulse wave coincided with lower tactile detection during systole. Furthermore, we tried to capture early SEPs at the upper arm to rule out differences in (peripheral) SEP amplitudes as explanation for altered conscious tactile perception across cardiac or respiratory cycles.

This study setup was intended to address the following research questions. (1) Does the interaction of cardiac activity and conscious tactile perception depend on decision confidence? (2) What is the precise temporal relationship between suppressed tactile detection and the kinetics of the pulse wave in the finger? (3) Does conscious tactile perception vary across the respiratory cycle and what is the relationship to respiratory modulation of the heartbeat?

## Materials and Methods

### Participants

Forty-one healthy humans (21 women, mean age = 25.5, age range: 19–37) participated in the study. Participants were predominantly right-handed with a mean laterality index of 90, SD = 17 (Oldfield, 1971). For four participants, the mean laterality index was not available.

### Ethics statement

All participants provided an informed consent. The experimental procedure and physiological measurements were approved by the ethics commission at the medical faculty of the University of Leipzig.

### Experimental design and statistical analysis

The experiment was designed to capture tactile detection of near-threshold stimuli (50% detection) and trials without stimuli (0% detection) across the cardiac and respiratory cycle. This resulted in three main stimulus-response conditions: (1) correct rejections of trials without stimulation, (2) undetected (misses), and (3) detected near-threshold stimuli (hits). False alarms (yes-responses) during trials without stimulation were very rare (mean false alarm rate = 6%, SD = 6%) and thus not further analyzed. Additionally, participants reported their decision confidence which allowed us to split trials by confidence.

We applied circular statistics to investigate whether conscious tactile perception was uniformly distributed across the cardiac and respiratory cycle or showed unimodal patterns. For each stimulus onset, the temporal distances to the preceding R-peak and expiration onset were calculated and put in relation to its current cardiac and respiratory cycle duration measured in degrees. Following for each participant, these angles were averaged for hits, misses, and correct rejections. For each stimulus-response condition, the resulting distributions of mean angles were tested across participants with the Rayleigh test for uniformity (Landler et al., 2018) from the R package “circular” (version 0.4-93). The application of circular statistics had two advantages. First, it accounted for cardiac and respiratory cycle duration variance within and between participants. Second, it allowed us to determine phases when detection differed without having to rely on arbitrary binning. However, it assumed that the different phases of the cardiac and respiratory cycle behave proportionally the same when cycle duration changes. That is why we complemented the circular statistics with a binning analysis that investigated the near-threshold detection rate for fixed time intervals relative to the preceding R-peak and expiration onset.

In repeated-measures ANOVAs, Greenhouse–Geisser correction was used to adjust for the lack of sphericity. *Post hoc t* tests *p* values were corrected for multiple comparisons with a false discovery rate (FDR) of 5% (Benjamini and Hochberg, 1995).

### Data and code availability

The code to run and analyze the experiment is available at <http://github.com/grundm/respirationCA>. The behavioral and physiological data [electrocardiogram (ECG), respiration, and oximetry] can be shared by the corresponding author on request if data privacy can be guaranteed.

### Stimuli and apparatus

Somatosensory stimulation was delivered via steel wire ring electrodes to the left index finger with a constant current stimulator (DS5; Digitimer). The anode was placed on the middle phalanx and the cathode on the proximal phalanx. The stimuli were single square-wave pulses with a duration of 0.2 ms and a near-threshold intensity (50% detection rate) which was assessed before an experimental block with an automatic procedure as described below, Behavioral paradigm, last paragraph. The stimulator was controlled by the waveform generator NI USB-6343 (National Instruments) and custom MATLAB scripts using the Data Acquisition Toolbox (The MathWorks Inc.).

### Behavioral paradigm

Participants had to report whether they perceived an electrical pulse and whether this yes/no-decision was confident or not. The experiment was separated into four blocks. Each block consisted of 150 trials. Participants received a near-threshold stimulus in 100 trials (mean intensity = 1.96 mA, range: 0.76–3.22 mA). In 50 trials, there was no stimulation (33% catch trials). The order of near-threshold and catch trials was pseudo-randomized for each block and participant. In total, there were 400 near-threshold and 200 catch trials.

Each trial started with a black fixation cross (black +) for a counter-balanced duration of 1.0–2.0 s (Fig. 1). It was followed by a salmon-colored fixation cross (0.62 s) to cue the stimulation at 0.5 s after the cue

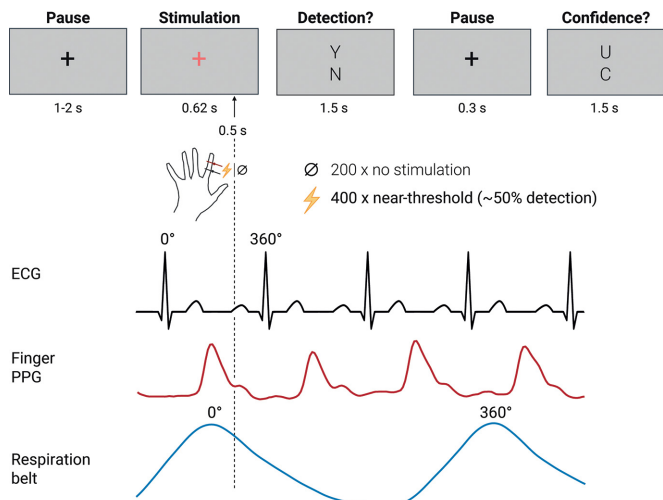


**Figure 1.** Experimental procedure and physiological parameters visualized for one exemplary trial. The tiles represent the participant's visual display and the times given below indicate the presentation duration. The near-threshold electrical finger nerve stimulation was always 0.5 s after the cue onset (salmon-colored fixation cross). Here, only one of four button response mappings is displayed (Y = yes; N = no; U = unconfident; C = confident). In total, 400 near-threshold trials and 200 trials without stimulation (33% catch trials) were presented in randomized order. Exemplary traces of ECG, finger photoplethysmography (PPG), and respiration belt below the trial procedure indicate that stimulus detection was analyzed relative to cardiac and respiratory cycles (0°–360°).

onset. With the cue offset, the participants had to report the detection of a tactile stimulus (yes/no). After the yes/no-button press, a pause screen was displayed for 0.3 s, before the participants were asked to report their decision confidence (confident/unconfident). With pressing the button for “confident” or “unconfident,” the new trial started. For both reports, the maximum response time was 1.5 s. Thus, the maximum possible trial duration was 5.8 s.

Participants indicated their perception and decision confidence with the right index finger on a two-button box. The buttons were arranged vertically. The four possible button response mappings were counterbalanced across participants, so that the top button could be assigned to “yes” or “no,” and “confident” or “unconfident,” respectively, for one participant.

Before the experiment, participants were familiarized with the electrical finger nerve stimulation and an automatic threshold assessment was performed to determine the stimulus intensity corresponding to the sensory threshold (50% detection rate). The threshold assessment entailed an up-and-down procedure (40 trials in the first run and 25 trials in subsequent runs), which served as a prior for the following Bayesian approach (psi method; 45 trials in first run and 25 trials in subsequent runs) from the Palamedes Toolbox (Kingdom and Prins, 2009) and closed with a test block (five trials without stimulation and 10 trials with stimulation intensity at the threshold estimate by psi method). Based on the test block results for the psi method threshold estimate and weighting in the results of the up-and-down procedure, the experimenter selected a near-threshold intensity candidate for the first experimental block. The visual display of the trials in the threshold assessment was similar to the trials in the experimental block (Fig. 1) but without the confidence rating and a shorter fixed intertrial interval (0.5 s). If a block resulted in a detection rate diverging strongly from 50% (<25% or >75%), the threshold assessment was repeated before the subsequent block to ensure a detection rate of ~50% throughout the whole experiment. The experimental procedure was controlled by custom MATLAB scripts using the Psychophysics Toolbox (Kleiner et al., 2007).

#### ECG acquisition

The ECG was recorded with the BrainAmp ExG (Brain Products) between two adhesive electrodes that were placed on the sternum and just below the heart on the left side of the thorax. A ground electrode was placed on the acromion of the right shoulder. The sampling frequency was 5000 Hz for 39 participants. Two participants were recorded with 1000 Hz.

#### Respiration acquisition

Respiration was measured with a respiration belt (BrainAmp ExG; Brain Products). The belt with a pressure-sensitive cushion was placed at the largest expansion of the abdomen during inspiration. The sampling frequency was 5000 Hz for 39 participants. Two participants were recorded with 1000 Hz.

#### Peripheral nerve activity acquisition

To examine the possibility to measure SEPs of peripheral nerve activity in response to near-threshold finger stimulation, two surface electrodes were placed with a distance of 2 cm at the left upper inner arm (below the biceps brachii) above the pathway of the median nerve in a subsample of 12 participants. The signal was recorded with a sampling rate of 5000 Hz, low-pass filtered at 1000 Hz, using a bipolar electrode montage (BrainAmp ExG; Brain Products).

#### Oximetry acquisition

The photoplethysmography was recorded with a finger clip SpO<sub>2</sub> transducer at the left middle finger at 50 Hz (OXI100C and MP150; BIOPAC Systems Inc.).

BIOPAC Systems Inc.).

#### Behavioral data analysis

The behavioral data were analyzed with R 4.0.3 in RStudio 1.3.10.923. First, trials were filtered for detection and confidence responses within the maximum response time of 1.5 s. Second, only blocks were considered with a near-threshold hit rate (HR) at least five percentage points above the false alarm rate. These resulted in 37 participants with four valid blocks, two participants with three valid blocks and two participants with two valid blocks. The frequencies of the response “confident” for correct rejections, misses, and hits were compared with paired *t* tests. Furthermore, the detection and confidence response times and resulting trial durations were compared between correct rejections, misses, and hits with paired *t* tests. The response times for hits and miss were additionally compared between confident and unconfident near-threshold trials.

#### Cardiac data analysis

ECG data were preprocessed with Kubios (version 2.2) to detect R-peaks. For two participants, the first four and the first twenty-two trials, respectively, had to be excluded because of a delayed start of the ECG recording. Additionally, one block of one participant and two blocks of another participant were excluded because of corrupted ECG data quality based on visual inspection (no R-peak detection possible).

First for correct rejections, misses, and hits, the circular distribution within the cardiac cycle was assessed with the Rayleigh test of uniformity and compared between the stimulus-response conditions with a randomization version of Moore's test for paired circular data (Moore, 1980) based on 10,000 permutations as implemented by (Pewsey et al., 2013). Additionally, this analysis was repeated for confident and unconfident hits and misses.

Second, instead of the relative position within the cardiac cycle, near-threshold trials were binned to four time intervals based on their temporal distance from the previous R-peak (0–200, 200–400, 400–600, and 600–800 ms). Then, dependent probabilities were calculated for each of

the four possible outcomes (unconfident misses, confident misses, unconfident hits, and confident hits) given the time interval. The probabilities were compared with  $t$  tests between time intervals separately for each of the four possible outcomes. FDR-correction was applied across all 24  $t$  tests. Furthermore, we used linear mixed-effects models (LMMs) with maximum likelihood estimation (Laplace approximation; glmer function in R) to evaluate the cardiac cycle effect on confidence beyond detection in near-threshold trials. Models without ["confidence ~ detection + (1|participant)"] and with the cardiac cycle information ["confidence ~ detection + cos(cardiac\_phase) + sin(cardiac\_phase) + (1|participant)"] were then compared using the anova function in R.

Additionally, we assessed whether metacognition changed across the cardiac cycle. For this purpose, response-specific meta- $d'$  was estimated for each cardiac interval using a hierarchical Bayesian model (MATLAB function fit\_meta\_d\_mcmc\_group.m) from the HMeta-d toolbox (Maniscalco and Lau, 2012; Fleming, 2017). Complementary to  $d'$  for yes/no-detection tasks, meta- $d'$  measures the sensitivity to distinguish with confidence ratings correct from incorrect yes/no-decisions and is calculated separately for yes and no responses (false alarms vs hits; misses vs correct rejections). For estimating meta- $d'$ , the Markov chain Monte Carlo (MCMC) method used three chains of 10,000 iterations with 1000 burn-in samples and default initial values from JAGS. We also ensured that  $\hat{R}$  was  $< 1.1$  for all model parameters of interest, indicating convergence of the model fit (Fleming, 2017). To account for perceptual sensitivity  $d'$  in measuring metacognitive sensitivity meta- $d'$ , M-ratios were calculated (meta- $d'$  divided by  $d'$  given yes or no response). An M-ratio of 1 indicates that confidence ratings can perfectly discriminate between correct and incorrect responses (Fleming and Lau, 2014). Compared with model-free approaches, M-ratio controls for differences in first order performance ( $d'$ ) as well as response biases ( $c$ ). For statistical testing whether M-ratios differed between yes/no-responses or cardiac cycle intervals, the differences of the corresponding group-level M-ratio posterior distributions (in log units) were calculated and assessed whether their 95% high-density intervals (HDIs) entailed zero or not (Kruschke, 2015; Fleming, 2017). The latter was interpreted as evidence for a difference.

Third, we analyzed the interbeat intervals (IBIs) in the course of a trial between the stimulus-response conditions. For this, two IBIs before, one during, and two after the stimulus onset were selected and compared with a two-way repeated measures ANOVA and *post hoc t* tests. To investigate whether changes of the IBI length were caused by systole or diastole, we applied a trapezoidal area algorithm (Vázquez-Seisdedos et al., 2011) to detect T-waves within the first poststimulus IBI ( $S + 1$ ). The T-wave end defines the end of systole and the onset of diastole. Systole and diastole durations were averaged for each participant and stimulus-response condition (correct rejection, miss, hit) and compared between the conditions across participants with FDR-corrected  $t$  tests. After visual inspection of T-wave detection results, two participants were excluded from the analysis, because the cardiac signal did not allow to consistently detect the T-wave. Additionally, in two trials of one participant the T-wave detection was not successful and 127 trials with a systole length three standard deviations below or above the participant mean at  $S + 1$  were excluded.

Furthermore, the relationship between heart slowing and detection performance was analyzed by calculating Pearson's correlation coefficients between heart slowing (ratio from IBI Stimulus to  $S + 1$ ) and near-threshold detection rate for (1) all trials and (2) correct rejections.

#### Oximetry data analysis

Oximetry data were analyzed with custom MATLAB scripts to detect pulse wave peaks with a minimum peak distance based on 140 heartbeats per minute (25.7 s) and a minimum peak prominence equal to a tenth of the data range in each block. Pulse wave cycles with a duration 1.5 times the median duration of the respective block were excluded from further processing. In R, pulse wave cycle data were merged with the behavioral data to apply the same exclusion criteria. Pulse wave peaks were located in the cardiac cycle to assess the duration since the previous R-peak (pulse wave transit time; PWTT) and its relative position in degree within the cardiac cycle.

#### Respiration data analysis

After visual inspection of the respiration traces, respiratory cycle detection was performed following the procedure by Power et al. (2020). First, outliers were replaced in a moving 1-s window with linearly interpolated values based on neighboring, non-outlier values. Local outliers were defined as values of more than three local scaled median absolute deviations (MAD) away from the local median within a 1-s window (Power et al., 2020). MAD was chosen for its robustness compared with standard deviation which is more affected by extreme values. Subsequently, the data were smoothed with a 1-s window Savitzky–Golay filter (Savitzky and Golay, 1964) to facilitate peak detection. Traces were then z-scored to identify local maxima (expiration onsets) and in the inverted trace local minima (expiration onsets) with the MATLAB findpeaks function. Local maxima and minima had to be at least 2 s apart with a minimum prominence of 0.9 times the interquartile range of the z-scored data. Respiratory cycles were defined as the interval from one expiration onset to the next expiration onset. For each participant, respiratory cycles with more than two times the median cycle duration were excluded from further analysis.

For each stimulus-response condition and participant, the mean angle direction of stimulus onsets within the respiratory cycle and their circular variance across trials were calculated. The distribution of mean angles of each stimulus-response condition was tested for uniformity with the Rayleigh test. Circular variance was defined as  $V = 1 - R$ , where  $R$  is the mean resultant length of each stimulus-response condition and participant with values between 0 and 1. Differences in circular variances between stimulus-response conditions were assessed with paired  $t$  tests. To investigate whether respiration phase-locking showed a relationship with task performance, Pearson's correlation coefficients between circular variance of respiration phases and near-threshold detection rate was calculated in (1) in all trials and (2) correct rejections.

Furthermore, we investigated whether participants gradually aligned their respiration to the stimulus onset in the beginning of the experiment. For the first 30 trials, the difference between each trial's stimulus onset angle and the mean angle within the first block was determined ("diff\_angle2mean"). The trial angle difference from the mean was used as a dependent variable in a random-intercept linear regression based on maximum likelihood estimation with trial number as independent variable: "diff\_angle2mean ~ 1 + trial + (1|participant)". The fit of this model was compared with a random-intercept only model "diff\_angle2mean ~ 1 + (1|participant)" in a  $\chi^2$  test to assess the effect of trial number on the angle difference. This analysis included only the 37 participants with a valid first block and excluded trials with false alarms.

Heart rate was analyzed across the respiratory cycle by assigning trials according to their respiration phase at stimulus onset to eight 45° intervals. For each interval the corresponding cardiac IBIs at stimulus onset were averaged for each participant and compared with FDR-corrected  $t$  tests.

Lastly, we compared the respiratory cycle duration between stimulus-response conditions by performing a one-way repeated-measures ANOVA and *post hoc t* tests. Furthermore, the inspiration onset within each respiratory cycle was determined to statistically compare expiration and inspiration duration between stimulus-response conditions with a two-way repeated measures ANOVA.

#### Phase-locking analysis between cardiac and respiratory activity

The  $n:m$  ( $n, m \in \mathbb{N}$ ) synchronization (Lachaux et al., 1999) was calculated in an intertrial setting for the stimulation onset as the following:

$$PLV_{cross} = \left| \frac{1}{n} \sum_{i=1}^n e^{j\phi_i} \right|$$

$$\phi_i = n\Phi_{i,resp} - m\Phi_{i,ecg},$$

where  $\Phi_{i,resp}$  and  $\Phi_{i,ecg}$  were the stimulation onset angles for the  $i$ -th trial within the respiratory (*resp*) and cardiac cycle (*ecg*), and  $j$  was the imaginary number. While  $m = 1$  was chosen for all participants, values for  $n$  were selected by calculating the ratio of the cardiac and respiratory frequency rounded to the nearest integer. The frequencies were estimated based on the mean cardiac and respiratory cycle durations at stimulus onset. The intertrial  $n:m$  synchronization at stimulation onset can



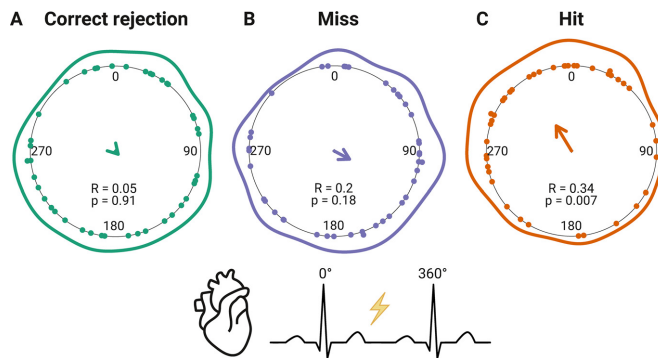


**Figure 2.** Distribution of mean angles (stimulus onset relative to cardiac cycle) for (A) correct rejections (green), (B) misses (purple), and (C) hits (red). Each dot indicates the mean angle of one participant. The line around the inner circle shows the density distribution of these mean angles. The direction of the arrow in the center indicates the mean angle across the participants while the arrow length represents the mean resultant length  $R$ . The resulting  $p$  value of the Rayleigh test of uniformity is noted below.

provide information about the extent to which the weighted phase difference of the two signals stays identical over trials. The calculated phase-locking value (PLV) lies between 0 and 1, with 0 indicating no intertrial coupling and 1 showing a constant weighted phase-difference of the two signals at the stimulation time.

#### SEP analysis

For the twelve participants with peripheral nerve recordings, stimulation artefacts were removed with a cubic monotonous Hermite spline interpolation from  $-2$  until  $4$  s relative to the trigger. Next, a 70-Hz high-pass filter was applied (fourth order Butterworth filter applied forwards and backwards) and the data were epoched  $-100$  to  $100$  ms relative to the trigger with  $-50$  to  $-2$  ms as baseline correction. Subsequently, epochs were averaged across for valid trials (yes/no and confidence response within maximum response time) with near-threshold stimuli and without stimulations.

## Results

### Detection and confidence responses

Participants ( $N = 41$ ) detected on average 51% of near-threshold stimuli ( $SD = 16\%$ ) and correctly rejected 94% of catch trials without stimulation ( $SD = 6\%$ ). On average, 188 catch trials (range: 93–200) and 375 near-threshold trials (range: 191–400) were observed. Participants reported to be “confident” about their yes/no-decision in 88% of the correct rejections ( $SD = 13\%$ ), in 71% of the misses ( $SD = 21\%$ ), and in 62% of the hits ( $SD = 18\%$ ). The confidence rate differed significantly between all conditions in paired  $t$  tests (CR vs miss:  $p = 3 \times 10^{-8}$ ; CR vs hit:  $p = 1 \times 10^{-9}$ ; miss vs hit:  $p = 0.019$ ). In total, we observed on average 184 misses (range: 58–303), 192 hits (range: 59–302), 177 correct rejections (range: 72–198), and 11 false alarms (range: 0–36). Two-third of the participants (27) had  $<10$  false alarms and four participants had zero false alarms. Because of zero or very few observations, false alarms were not further analyzed.

In near-threshold trials, participants reported their yes/no-decision later than for correct rejections (mean  $\pm$  SD:  $RT_{Hit} = 641 \pm 12$  ms,  $RT_{Miss} = 647 \pm 12$  ms,  $RT_{CR} = 594 \pm 10$  ms; paired  $t$  test hit vs CR:  $p = 0.02$ , miss vs CR:  $p = 3 \times 10^{-8}$ ). The yes/no-response times for hits and misses did not differ significantly ( $p = 0.43$ ). Additionally in unconfident compared with confident

near-threshold trials, yes/no-responses were on average 221 ms slower (mean  $\pm$  SD:  $RT_{Near\_unconf} = 789 \pm 11$  ms,  $RT_{Near\_conf} = 569 \pm 9$  ms; paired  $t$  test:  $p = 2 \times 10^{-16}$ ). Splitting near-threshold trials by confidence resulted in on average 49 unconfident misses (range: 6–143), 135 confident misses (range: 29–289), 70 unconfident hits (range: 9–181), and 122 confident hits (range: 24–277).

### Cardiac cycle

First, we addressed the question whether stimulus detection differed along the cardiac cycle. For hits, mean angles within the cardiac cycle were not uniformly distributed ( $R = 0.34$ ,  $p = 0.007$ ; Fig. 2), indicating a relation between cardiac phase and stimulus detection. Sixteen participants had a mean angle for hits in the last quarter of the cardiac cycle ( $270^\circ$ – $360^\circ$ ). The Rayleigh tests were not significant for misses ( $R = 0.20$ ,  $p = 0.18$ ) and correct rejections ( $R = 0.05$ ,  $p = 0.91$ ).

Additionally, we tested whether there was a bias for the presentation of near-threshold stimuli within the cardiac cycle and calculated a Rayleigh test for each participant. None of these tests was significant (all FDR-corrected  $p > 0.31$ ). With a randomization version of Moore’s test for paired circular data based on 10,000 permutations the distributions of correct rejections, misses, and hits were statistically compared with each other. The distribution of hits and misses differed significantly ( $R = 1.27$ ,  $p = 0.01$ ), whereas the distributions of correct rejections and misses ( $R = 0.84$ ,  $p = 0.13$ ), and correct rejections and hits did not ( $R = 0.41$ ,  $p = 0.62$ ).

Second, we repeated the analysis by splitting near-threshold trials based on the reported decision confidence (Fig. 3). The unimodal distribution was also present for confident hits ( $R = 0.38$ ,  $p = 0.002$ ) but not for unconfident hits ( $R = 0.10$ ,  $p = 0.69$ ). Eighteen participants had a mean angle for confident hits in the last quarter of the cardiac cycle ( $270^\circ$ – $360^\circ$ ). Confident misses also showed a unimodal distribution ( $R = 0.28$ ,  $p = 0.04$ ). Unconfident misses ( $R = 0.22$ ,  $p = 0.14$ ), confident correct rejections ( $R = 0.005$ ,  $p = 1.00$ ), and unconfident correct rejections ( $R = 0.01$ ,  $p = 1.00$ ) did not support rejecting the null hypotheses of a uniform distribution. Two participants were excluded from the analysis of unconfident correct rejections because of zero unconfident correct rejections (mean  $n = 20$ ,  $SD = 22$ , range: 0–88).

Third, near-threshold trials were analyzed regarding their dependent probabilities of the four possible outcomes (unconfident misses, confident misses, unconfident hits, confident hits) given one of four time intervals after the R-peak (0–200, 200–400, 400–600, 600–800 ms). FDR-corrected  $t$  tests between time intervals for each outcome resulted in significant differences only for confident hits between the last interval (600–800 ms) and the three other intervals (0–200 ms:  $p = 0.012$ ; 200–400 ms:  $p = 0.0008$ ; 400–600 ms:  $p = 0.0012$ ). The significant comparison of LMMs without and with the cardiac cycle information ( $\chi^2 = 11.2$ ,  $p = 0.004$ ), indicated that the cardiac cycle explained variance of confidence decisions beyond their relationship with hit/miss responses.

Metacognitive efficiency was assessed across the cardiac cycle with response-specific M-ratios for each interval based on

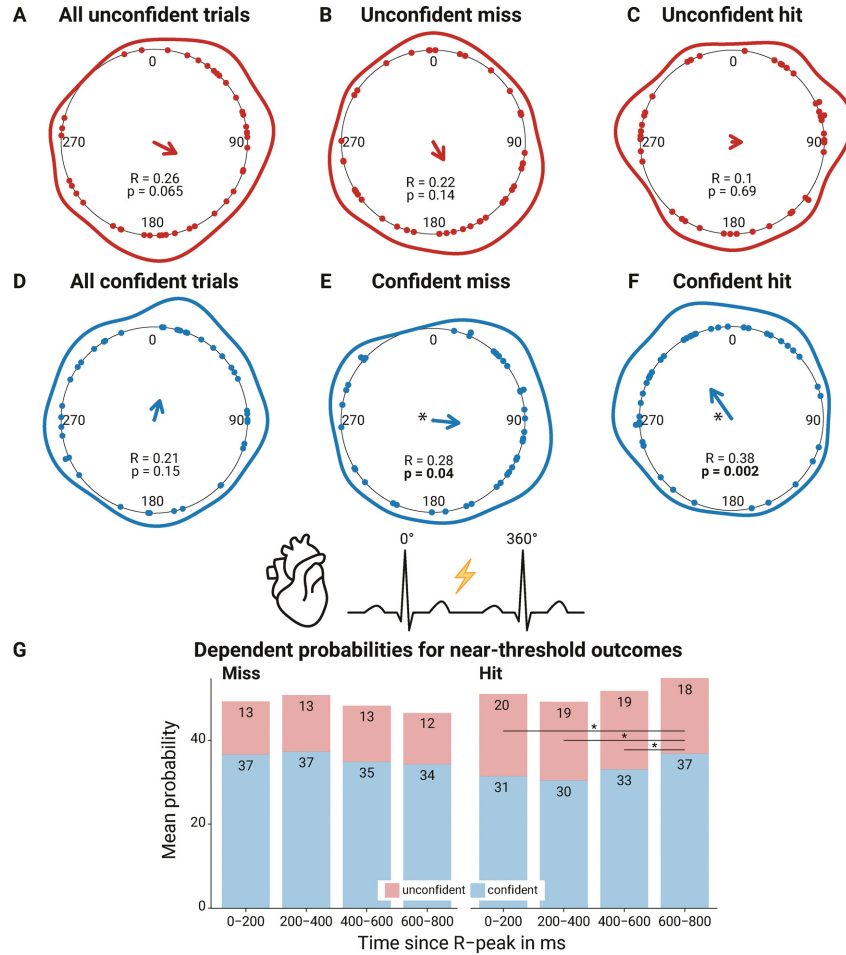


**Figure 3.** Circular distribution within the cardiac cycle of unconfident/confident trials and unconfident/confident misses and hits (*A–F*), dependent probabilities of unconfident/confident miss/hit at four time intervals after the R-peak (*G*), and metacognitive efficiency across the cardiac cycle (*H*). The distributions of mean angles (stimulus onset relative to cardiac cycle) are shown for (*A*) all unconfident trials (correct rejections, misses, and hits), (*B*) unconfident misses (red), (*C*) unconfident hits (red), (*D*) all confident trials (correct rejections, misses, and hits), (*E*) confident misses (blue), and (*F*) confident hits (blue). In *A–F*, each dot indicates the mean angle of one participant. The line around the inner circle shows the density distribution of these mean angles. The direction of the arrow in the center indicates the mean angle across the participants while the arrow length represents the mean resultant length  $R$ . The resulting  $p$  value of the Rayleigh test of uniformity is noted below and written in bold if significant. *G*, Mean dependent probabilities for the four possible outcomes of near-threshold trials given a time interval since the previous R-peak. The numbers for one time interval do not add up exactly to 100% across confident/unconfident misses and hits because of rounding and showing the mean across participants. The asterisks between the bars for confident hits indicate significant  $t$  tests. (FDR-corrected  $p < 0.01$ ).

Bayesian hierarchical models (Fleming, 2017) for yes/no-responses (mean number of no-responses per cardiac interval = [88, 90, 84, 67], SD = [25, 24, 25, 29]; mean number of no-responses per cardiac interval = [50, 48, 49, 38], SD = [22, 22, 21, 17]). The means of the group-level M-ratio posterior distribution for no-responses were all below 1 across the cardiac cycle (mean group-level posterior distribution M-ratio(no) = [0.59, 0.56, 0.59, 0.58], SD = [0.75, 0.52, 0.45, 0.34]; Fig. 4), whereas this was not the case for yes-responses: while the mean of the group-level M-ratio posterior distribution for yes-responses was below 1 at 0–

200 ms after the R-peak, it was above 1 at 200–400 ms, and stabilized a bit below 1 at 400–800 ms (mean group-level posterior distribution M-ratio(yes) = [0.81, 1.05, 0.93, 0.95], SD = [0.36, 0.09, 0.23, 0.15]).

For each cardiac cycle interval, the difference of the group-level M-ratio posterior distribution (in log units) between yes/no-responses was assessed with 95% HDIs. For 200–400 and 600–800 ms, the 95% HDIs did not entail zero, thus providing evidence that metacognitive efficiency was higher for yes compared with no-responses. When comparing the group-level M-

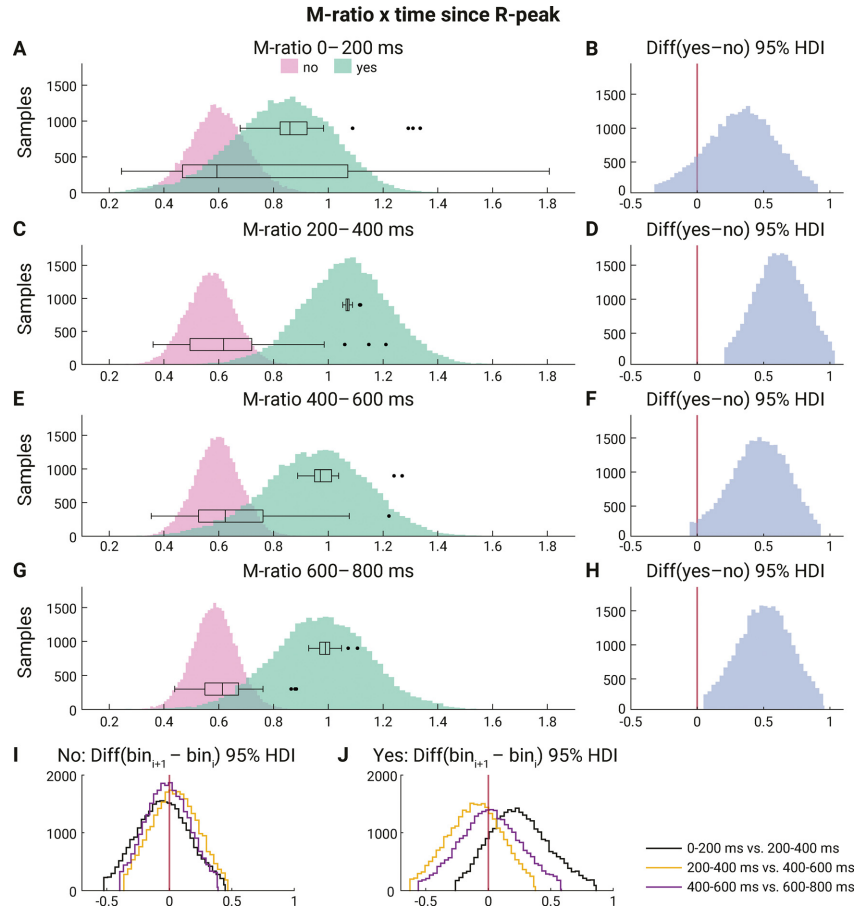


**Figure 4.** Response-specific metacognitive efficiency (M-ratios) across the cardiac cycle. At four cardiac intervals after the R-peak (**A, C, E, G**), the posterior distributions of group-level M-ratios are shown for no (pink; correct rejection vs miss) and yes-responses (green; hit vs false alarm). On top of these histograms of MCMC samples, boxplots represent the participant-level M-ratios for yes/no-responses. M-ratios of 1 indicate that confidence ratings can perfectly discriminate between correct and incorrect responses. M-ratios below 1 indicate inefficient metacognition. The second column shows the difference between the posterior distributions (in log units) of yes/no-responses as the 95% HDIs at the four cardiac cycle intervals (**B, D, F, H**). The last row shows the 95% HDIs (in log units) between subsequent cardiac intervals ( $bin_{i+1} - bin_i$ ) for yes/no-responses (**I, J**). These 95% HDIs indicate a credible difference between the corresponding group-level M-ratios if zero (red vertical line) is not included (**D, H**).

ratio posterior distribution (in log units) between subsequent cardiac cycle intervals within yes/no-responses, the 95% HDIs always entailed zero. Hence, there was no statistical evidence for an overall modulation of metacognition across the cardiac cycle.

**Cardiac IBI**

For each stimulus-response condition (hit, miss, and correct rejection), we extracted the IBI entailing the stimulus onset, as well as the two preceding and subsequent IBIs (Fig. 5A). We used a two-way repeated measures ANOVA to test the factors time and stimulus-response condition, and their interaction on IBIs. The main effect of time ( $F_{(2,73,109.36)} = 35.60, p = 3 \times 10^{-15}$ ) and the interaction of time and stimulus-response condition ( $F_{(4,89,195.55)} = 4.92, p = 0.0003$ ) were significant. There was no

significant main effect of stimulus-response condition on IBIs ( $F_{(1,42,56.75)} = 2.35, p = 0.12$ ). Following, *post hoc t* tests were calculated at each IBI between the stimulus-response conditions ( $5 \times 3$ ) and within each stimulus-response condition between subsequent IBIs ( $3 \times 4$ ), resulting in 27 FDR-corrected *p* values. At *S* + 1, the IBIs for hits were significantly longer than for misses ( $\Delta IBI = 5.2$  ms, FDR-corrected  $p = 0.024$ ) and correct rejections ( $\Delta IBI = 4.4$  ms, FDR-corrected  $p = 0.017$ ). The IBIs between misses and correct rejections did not differ significantly (FDR-corrected  $p = 0.62$ ). At *S* + 2, the IBIs for hits were still longer compared with correct rejections ( $\Delta IBI = 5.3$  ms, FDR-corrected  $p = 0.014$ ) but not to misses (FDR-corrected  $p = 0.25$ ). Within each stimulus-response condition (hit, miss, and correct rejection) subsequent IBIs differed significantly (FDR-corrected  $p < 0.005$ ).

Furthermore, the heart slowing ratio in all trials as well as in correct rejections (IBI Stimulus to S + 1) was correlated with near-threshold detection rate. This resulted in a strong correlation of heart slowing and detection task performance across participants (all trials:  $r = 0.53$ ,  $p = 0.0004$ ; correct rejections:  $r = 0.58$ ,  $p = 0.00006$ ).

To determine whether the longer IBIs at S + 1 for hits as compared with misses and correct rejections, was because of longer systole or diastole, we automatically detected the T-wave end to separate both cardiac phases for statistical comparison. At S + 1, the length of systoles was on average 324 ms (SD = 24 ms), and the length of diastoles 535 ms (SD = 107). Only diastoles for hits were significantly longer compared with misses ( $\Delta IBI = 6.3$  ms, FDR-corrected  $p = 0.006$ ) and correct rejections at S + 1 ( $\Delta IBI = 5.1$  ms, FDR-corrected  $p = 0.006$ ). Systoles at S + 1 showed no significant differences between the three conditions (hit vs miss: FDR-corrected  $p = 0.81$ ; hit vs CR: FDR-corrected  $p = 0.81$ ; miss vs CR: FDR-corrected  $p = 0.81$ ).

Furthermore, IBIs of trials with confident and unconfident decisions independent of stimulus presence and yes/no-response (excluding false alarms) were compared with a two-way repeated measures ANOVA (Fig. 5B). The main effects time ( $F_{(2,71,108.31)} = 42.37$ ,  $p = 2 \times 10^{-16}$ ) and confidence ( $F_{(1,40)} = 5.36$ ,  $p = 0.026$ ), as well as the interaction of time and confidence were significant ( $F_{(2,73,109.05)} = 30.79$ ,  $p = 2 \times 10^{-16}$ ). *Post hoc t* tests between the two confidence categories for each IBI (1 × 5) and within each confidence category between subsequent IBIs (2 × 4) revealed significant longer poststimulus IBIs for unconfident compared with confident decisions at S + 1 ( $\Delta IBI = 4.6$  ms, FDR-corrected  $p = 0.005$ ) and S + 2 ( $\Delta IBI = 10.6$  ms, FDR-corrected  $p = 6 \times 10^{-7}$ ). All subsequent IBIs differed significantly within each confidence category (FDR-corrected  $p < 0.05$ ). When repeated for near-threshold trials only, the difference between confidence categories was still present within each awareness condition: unconfident hits and misses showed longer IBIs at S + 2 compared with confident hits ( $\Delta IBI = 5.7$  ms, FDR-corrected  $p = 0.047$ ) and confident misses, respectively ( $\Delta IBI = 10.2$  ms, FDR-corrected  $p = 0.008$ ).

Additionally, we tested whether the poststimulus heart slowing ratio (IBI S + 1 and S + 2 relative to Stimulus) differed in near-threshold trials between detection and confidence (Fig. 5C,D). This approach has the advantage to account for the preceding IBI Stimulus when comparing the IBI differences at S + 1 and S + 2. A two-way repeated measures

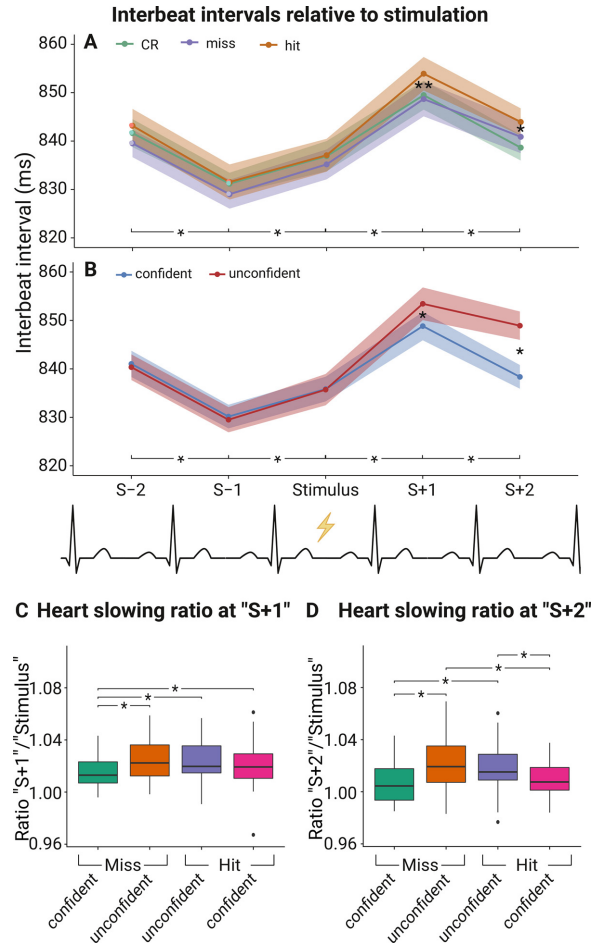


**Figure 5.** IBIs before and after the stimulus onset for (A) correct rejections (green), misses (purple), and hits (orange), and for (B) confident (blue) and unconfident (red) decisions. Confidence bands reflect within-participant 95% confidence intervals. The label Stimulus on the y-axis indicates the cardiac cycle when the stimulation or cue only were present. The labels S - 1 and S + 1 indicate the preceding and following intervals, respectively. In A, the two asterisks at S + 1 indicate significant *t* tests between hits and misses (FDR-corrected  $p = 0.024$ ), and between hits and correct rejections (FDR-corrected  $p = 0.017$ ). The one asterisk at S + 2 in A indicates a significant *t* test between hits and correct rejections (FDR-corrected  $p = 0.014$ ). In B, the asterisks at S + 1 and S + 2 indicate significant *t* tests between confident and unconfident decisions (S + 1: FDR-corrected  $p < 0.005$ ; S + 2: FDR-corrected  $p = 6 \times 10^{-7}$ ). The lines with asterisks on the bottom indicate significant *t* tests for subsequent IBIs within all conditions (FDR-corrected  $p < 0.05$ ). In C, D, the ratio of IBIs at S + 1 and S + 2 relative to Stimulus are shown for unconfident/confident misses and hits. The boxplots indicate the median (centered line), the 25th/75th percentiles (box), 1.5 times the interquartile range or the maximum value if smaller (whiskers), and outliers (dots beyond the whisker range). The asterisks between the boxplots indicate significant *t* tests (FDR-corrected  $p < 0.05$ ).

ANOVA showed a main effect between confidence categories (S + 1:  $F_{(1,40)} = 11.27$ ,  $p = 0.02$ ; S + 2:  $F_{(1,40)} = 28.98$ ,  $p = 0.000003$ ) but not for detection (S + 1:  $F_{(1,40)} = 4.04$ ,  $p = 0.051$ ; S + 2:  $F_{(1,40)} = 0.13$ ,  $p = 0.73$ ). At S + 1, *post hoc t* tests showed significant lower heart slowing ratios relative to Stimulus for confident misses compared with unconfident

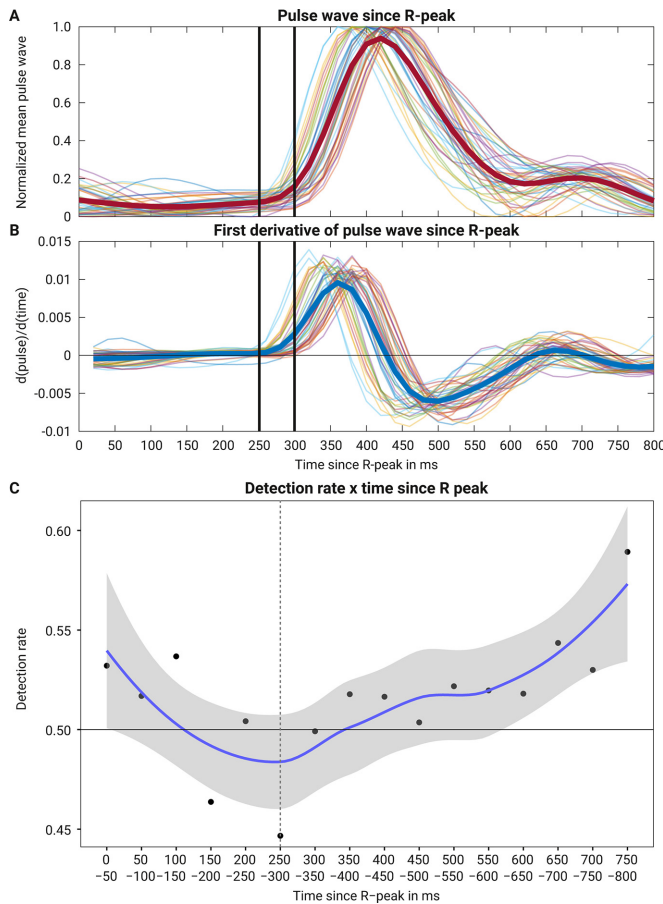


**Figure 6.** Pulse wave and detection relative to cardiac cycle. **A**, Mean pulse waves measured at the left middle finger across all participants (red thick line) and for each participant (colored thin lines) locked to preceding R-peak. **B**, First derivative of the mean pulse waves indicating the onset of the arriving pulse wave in the finger. The time window with the lowest detection rate is indicated with vertical thick black lines. **C**, Detection rate of near-threshold trials in 50-ms stimulus onset intervals since preceding R-peak. The black dots indicate the mean across participants. The blue line is the locally smoothed loess curve with a 95% confidence interval (gray) across these means.

misses (FDR-corrected  $p = 0.001$ ), unconfident hits (FDR-corrected  $p = 0.00002$ ), and confident hits (FDR-corrected  $p = 0.04$ ). At  $S + 2$ , heart slowing ratios relative to Stimulus were significantly lower for confident misses compared with unconfident misses (FDR-corrected  $p = 0.0001$ ) and unconfident hits (FDR-corrected  $p = 0.0002$ ), and for confident hits compared with unconfident hits (FDR-corrected  $p = 0.001$ ) and unconfident misses (FDR-corrected  $p = 0.0004$ ).

#### Pulse wave relative to electric cardiac cycle

Next to the electric cardiac cycle, we assessed whether stimulus detection was dependent on the pulse wave cycle measured at the left middle finger. Pulse wave peaks were located in the cardiac cycle by calculating the time to the preceding R-peak:

the PWTT and the PWTT relative to its current cardiac cycle in degree. The PWTT was on average 405 ms (SD = 24 ms, range: 354–439 ms). The pulse wave peak occurred on average in the middle of the cardiac cycle (mean angle  $M_{PWTT} = 178^\circ$ ,  $R = 0.91$ ,  $p = 0$ ) after the mean angle of confident misses ( $M_{Confident\ miss} = 96^\circ$ ) and before the mean angle of confident hits ( $M_{Confident\ hit} = 325^\circ$ ).

For putting the observed correlations between detection and the cardiac cycle in relation to the pulse wave peak, the analysis of near-threshold HRs during different stimulus onset intervals after the R-peak was repeated limited to 0–400 ms with shorter intervals (50 ms) and without splitting by confidence. A one-way repeated-measures ANOVA showed a main effect by time interval on near-threshold detection rate ( $F_{(5,64,225,46)} = 3.15$ ,  $p = 0.007$ ). The near-threshold HRs were significantly decreased before the pulse wave peak (mean PWTT = 405 ms) during the interval of 250–300 ms compared with the interval of 0–50 ms (FDR-corrected  $p = 0.038$ ). The interval 250–300 ms was plotted on the average pulse wave locked to the preceding R-peak and its slope (difference between adjacent samples, first derivative) to determine the onset of the pulse wave arrival in the finger. The first derivatives of participant's mean pulse waves showed that after 250 ms the pulse wave slopes substantially increased indicating the onset of the arriving pulse waves (Fig. 6B).

#### Respiratory cycle

First, we investigated whether conscious tactile perception depends on the stimulus onset relative to the respiratory cycle. Thus, we calculated the mean angles for hits, misses, and correct rejections for each participant and tested their circular distribution with the Rayleigh test of uniformity. For all conditions, uniformity was rejected in favor of an alternative unimodal distribution (correct rejections:  $R = 0.58$ ,  $p = 4 \times 10^{-7}$ ; misses:  $R = 0.54$ ,  $p = 2 \times 10^{-6}$ ; hits:  $R = 0.65$ ,  $p = 1 \times 10^{-8}$ ; Fig. 7). These unimodal distributions were centered at stimulus onset for the three conditions (mean angle  $M_{correct\ rejection} = 3.2^\circ$ ,  $M_{miss} = 5.0^\circ$ , and  $M_{hit} = 15.1^\circ$ ). Furthermore, we analyzed the circular distribution for each participant and stimulus-response condition. For hits, 38 of 41 participants showed a significant Rayleigh test after FDR-correction. For misses, 30 participants had a significant Rayleigh test, and for correct rejections, 32 participants. To assess whether the strength of the respiration locking differed significantly between hits, misses, and correction rejections, the circular variance of stimulus onset angles across trials was calculated for each stimulus-response condition and compared with  $t$  tests. Hits had a lower circular variance than misses ( $\Delta V = -0.044$ ,  $t_{(40)} = -3.17$ ,  $p = 0.003$ ) and correct

rejections ( $\Delta V = -0.035$ ,  $t_{(40)} = -2.78$ ,  $p = 0.008$ ), i.e., exhibited a stronger clustering around the mean direction. There was no significant difference in circular variance between misses and correct rejections ( $p = 0.44$ ). Furthermore, the circular variance of respiration phases in all trials as well as in correct rejections showed a negative medium correlation with near-threshold detection rate across participants (all trials:  $r = -0.38$ ,  $p = 0.013$ ; correct rejections:  $r = -0.41$ ,  $p = 0.008$ ).

We tested whether detection rates differed along the respiratory cycle. Thus, we binned near-threshold trials based on their relative position within the respiratory cycle in four quadrants ( $0^\circ$ – $90^\circ$ ,  $90^\circ$ – $180^\circ$ ,  $180^\circ$ – $270^\circ$ , and  $270^\circ$ – $360^\circ$ ), a one-way repeated-measures ANOVA was significant for the main effect quadrant on near-threshold detection rate ( $F_{(2.64, 105.44)} = 3.69$ ,  $p = 0.018$ ). *Post hoc t* tests revealed that only the first quadrant ( $0^\circ$ – $90^\circ$ ) showed significantly greater HRs compared with all other quadrants ( $90^\circ$ – $180^\circ$ :  $\Delta HR = 3.8\%$ , FDR-corrected  $p = 0.03$ ;  $180^\circ$ – $270^\circ$ :  $\Delta HR = 3.7\%$ , FDR-corrected  $p = 0.03$ ;  $270^\circ$ – $360^\circ$ :  $\Delta HR = 2.3\%$ , FDR-corrected  $p = 0.04$ ).

Comparing cardiac IBIs between eight  $45^\circ$  intervals across the respiratory cycle showed a significant increase of IBIs starting with the onset of expiration (increase from  $0^\circ$  to  $225^\circ$ ), and a decrease starting with the onset of inspiration (decrease from  $225^\circ$  to  $360^\circ$ ; Fig. 7E). The inspiration onset was on average at  $211^\circ$  (range:  $187$ – $250^\circ$ ) within the respiratory cycle which started with the expiration onset ( $R = 0.97$ ,  $p = 3 \times 10^{-16}$ ).

Second, the distribution of mean angles was assessed for confident and unconfident decisions. Hits, misses, and correct rejections were split by decision confidence and the resulting distributions were evaluated with the Rayleigh test for uniformity. All stimulus-response conditions showed for unconfident and confident decisions a significant unimodal distribution locked around the stimulus onset: unconfident correct rejections (mean angle  $M_{\text{unconf\_CR}} = 18.3^\circ$ ;  $R = 0.41$ ,  $p = 0.001$ ), confident correct rejections ( $M_{\text{conf\_CR}} = 2.2^\circ$ ;  $R = 0.58$ ,  $p = 4 \times 10^{-7}$ ), unconfident misses ( $M_{\text{unconf\_miss}} = 13.4^\circ$ ;  $R = 0.45$ ,  $p = 0.0001$ ), confident misses ( $M_{\text{conf\_miss}} = 6.7^\circ$ ,  $R = 0.51$ ;  $p = 0.00001$ ), unconfident hits ( $M_{\text{unconf\_hit}} = 10.4^\circ$ ;  $R = 0.51$ ,  $p = 0.0001$ ), and confident hits ( $M_{\text{conf\_hit}} = 15.2^\circ$ ;  $R = 0.67$ ,  $p = 4 \times 10^{-9}$ ). Two participants had zero unconfident correct rejections and were not considered in the respective Rayleigh test.

Third, to examine aforementioned phase effects further, we investigated whether participants adjusted their respiration rhythm to the paradigm in the beginning of the experiment. Thus, for the

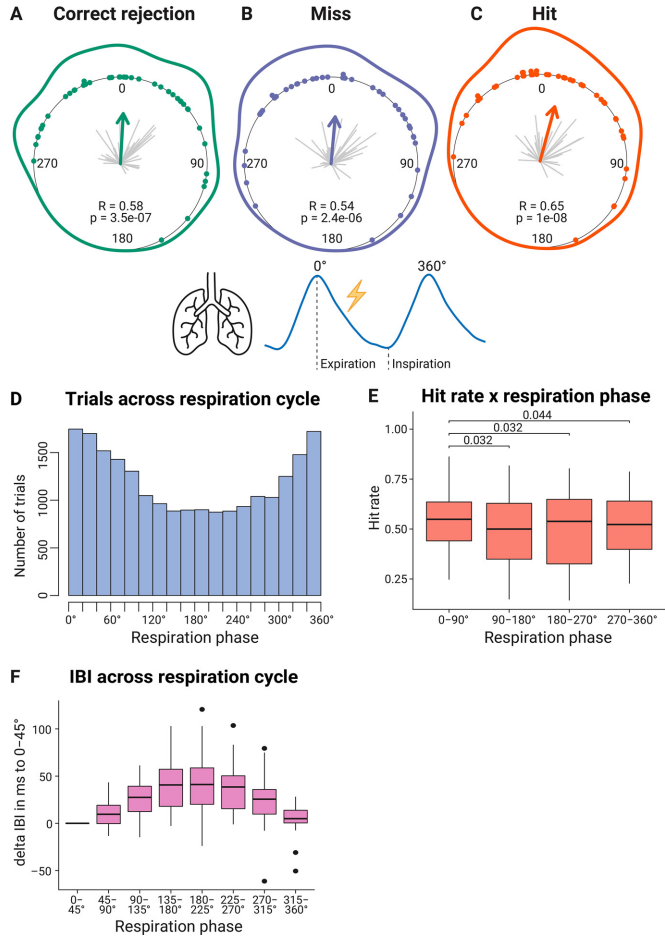


**Figure 7.** Circular distribution of mean stimulus onsets relative to the respiratory cycle for (A) correct rejections (green), (B) misses (purple), and (C) hits (red). Zero degree corresponds to expiration onset. Each dot indicates the mean angle of one participant. The gray lines originating in the center of the inner circle represent the resultant lengths  $R_i$  for each participant's mean angle. A longer line indicates a less dispersed intraindividual distribution ( $V_i = 1 - R_i$ ). The direction of the arrow in the center indicates the mean angle across the participants while the arrow length represents the mean resultant length  $R$ . The line around the inner circle shows the density distribution of these mean angles. The resulting  $p$  value of the Rayleigh test of uniformity is noted below. D, Histogram of respiration phases. Cumulative number of trials across all trials and participants for the relative position of the stimulus onset within the respiratory cycle binned in  $20^\circ$  intervals from  $0^\circ$  to  $360^\circ$ . The Rayleigh test across all trials and participants was significant ( $R = 0.18$ ,  $p = 2 \times 10^{-29}$ ). E, Detection rates for each quadrant of the respiratory cycle. Lines with  $p$  values above the boxplots indicate significant FDR-corrected  $t$  tests of all possible combinations. F, IBI differences for each eighth of the respiratory cycle relative to the first eighth ( $0^\circ$ – $45^\circ$ ). The boxplots (E, F) indicate the median (centered line), the 25th/75th percentiles (box), 1.5 times the interquartile range or the maximum value if smaller (whiskers), and outliers (dots beyond the whisker range).

first 30 trials of the first block, a random-intercept linear regression model with maximum likelihood estimation (lmer function in R) was calculated to evaluate the effect of trial number on trial angle difference from the mean for each participant. The angle difference was determined between the stimulus onset angle within the respiratory cycle of each trial and the mean of all angles in the first block ("diff\_angle2mean"). This analysis included 37 participants with a

first block and excluded trials with false alarms. Comparing the model “diff\_angle2mean  $\sim 1 + \text{trial} + (1|\text{participant})$ ” with a random intercept-only model “diff\_angle2mean  $\sim 1 + (1|\text{participant})$ ” revealed an effect of trial on the difference to the angle mean within the first 30 trials of the first block ( $\chi^2 = 5.84$ ,  $p = 0.016$ ). The fixed-effect slope was  $b_1 = -0.47$  and the mean of the random-intercepts  $b_0 = 79.7$  (diff\_angle2mean =  $b_1 \times \text{trial} + b_0$ ).

### Respiratory cycle duration

Given the previously reported heart slowing during conscious tactile perception (Motyka et al., 2019), we tested whether a similar effect was also present in the respiratory rhythm. Indeed, the mean duration of respiratory cycles differed between response categories (Fig. 8), as indicated by a one-way repeated-measures ANOVA ( $F_{(1.49, 59, 61)} = 13.11$ ,  $p = 0.0001$ ). *Post hoc t* tests showed that respiratory cycles accompanying misses (mean  $t = 3.86$  s) were significantly longer than respiratory cycles with correct rejections (mean  $t = 3.82$  s,  $\Delta t = 40$  ms, FDR-corrected  $p = 0.002$ ) and with hits (mean  $t = 3.77$  s,  $\Delta t = 91$  ms, FDR-corrected  $p = 0.0002$ ). Respiratory cycles with hits were also significantly shorter than correct rejections ( $\Delta t = 50$  ms, FDR-corrected  $p = 0.014$ ).

Additionally, we analyzed whether the respiratory cycle duration differed between confident and unconfident hits and misses. There was a main effect by detection ( $F_{(1,40)} = 14.64$ ,  $p = 0.0004$ ) but not by confidence ( $F_{(1,40)} = 1.15$ ,  $p = 0.29$ ) on respiratory cycle duration in a two-way repeated measures ANOVA. The interaction of detection and confidence was not significant ( $F_{(1,40)} = 0.83$ ,  $p = 0.37$ ).

Furthermore, we determined the expiration and inspiration duration for each respiratory cycle and compared them between hits, misses, and correct rejections. A two-way repeated measures ANOVA showed significant main effects of respiration phase (expiration longer than inspiration:  $F_{(1,40)} = 125.03$ ,  $p = 7 \times 10^{-14}$ ) and stimulus-response condition ( $F_{(1,45,58)} = 12.25$ ,  $p = 0.00002$ ). The interaction of respiration phase and stimulus-response condition was not significant ( $F_{(1,58,63,15)} = 0.22$ ,  $p = 0.75$ ). None of the six *post hoc t* tests between stimulus-response conditions for each respiration phase was significant after FDR-correction. The uncorrected  $p$  values did not show evidence that the respiratory cycle duration differences were caused by the expiration or inspiration phase (expiration, correct rejection vs miss:  $p = 0.04$ ; correct rejection vs hit:  $p = 0.21$ ; miss vs hit:  $p = 0.02$ ; inspiration, correct rejection vs miss:  $p = 0.09$ ; correct rejection vs hit:  $p = 0.06$ ; miss vs hit:  $p = 0.01$ ).

### Phase-locking between cardiac and respiratory activity

Because of the natural coupling of cardiac and respiratory rhythms (Dick et al., 2014), we investigated whether phase-locking of both rhythms is associated with conscious tactile perception. PLVs were calculated across trials using n:m synchronization (Tass et al., 1998; Lachaux et al., 1999) to account for the different frequency bands of the two signals. PLVs were compared between hits, misses, and correct rejections with a one-way repeated-measures ANOVA. The ANOVA showed no significant main effect of stimulus-response condition on PLVs between cardiac and respiratory activity ( $F_{(1,98,79,15)} = 1.72$ ,  $p = 0.19$ ).

### Peripheral nerve activity

For the subsample of twelve participants with peripheral nerve recordings at the left upper arm, there was no SEP associated with near-threshold stimuli. Also, the grand mean across participants did not show a difference between trials with and without

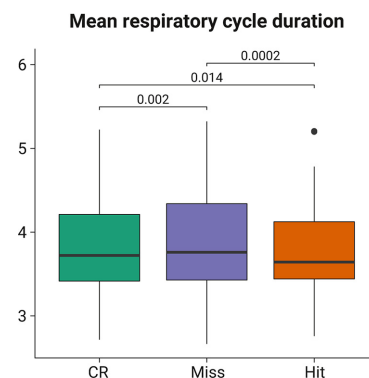


**Figure 8.** Mean respiratory cycle duration in seconds for correct rejections (green), misses (purple), and hits (red). The boxplots indicate the median (centered line), the 25th/75th percentiles (box), 1.5 times the interquartile range or the maximum value if smaller (whiskers), and outliers (dots beyond the whisker range). Significant *post hoc t* tests are indicated above the boxplot with a black bar and the respective FDR-corrected  $p$  value.

near-threshold stimulation. We concluded that near-threshold stimulation intensities (in the given subsample on average 1.88 mA, range: 0.79–2.50 mA) did not produce sufficiently high peripheral SEPs to measure them non-invasively from the inner side of the upper arm. Hence, we did not further pursue the analysis of peripheral SEPs. (Yet note that peripheral SEPs were observed in a pilot study with the same acquisition setup but applying superthreshold stimulation intensities of 6 mA.)

### Discussion

In this study, we confirm our previous finding that stimulus detection varies along the cardiac cycle (Motyka et al., 2019; Al et al., 2020, 2021). With the additional recording of photoplethysmography, decision confidence, and respiratory activity, we obtain several new findings regarding the integration of cardiac and respiratory signals in perceptual decision-making: we precisely pinpoint the period of lowest tactile detection rate at 250–300 ms after the R-peak, and we show a variation of confidence ratings across the cardiac cycle. A further new finding is that confidence ratings are the major determinant of cardiac deceleration. We confirm previous findings of an alignment of the respiratory cycle to the task cycle and we observed that this alignment follows closely the modulation of heart frequency (HF) across the respiratory cycle (sinus arrhythmia) with preferred stimulation onsets during periods of highest HF. Detection rate was highest in the first quarter of the respiratory cycle (after expiration onset), and temporal clustering during the respiratory cycle was more pronounced for hits than for misses and, interindividually, stronger respiratory phase-locking was associated with higher detection rates. Taken together, our findings show how tuning to respiration and closely linked cardio-respiratory signals are integrated to achieve optimal task performance.

### Detection varies across the cardiac cycle and is lowest 250–300ms after R-peak

While replicating the unimodal distribution of hits within the cardiac cycle here for the third time in an independent study of

somatosensory detection (Motyka et al., 2019; Al et al., 2020, 2021), we now located the decreased near-threshold detection rate more precisely 250–300 ms after the R-peak, before the pulse wave peak (405 ms) in the middle of the cardiac cycle (178°). The slope of the pulse wave showed a take-off around 250 ms after the preceding R-peak, indicating the onset of the pulse wave arrival. The explanation of the cardiac cycle effect on somatosensory detection stays speculative. In our previous study (Al et al., 2020), we found this systolic suppression to be associated with a change in sensitivity and with a reduction of the P300 SEP component which is commonly assumed to encode prediction (errors; Friston, 2005). We therefore postulated that the prediction of the pulse-wave associated peripheral nerve activation (Macefield, 2003) also affects the perception of other weak stimuli in the same time window since they are wrongly assumed to be a pulse-related “artifact.” Our new finding of temporally locating the lower tactile detection at the pulse wave onset and not during maximal peripheral vascular changes in the finger further supports this view. Perception of heartbeats has been reported to occur in the very same time interval of 200–300 ms after the R-peak (Yates et al., 1985; Brener and Kluitse, 1988; Ring and Brener, 1992). While this temporal judgment is unlikely to be solely based on the pulse wave in the finger, heartbeat sensations were mainly localized on the chest (Khalsa et al., 2009; Hassanpour et al., 2016), it is consistent with the prediction of strongest heartbeat-related changes at 250–300 ms and an attenuated detection of weak stimuli presented in the same time window.

#### Confidence ratings vary across the cardiac cycle

We also show that the cardiac cycle had a relationship with confidence ratings, in addition to the association of hit/miss responses with confidence ratings. When comparing the dependent probabilities of the four possible outcomes in near-threshold trials (unconfident/confident miss/hit), only the number of confident hits increased at the end of the cardiac cycle (600–800 ms) compared with 0–600 ms.

By determining  $M$ -ratios relating meta- $d'$  to  $d'$ , we show that metacognitive efficiency for yes-responses is generally higher than for no-responses [close to 1 (“optimal”) vs below 1 (“inefficient”)]. In our data, there was no evidence for an overall modulation of metacognition across the cardiac cycle. Qualitatively, while metacognition for no-responses is clearly smaller than 1 (“inefficient”) for all cardiac intervals, metacognition for yes-responses seems to be shifted below 1 (“inefficient”) at the onset of systole (0–200 ms after R-peak), shifted above 1 (“superoptimal”) during the period of 200–400 ms, and stabilizing over 1 at 400–800 ms. Future research must show whether this qualitative observation can be replicated. If so, the systolic variation might be related to a decisional conflict during an interval with the highest uncertainty whether a weak pulse was generated internally (heartbeat) or applied externally (Allen et al., 2019).

The higher confidence ratings for misses than for hits are most likely because of the higher expectation of no-responses which is ~66%, given 1/3 null trials and 2/3 “50% near-threshold” trials. For visual decision-making, confidence has been shown to be influenced by probabilities and, hence, expectations that a stimulus would occur (Sherman et al., 2015) and that the decision would be correct (Aitchison et al., 2015). In an independent fMRI study with near-threshold somatosensory stimuli using a four-point confidence scale, we equally found lower confidence for hits than for misses (Grund et al., 2021). It is not as straightforward to explain the overall lower metacognitive efficiency for no-responses versus yes-responses. We speculate that it

is probably related to the different likelihoods of the respective decisional alternatives: among the no-responses “Miss” and “Correct rejection” have an almost equal likelihood while among yes-responses “Hits” are much more likely than “False alarms.”

#### Heart slowing and perceptual decision-making

In the present study, we confirmed cardiac deceleration related to the parasympathetic correlate of the orienting response to a change in the environment (Sokolov, 1963) for all trial types even for trials without stimulation and we also confirmed the previously reported more pronounced heart deceleration with conscious perception (Park et al., 2014; Cobos et al., 2019; Motyka et al., 2019). Interestingly, however, when confidence ratings were taken into account this effect was reduced (particularly at two IBIs after the stimulation) and our findings indicate that heart rate slowing is mainly because of confidence rating, such that unconfident decision are associated with stronger heart rate slowing. Increased heart slowing for unconfident decisions might be associated with uncertainty, because heart slowing has been reported for the violation of performance-based expectations in a learning paradigm (Crone et al., 2003), for errors in a visual discrimination task (Łukowska et al., 2018), and for error keystrokes by pianists (Bury et al., 2019). Previous studies have linked heart rate changes with confidence. For example, in a visual discrimination task, confidence has been associated with heart acceleration which, in turn, attenuated the heart slowing caused by the orienting response to the stimulus (Allen et al., 2016). Since this effect was reversed by a subliminal and arousing negative emotional cue, confidence was interpreted as an integration of exteroceptive and interoceptive signals (Allen et al., 2016, 2019). A related phenomenon may underlie our results, in that rapid heart rate changes are transmitted upstream to be integrated in the decision process and particularly its metacognitive aspects.

Variations in the cardiac cycle were mainly because of changes in the length of diastoles which is in line with previous literature showing that cardiac cycle length is mainly modulated by diastole (Levick, 1991).

Interestingly, the extent of cardiac deceleration (we tested for all trials and for correct rejections) showed a positive correlation with near-threshold detection across participants. This is the case despite the fact that in all participants near-threshold stimulation intensity was adjusted before the experiment such that they detected ~50% of the stimulus trials. We thus have to assume that from the starting point of ~50% detection rate (without adjustment of the respiration), those participants who had a more pronounced heart slowing during the experiment improved their detection rate more than other participants.

#### Respiration locking and perceptual decision-making

Localizing stimulus onsets in the respiratory cycle revealed that (expected) stimulus onsets were locked to respiration. During the first thirty trials, the angular difference of onset time points to the mean angle showed a linear decrease as participants adapted their respiration rhythm to the paradigm. Intraindividual circular variance of stimulation onsets was lower for hits than misses, indicating a more pronounced respiratory phase-clustering went along with a higher likelihood of hits. HRs were greater in the first quadrant after expiration onset compared with all other three quadrants of the respiratory cycle. Furthermore, there was a negative correlation between intraindividual circular variance of respiration phases in all trials (and also correct rejections) and near-threshold detection rate across all



participants. Together these results suggest that respiration-locking is beneficial for task performance.

Interestingly, the frequency distribution of stimulation onsets closely matched heart rate changes along the respiratory cycle. Heart rate showed the well-known increase with expiration and decrease with inspiration (sinus arrhythmia), and stimulus onsets occurred most frequently during the period with shortest IBIs, i.e., highest heart rate. It is known that not only heart rate but also neural excitability changes during the respiratory cycle. In a recent study, the course of alpha power, known to be inversely related to excitability, across the respiratory cycle has been shown to facilitate perceptual sensitivity during late inspiration (Kluger et al., 2021), start of the time period when in our study most stimuli were timed. Also for tactile stimuli, it has been shown that alpha power in central brain areas is related to conscious detection (Schubert et al., 2009; Nierhaus et al., 2015; Craddock et al., 2017; Forschack et al., 2020; Stephani et al., 2021). Taken together, respiration phase locking might be used to increase the likelihood to detect faint stimuli in a phase of highest cortical excitability (attention).

While the mean angle across all participants locked at expiration onset, participant's individual mean angles ranged from late inspiration to early expiration (approximately  $>270^\circ$  and  $<90^\circ$ ). The inspiration onset was on average at  $211^\circ$ . Thus, the current data does not allow to determine whether participants tuned their inspiration or expiration onset. Possibly participants adapted their respiration rhythm to the cue onset which occurred 500 ms before the stimulus onset. Given a mean respiratory cycle duration of 3.82 s, the cue onset was  $47^\circ$  before the stimulus onset.

In conclusion, the two predominant body rhythms modulate conscious tactile perception. Our data indicate that phase-locking of respiration facilitates perception by optimal timing of stimuli in periods of highest heart rate and cortical excitability. Tactile detection and related decision confidence also vary characteristically during the cardiac cycle and the effects seem best explained by an interoceptive predictive coding account which is meant to model and suppress bodily changes related to the heartbeat.

## References

- Aitchison L, Bang D, Bahrami B, Latham PE (2015) Doubly Bayesian analysis of confidence in perceptual decision-making. *PLoS Comput Biol* 11: e1004519.
- Al E, Iliopoulos F, Forschack N, Nierhaus T, Grund M, Motyka P, Gaebler M, Nikulin VV, Villringer A (2020) Heart-brain interactions shape somatosensory perception and evoked potentials. *Proc Natl Acad Sci USA* 117:10575–10584.
- Al E, Iliopoulos F, Nikulin VV, Villringer A (2021) Heartbeat and somatosensory perception. *Neuroimage* 238:118247.
- Allen M, Frank D, Schwarzkopf DS, Fardo F, Winston JS, Hauser TU, Rees G (2016) Unexpected arousal modulates the influence of sensory noise on confidence. *Elife* 5:e18103.
- Allen M, Levy A, Parr T, Friston KJ (2019) The body's eye: the computational anatomy of interoceptive inference. *bioRxiv*. 603928.
- Azzalini D, Rebollo I, Tallon-Baudry C (2019) Visceral signals shape brain dynamics and cognition. *Trends Cogn Sci* 23:488–509.
- Babo-Rebello M, Richter CG, Tallon-Baudry C (2016) Neural responses to heartbeats in the default network encode the self in spontaneous thoughts. *J Neurosci* 36:7829–7840.
- Benjamini Y, Hochberg Y (1995) Controlling the false discovery rate: a practical and powerful approach to multiple testing. *J R Stat Soc Series B Stat Methodol* 57:289–300.
- Brener J, Kluitse C (1988) Heartbeat detection: judgments of the simultaneity of external stimuli and heartbeats. *Psychophysiology* 25:554–561.
- Bury G, García-Huésca M, Bhattacharya J, Ruiz MH (2019) Cardiac afferent activity modulates early neural signature of error detection during skilled performance. *Neuroimage* 199:704–717.
- Cobos MI, Guerra PM, Vila J, Chica AB (2019) Heart-rate modulations reveal attention and consciousness interactions. *Psychophysiology* 56: e13295.
- Craddock M, Poliakoff E, El-dereby W, Klepousniotou E, Lloyd DM (2017) Pre-stimulus alpha oscillations over somatosensory cortex predict tactile misperceptions. *Neuropsychologia* 96:9–18.
- Critchley HD, Harrison NA (2013) Visceral influences on brain and behavior. *Neuron* 77:624–638.
- Critchley HD, Garfinkel SN (2015) Interactions between visceral afferent signaling and stimulus processing. *Front Neurosci* 9:286.
- Crone EA, Veen FM, van der Molen MW, van der Somsen RJM, Beek B, van Jennings JR (2003) Cardiac concomitants of feedback processing. *Biol Psychol* 64:143–156.
- Dick TE, Hsieh Y-H, Dhingra RR, Baekey DM, Galán RF, Wehrwein E, Morris KF (2014) Cardiorespiratory coupling: common rhythms in cardiac, sympathetic, and respiratory activities. *Prog Brain Res* 209:191–205.
- Fleming SM (2017) HMeta-d: hierarchical Bayesian estimation of metacognitive efficiency from confidence ratings. *Neurosci Conscious* 2017:nix007.
- Fleming SM, Lau HC (2014) How to measure metacognition. *Front Hum Neurosci* 8:443.
- Forschack N, Nierhaus T, Müller MM, Villringer A (2020) Dissociable neural correlates of stimulation intensity and detection in somatosensation. *Neuroimage* 217:116908.
- Friston K (2005) A theory of cortical responses. *Philos Trans R Soc Lond B Biol Sci* 360:815–836.
- Galvez-Pol A, McConnell R, Kilner JM (2020) Active sampling in visual search is coupled to the cardiac cycle. *Cognition* 196:104149.
- Grund M, Forschack N, Nierhaus T, Villringer A (2021) Neural correlates of conscious tactile perception: an analysis of BOLD activation patterns and graph metrics. *Neuroimage* 224:117384.
- Hassanpour MS, Yan L, Wang DJJ, Lapidus RC, Arevian AC, Simmons WK, Feusner JD, Khalsa SS (2016) How the heart speaks to the brain: neural activity during cardiorespiratory interoceptive stimulation. *Philos Trans R Soc Lond B Biol Sci* 371:20160017.
- Huijbers W, Pennartz CMA, Beldzik E, Domagalik A, Vinck M, Hofman WF, Cabeza R, Daselaar SM (2014) Respiration phase-locks to fast stimulus presentations: implications for the interpretation of posterior midline “deactivations.” *Hum Brain Mapp* 35:4932–4943.
- Khalsa SS, Rudrauf D, Feinstein JS, Tranel D (2009) The pathways of interoceptive awareness. *Nat Neurosci* 12:1494–1496.
- Kingdom FAA, Prins N (2009) *Psychophysics*. San Diego: Academic Press Inc.
- Kleiner M, Brainard D, Pelli D, Ingling A, Murray R, Broussard C (2007) What's new in psychtoolbox-3. *Perception* 36:1–16.
- Kluger DS, Balestrieri E, Busch NA, Gross J (2021) Respiration aligns perception with neural excitability. *bioRxiv* 2021.03.25.436938.
- Kralemann B, Frühwirth M, Píkovský A, Rosenblum M, Kenner T, Schaefer J, Moser M (2013) In vivo cardiac phase response curve elucidates human respiratory heart rate variability. *Nat Commun* 4:2418–2419.
- Kruschke JK (2015) *Doing Bayesian data analysis*, Ed 2. San Diego: Academic Press.
- Lachaux JP, Rodriguez E, Martinerie J, Varela FJ (1999) Measuring phase synchrony in brain signals. *Hum Brain Mapp* 8:194–208.
- Landler L, Ruxton GD, Malkemper EP (2018) Circular data in biology: advice for effectively implementing statistical procedures. *Behav Ecol Sociobiol* 72:128.
- Levick JR (1991) *An introduction to cardiovascular physiology*. Oxford: Butterworth-Heinemann.
- Lukowska M, Sznajder M, Wierzczoń M (2018) Error-related cardiac response as information for visibility judgements. *Sci Rep* 8:1131.
- Macefield VG (2003) Cardiovascular and respiratory modulation of tactile afferents in the human finger pad. *Exp Physiol* 88:617–625.
- Maniscalco B, Lau H (2012) A signal detection theoretic approach for estimating metacognitive sensitivity from confidence ratings. *Conscious Cogn* 21:422–430.
- Moore BR (1980) A modification of the Rayleigh test for vector data. *Biometrika* 67:175–180.

- Motyka P, Grund M, Forschack N, Al E, Villringer A, Gaebler M (2019) Interactions between cardiac activity and conscious somatosensory perception. *Psychophysiology* 56:e13424.
- Nierhaus T, Forschack N, Piper SK, Holtze S, Krause T, Taskin B, Long X, Stelzer J, Margulies DS, Steinbrink J, Villringer A (2015) Imperceptible somatosensory stimulation alters sensorimotor background rhythm and connectivity. *J Neurosci* 35:5917–5925.
- Ohl S, Wohltat C, Kliegl R, Pollatos O, Engbert R (2016) Microsaccades are coupled to heartbeat. *J Neurosci* 36:1237–1241.
- Oldfield RC (1971) The assessment and analysis of handedness: the Edinburgh inventory. *Neuropsychologia* 9:97–113.
- Park HD, Barnoud C, Trang H, Kannape OA, Schaller K, Blanke O (2020) Breathing is coupled with voluntary action and the cortical readiness potential. *Nat Commun* 11:289–288.
- Park HD, Correia S, Ducorps A, Tallon-Baudry C (2014) Spontaneous fluctuations in neural responses to heartbeats predict visual detection. *Nat Neurosci* 17:612–618.
- Perl O, Ravia A, Rubinson M, Eisen A, Soroka T, Mor N, Secundo L, Sobel N (2019) Human non-olfactory cognition phase-locked with inhalation. *Nat Hum Behav* 3:501–512.
- Pewsey A, Neuhauser M, Ruxton GD (2013) *Circular statistics in R*. Oxford: Oxford University Press.
- Power JD, Lynch CJ, Dubin MJ, Silver BM, Martin A, Jones RM (2020) Characteristics of respiratory measures in young adults scanned at rest, including systematic changes and “missed” deep breaths. *Neuroimage* 204:116234.
- Ring C, Brener J (1992) The temporal locations of heartbeat sensations. *Psychophysiology* 29:535–545.
- Savitzky A, Golay MJE (1964) Smoothing and differentiation of data by simplified least squares procedures. *Anal Chem* 36:1627–1639.
- Schubert R, Haufe S, Blankenburg F, Villringer A, Curio G (2009) Now you'll feel it, now you won't: EEG rhythms predict the effectiveness of perceptual masking. *J Cogn Neurosci* 21:2407–2419.
- Seth AK, Friston KJ (2016) Active interoceptive inference and the emotional brain. *Philos Trans R Soc Lond B Biol Sci* 371:20160007.
- Sherman MT, Seth AK, Barrett AB, Kanai R (2015) Prior expectations facilitate metacognition for perceptual decision. *Conscious Cogn* 35:53–65.
- Sokolov EN, (1963) Higher Nervous Functions: The Orienting Reflex. *Annu Rev Physiol* 25:545–580.
- Stephani T, Hodapp A, Idaji MJ, Villringer A, Nikulin VV (2021) Neural excitability and sensory input determine intensity perception with opposing directions in initial cortical responses. *Elife* 10:e67838.
- Tass P, Rosenblum MG, Weule J, Kurths J, Pikovsky A, Volkman J, Schnitzler A, Freund H-J (1998) Detection of n:m phase locking from noisy data: application to magnetoencephalography. *Phys Rev Lett* 81:3291–3294.
- Vázquez-Seisdedos CR, Neto JE, Reyes EJM, Klautau A, de Oliveira RCL (2011) New approach for T-wave end detection on electrocardiogram: performance in noisy conditions. *Biomed Eng Online* 10:77.
- Yates AJ, Jones KE, Marie GV, Hogben JH (1985) Detection of the heartbeat and events in the cardiac cycle. *Psychophysiology* 22:561–567.
- Zelano C, Jiang H, Zhou G, Arora N, Schuele S, Rosenow J, Gottfried JA (2016) Nasal respiration entrains human limbic oscillations and modulates cognitive function. *J Neurosci* 36:12448–12467.

## **Chapter 4**

### 4 Study 3: Neural correlates of conscious tactile perception: An analysis of BOLD activation patterns and graph metrics

**Martin Grund**, Norman Forschack, Till Nierhaus, and Arno Villringer

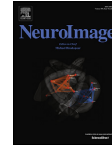
Published in *NeuroImage* in 2021.





Contents lists available at ScienceDirect

NeuroImage

journal homepage: [www.elsevier.com/locate/neuroimage](http://www.elsevier.com/locate/neuroimage)

## Neural correlates of conscious tactile perception: An analysis of BOLD activation patterns and graph metrics



Martin Grund<sup>a,\*</sup>, Norman Forschack<sup>a,b</sup>, Till Nierhaus<sup>a,c</sup>, Arno Villringer<sup>a,d</sup>

<sup>a</sup> Department of Neurology, Max Planck Institute for Human Cognitive and Brain Sciences, Stephanstr. 1A, 04103 Leipzig, Germany

<sup>b</sup> Experimental Psychology and Methods, Faculty of Life Sciences, University of Leipzig, 04109 Leipzig, Germany

<sup>c</sup> Neurocomputation and Neuroimaging Unit, Department of Education and Psychology, Freie Universität Berlin, 14195 Berlin, Germany

<sup>d</sup> MindBrainBody Institute, Berlin School of Mind and Brain, Charité – Universitätsmedizin Berlin and Humboldt-Universität zu Berlin, 10099 Berlin, Germany

### ARTICLE INFO

#### Keywords:

Somatosensory processing  
Perceptual awareness  
Consciousness  
Functional connectivity  
Graph theory  
fMRI

### ABSTRACT

Theories of human consciousness substantially vary in the proposed spatial extent of brain activity associated with conscious perception as well as in the assumed functional alterations within the involved brain regions. Here, we investigate which local and global changes in brain activity accompany conscious somatosensory perception following electrical finger nerve stimulation, and whether there are whole-brain functional network alterations by means of graph metrics. Thirty-eight healthy participants performed a somatosensory detection task and reported their decision confidence during fMRI. For conscious tactile perception in contrast to undetected near-threshold trials (misses), we observed increased BOLD activity in the precuneus, the intraparietal sulcus, the insula, the nucleus accumbens, the inferior frontal gyrus and the contralateral secondary somatosensory cortex. For misses compared to correct rejections, bilateral secondary somatosensory cortices, supplementary motor cortex and insula showed greater activations. The analysis of whole-brain functional network topology for hits, misses and correct rejections, did not result in any significant differences in modularity, participation, clustering or path length, which was supported by Bayes factor statistics. In conclusion, for conscious somatosensory perception, our results are consistent with an involvement of (probably) domain-general brain areas (precuneus, insula, inferior frontal gyrus) in addition to somatosensory regions; our data do not support the notion of specific changes in graph metrics associated with conscious experience. For the employed somatosensory submodality of fine electrical current stimulation, this speaks for a global broadcasting of sensory content across the brain without substantial reconfiguration of the whole-brain functional network resulting in an integrative conscious experience.

### 1. Introduction

In the debate on the neural correlates of consciousness, several crucial issues are still not resolved. First, regarding the involved brain regions, some studies assume only areas related to the particular perceptual modality to be necessary (Aukstulewicz et al., 2012; Schröder et al., 2019), others emphasize the role of a parietal hot zone (Boly et al., 2017; Koch et al., 2016) whereas some theories - most notably the global workspace theory (Baars, 1988; Dehaene et al., 2006; Mashour et al., 2020) - assume conscious experience to depend on the involvement of widespread particularly fronto-parietal brain regions (Naghavi and Nyberg, 2005; Rees et al., 2002). Second, regarding the neurophysiological processes occurring *within* the involved brain regions, recent studies are suggesting specific alterations in their connectivity which can be identified by effects of transcranial stimulation

(Casali et al., 2013) or using graph-theoretical metrics on fMRI data (Godwin et al., 2015; Sadaghiani et al., 2015).

For the somatosensory domain, previous fMRI activation studies have suggested the ipsilateral and contralateral secondary somatosensory cortices as the most promising candidates for conscious tactile perception (Moore et al., 2013; Schröder et al., 2019). Furthermore, recurrent interaction of S2 with S1 may play an important role for tactile detection (Aukstulewicz et al., 2012). Research focusing on tactile illusions has shown that S1 is activated somatotopically in correspondence with the illusory percept and body ownership (Blankenburg et al., 2006; Martuzzi et al., 2015). In this context, the temporal parietal junction (TPJ) plays a major role for bodily self-consciousness (De Ridder et al., 2007; Ionta et al., 2014). The insula has been consistently reported to be associated with conscious tactile perception (Moore et al., 2013) and described as a central hub for interoception (Ronchi et al., 2015) and self-identification (Park and Blanke, 2019). Interestingly, in another recent study, the insula together with anterior cingulate cor-

\* Corresponding author.

E-mail address: [mgrund@cbs.mpg.de](mailto:mgrund@cbs.mpg.de) (M. Grund).

<https://doi.org/10.1016/j.neuroimage.2020.117384>

Received 12 May 2020; Received in revised form 10 September 2020; Accepted 12 September 2020

Available online 17 September 2020

1053-8119/© 2020 The Authors. Published by Elsevier Inc. This is an open access article under the CC BY-NC-ND license (<http://creativecommons.org/licenses/by-nc-nd/4.0/>)

tex coded for uncertainty across stimulation intensities (Schröder et al., 2019). In the same study, frontal and parietal activations in tactile detection paradigms have been interpreted as serving the task (e.g., reporting a percept) but not the conscious sensory experience (Schröder et al., 2019). Yet, the above-mentioned ideas of a “global workspace” involving mainly fronto-parietal activity (Dehaene et al., 2006), or of a posterior cortical hot zone integrating sensory cortices (Koch et al., 2016) are conceived to be domain-general thus also applying to the tactile consciousness.

While most of the above-mentioned studies relied on the analysis of BOLD activation patterns, the question, whether functional connectivity changes or not, can be assessed using graph metrics (Bassett and Sporns, 2017). For this purpose, cortical and subcortical regions of interest (ROIs) are defined as nodes and their temporal relationships as edges (i.e., their connection; Bullmore and Bassett, 2011). The resulting network topologies are assessed with graph-theoretical measures such as modularity and clustering coefficient and compared between aware and unaware target trials (Godwin et al., 2015; Sadaghiani et al., 2015; Weisz et al., 2014). Modularity captures the global organization of nodes in subnetworks, whereas the clustering coefficient indicates whether a node’s neighbors are also connected, thus forming local clusters. Measures of integration (e.g., characteristic path length) describe the general connectivity between all nodes, whereas measures of centrality (e.g., participation coefficient) reveal important nodes in the network. In this framework, visual awareness has recently been suggested to be accompanied by a decreased modularity and increased participation coefficient of the post-stimulus network topology in fMRI (Godwin et al., 2015). Importantly, these topologies had explanatory power beyond local BOLD amplitudes and baseline functional connectivity (Godwin et al., 2015). Globally, this indicates a lower segregation of nodes into distinct networks and locally a higher centrality of all nodes. A more integrated state accompanying stimulus awareness (Godwin et al., 2015) is supposed to facilitate broadcasting of sensory information to other brain areas (Dehaene et al., 2006; Dehaene and Changeux, 2011). These widespread changes in functional connectivity have been interpreted as evidence supporting global models of awareness, e.g., the global workspace theory (Dehaene et al., 2006; Dehaene and Changeux, 2011). Whether these changes in graph metrics generalize to other sensory modalities is not yet answered.

In the present study, building on our previous experience in studies on neural processes underlying conscious and unconscious somatosensory processing (Blankenburg et al., 2003; Förschack et al., 2020; 2017; Nierhaus et al., 2015; Schubert et al., 2006), we used a “classical” fMRI detection paradigm in which aware and unaware trials of physically identical near-threshold stimuli are contrasted (Aru et al., 2012; Baars, 1988). Notably, our fMRI paradigm included a nine-second pause between stimulation and report, which made the assessment of functional network topologies with graph metrics possible. Therefore, our study design allowed to assess BOLD activity patterns and graph metrics independently, as well as to relate the two measures directly.

Two other features of our paradigm are important: (i) a confidence rating was included for each trial allowing for an analysis of confident decisions only and (ii) the paradigm included 25% catch trials. By comparing the contrast of undetected stimuli to correctly rejected catch trials, neural processes associated with non-conscious stimulus processing of near-threshold stimuli can be assessed. In a previous study on sub-threshold stimuli, we had shown that they were associated with a deactivation of somatosensory brain regions (Blankenburg et al., 2003); however, it is not clear whether this is also true for stronger stimuli near the detection threshold.

Thus, our study aimed to address the following main questions:

- Do BOLD activation patterns following somatosensory near-threshold stimuli match the predictions of major consciousness theories, i.e., does the contrast detected/undetected lead to increased activity only in somatosensory areas (Schröder et al., 2019), in a

fronto-parietal network (global workspace theory), or in a more restricted temporo-parietal-occipital hot zone (Koch et al., 2016)?

- Do graph metrics change with the conscious experience of somatosensory stimuli as shown for the visual system by Godwin et al. (2015), and do the affected areas match activated brain areas?
- Which neural changes are associated with non-perceived, but near-threshold somatosensory stimuli?

## 2. Materials and methods

### 2.1. Participants

Thirty-eight healthy humans (19 women; mean age = 27.3, age range: 23–36) participated in the study. They had normal or corrected-to-normal vision and were right-handed (mean laterality index = 85, range: 60–100; Oldfield, 1971).

### 2.2. Ethics statement

All participants provided informed consent (including no contraindication for MRI), and all experimental procedures were approved by the ethics commission at the medical faculty of the University of Leipzig.

### 2.3. Experimental design and statistical analysis

The experimental design of the tactile detection task had the intention to generate different sensory experiences for physically identical stimulus presentations. Brain activity accompanying these sensory experiences was sampled with BOLD fMRI (see fMRI data acquisition for details). The tactile stimulation was applied as a single electrical pulse to the left index finger. The stimulation intensity was set to the individual sensory threshold, before each of the four acquisition blocks, such that participants reported a stimulus detection (“hit”) in about 50% of the trials. One hundred near-threshold trials were intermingled with 20 clearly perceivable, supra-threshold trials and 40 catch trials without stimulation as control conditions. Participants had to report their perception (yes/no) and decision confidence (see “behavioral paradigm” for details). This led to three within-participant factors of interest: (a) rejected catch trials without stimulation (correct rejections), (b) non-perceived near-threshold trials (misses), and (c) perceived near-threshold trials (hits). We did not include false alarms (reported “yes” in catch trials without stimulation) due to the low false alarm rate (mean FAR = 3.3%,  $SD = 6.0\%$ ). 17 of 31 participants reported zero false alarms.

We compared the graph metrics between hits, misses and correct rejections across participants with the Wilcoxon’s signed-rank test (see Graph-theoretical analysis for details). For each graph metric, the  $p$ -values of the 24 paired Wilcoxon’s signed-rank tests were corrected for multiple comparisons with a false discovery rate (FDR) of 5% (Benjamini and Hochberg, 1995). The BOLD response amplitudes were modeled for the three (detection related) within-participant factors and compared them with a mixed-effects meta-analysis (3dMEMA; Chen et al., 2012). We controlled for multiple comparisons with family-wise error correction (see fMRI contrast analysis for details).

### 2.4. Data and code availability

The code to run the experiment, the behavioral data, and the code to analyze the behavioral and MRI data are available at <http://github.com/grundm/graphCA>. Due to a lack of consent of the participants, structural and functional MRI data cannot be shared publicly, and can only be made available upon reasonable request if data privacy can be guaranteed according to the rules of the European General Data Protection Regulation (EU GDPR). The respective research group has to sign a data use agreement to follow these rules. This statement is in line with our institute’s policies and requirements by our funding bodies.

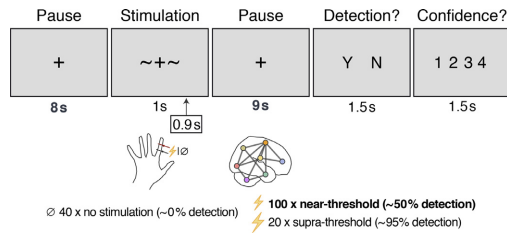


**Fig. 1.** Experimental paradigm visualized across one trial (21 s). The tiles represent the participant's visual display and the times given below indicate the presentation duration. In total, each participant completed 160 trials across 4 blocks, including 100 near-threshold trials. Electrical nerve stimulation was applied to the left index finger 0.9 s after cue onset (~+~) to temporally align yes/no-decisions, which presumably had to be made at cue offset. Participants only reported their target detection decision (yes/no) following a long pause of 9 s in order to model the brain's post-stimulus functional network without a button press-related signal. The detection decision was followed by a confidence rating on a scale from 1 (very unconfident) to 4 (very confident). Every 0.75 s, a full MRI brain volume (BOLD) was acquired with a 3-mm isotropic resolution.

## 2.5. Behavioral paradigm

Participants had both to report the perception (yes/no) of electrical pulses applied to their left index finger and rate their confidence about their decision. Single square-wave pulses (0.2 ms) were generated with a constant current stimulator (DS5; Digitimer, United Kingdom) at individually assessed intensities near (mean intensity = 1.85 mA, range: 1.01–3.48 mA) and supra (mean intensity = 2.18 mA, range: 1.19–3.89 mA) perceptual threshold reflecting 50% and 100% detection rate. Additionally, 25% of all trials were catch trials without stimulation.

Each trial (21 s) started with a fixation cross (1 s), followed by a cue (1 s) indicating an electrical pulse was soon to follow (Fig. 1). The stimulation onset was always 100 ms before cue offset in order to temporally align the stimulation with the detection decisions. For aware trials participants' detection decisions presumably occur the instant the stimulation is noticed. However, for unaware trials they can only conclude there was no stimulus at cue offset. If the stimulus onsets had been pseudo-randomized across the cue window, the yes-decision would have occurred on average half of the cue window earlier than the no-decision. The actual reporting of the decision was delayed by 9 s to allow a movement-free time window for analyses. Participants had 1.5 s to report if they felt the stimulus or not by pressing the corresponding button for yes or no. Subsequently they had another 1.5 s to report their confidence about the yes/no-decision on a scale from 1 (very unconfident) to 4 (very confident). Any remaining time in the confidence rating window, following the rating, was added to a 7 s fixation cross creating an inter-trial interval of at least 7 s. Participants were instructed to place their right four fingers on a four-button box. The second and third buttons were controlled by the right middle finger and the ring finger to report the decision for yes or no. The outer buttons were controlled by the index finger and the little finger additionally to report the confidence decision on the full four-point scale. All button-response mappings were counterbalanced across participants. Hence depending on the mapping, the middle finger or the ring finger indicated "yes", and the four-point confidence scale started with "very confident" or "very unconfident" at the index finger.

Each block had in total 40 trials and lasted 14 min: 10 trials without stimulation, 25 with near-threshold intensity, and 5 with supra-threshold intensity, delivered in pseudo-randomized order. Before each block, individual thresholds were assessed with an up-and-down method followed by the psi method from the Palamedes Toolbox (Kingdom and Prins, 2009). The threshold procedure followed that of the actual ex-

perimental trials but excluded the long pause and confidence response. Participants performed 4 blocks sequentially (circa 80 min). The experimental procedure was controlled by custom MATLAB scripts (The MathWorks Inc., Natick, Massachusetts) using Psychophysics Toolbox (Kleiner et al., 2007).

## 2.6. fMRI data acquisition

While participants performed the task, we acquired whole-brain BOLD contrast images with a 32-channel head coil on a Siemens MAGNETOM Prisma 3 Tesla scanner. For sub-second, whole-brain images, we used a Multi-Band (MB) echo-planar imaging (EPI) sequence (Moeller et al., 2010; Setsompop et al., 2012) with an MB acceleration factor of 3 (TR = 750 ms, TE = 25 ms, flip angle = 55°, receiver bandwidth = 1815 Hz/px, partial Fourier = 7/8). No GRAPPA acceleration was applied (iPAT factor = 1). In each of the 4 blocks we acquired 1120 brain volumes (14 min), each consisting of 36 axial slices with a field of view of 192 × 192 mm<sup>2</sup> (64 × 64 voxel) and a 0.5-mm gap resulting in 3-mm isotropic voxels.

For magnetic distortion correction of the EPI scans, B0 images were obtained from double-echo GRE images (TR = 750 ms, TE<sub>1</sub> = 4.92 ms, ΔTE = 2.46 ms, echo spacing = 0.66 ms, flip angle = 45°), with the same voxel geometry as used for the EPI scans. The receiver bandwidth was 822 Hz/pixel.

For normalizing the EPI scans and extracting nuisance regressors of core white matter voxels and ventricles, we used previously acquired T1-sensitive brain images of the participants with a 32-channel head coil or for two participants with a 20-channel head/neck coil on 3-Tesla Siemens MAGNETOM Prisma, Skyra, TrioTim or Verio scanner. The MPRAGE sequence covered the whole brain (176 × 240 × 256 mm<sup>3</sup>) with an isotropic voxel resolution of 1 mm and slightly varied regarding the echo time and the receiver bandwidth across participants (TR = 2.3 s, TE = [2.01 (2), 2.96 (9), 2.98 (19), 4.21 (5)] ms, inversion time TI = 900 ms, flip angle = 9°, bandwidth = [238 (10), 240 (16), 241 (9)] Hz/px). For two participants, the sequence parameters were more different (TR = 1.3 s, TE = 3.5 ms, inversion time = 650 ms, flip angle = 8°/10°, bandwidth = 190 Hz/px).

## 2.7. Behavioral data analysis

The behavioral data was analyzed with R 3.6.0 in RStudio 1.2.1335. Data by four participants was incomplete due to technical issues and failed data acquisition. The blocks of the remaining 34 participants were evaluated for successful near-threshold assessments if at least 4 null and 17 near-threshold trials with a yes/no and confidence response were recorded. This meant that only blocks with a hit rate at least 5 percentage points larger than the false alarm rate and participants with an average hit rate of 20–80% were further processed. This resulted in 31 participants with on average 89 near-threshold trials (range: 66–100). The distribution of mean detection rates is visualized in Fig. 2a. For the confidence ratings, we calculated conditional probabilities for each confidence rating given a stimulus-response condition: correct rejection, near-threshold miss, near-threshold hit, and supra-threshold hit (Fig. 2b). The conditional probabilities were compared with paired *t*-tests between neighboring conditions (correct rejection vs. near-miss, near-miss vs. near-hit, near-hit vs. supra-hit). The twelve *p*-values were FDR-corrected with a false discovery rate of 5% (Benjamini and Hochberg, 1995) and visualized with the means in Fig. 2b.

## 2.8. fMRI preprocessing

Each EPI block was preprocessed with custom bash scripts using AFNI 18.2.17, FSL 5.0.11, and FreeSurfer 6.0.0 (Cox, 1996; Fischl, 2012; Smith et al., 2004). The code is available on <http://github.com/grundm/graphCA>. After removing the initial 10 volumes, the time series

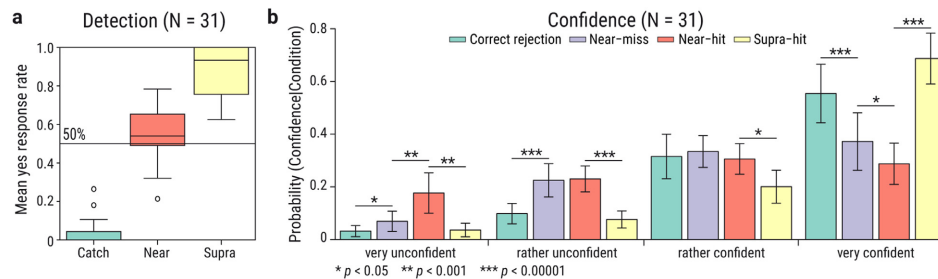


**Fig. 2.** Mean detection rate and decision confidence across participants. (a) Detection rates for each trial condition: without stimulation (catch trials) and with near- and supra-threshold stimulation. The central line indicates the median in each box. The whiskers indicate 1.5 times the interquartile range or the maximum value if smaller. Circles indicate values beyond this whisker range. (b) Mean conditional probabilities for each confidence rating given a stimulus-response condition: correct rejection (green), near-threshold misses (purple), near-threshold hits (red), and supra-threshold hits (yellow). Error bars indicate within-participants 95% confidence intervals (Morey, 2008). Horizontal lines indicate significant paired t-tests with FDR-corrected  $p$ -values between neighboring conditions (Benjamini and Hochberg, 1995).

were despiked and corrected for slice timing. Subsequently, the volumes were corrected for motion and distortion using field maps acquired at the beginning of the experiment. We applied a non-linear normalization to MNI space (AFNI 3dQwarp). Next to the realignment to correct for motion, we calculated the euclidean norm (enorm) to censor volumes with large motion for the functional connectivity and BOLD contrast analyses. Volumes were ignored when they exceeded motion  $> 0.3$  mm (enorm =  $\sqrt{\text{sum squares}}$  of motion parameters; AFNI 1d\_tool.py -censor\_motion). Compared to the framewise displacement (FD =  $\text{sum}(\text{abs})$  of motion parameters; Power et al., 2012), the euclidean norm has the advantage to represent appropriately large motion, e.g., the six parameters “6 0 0 0 0 0” and “1 1 1 1 1 1” would be the same for FD (FD = 6) in contrast to a enorm of 6 and 2.45, respectively. Modeling the functional connectivity and the BOLD contrasts was done with AFNI 19.1.05.

### 2.9. fMRI whole-brain contrast analysis

For the BOLD contrast analysis, the data was additionally smoothed with a 7-mm FWHM kernel and scaled to a mean of 100 and maximum of 200. In the final step, we calculated a nuisance regression to control for (a) motion with Friston’s 24-parameter model (Friston et al., 1996), (b) signal outliers and their derivatives, (c) each 3 first principal components of core voxels in ventricle and white matter masks separately, and (d) a constant and trends up to polynomial of degree six ( $\sim$ high-pass filter  $> 0.0046$  Hz) separately for each block.

We calculated an individual general linear model (GLM) for each participant with AFNI 3dREMLfit that combined all blocks and modeled the BOLD response as a gamma function for the following conditions: correct rejections, near-threshold misses, and near-threshold hits. A second model included confident correct rejections, confident misses, and confident hits (pooled confidence ratings of 3 and 4). Furthermore, two BOLD response regressors for the button presses of the yes/no-decision and the confidence rating were included. The regressors of the nuisance regression served as baseline regressors (AFNI 3dDeconvolve -ortvec).

The estimated regression coefficients for the aware and unaware condition were tested against each other with a mixed-effects meta-analysis (3dMEMA; Chen et al., 2012). This approach accounts for within-participant variability by using the corresponding  $t$ -statistics of the regression coefficients from each participant. Additionally, the detection rate was used as a covariate to account for the interindividual variance. The resulting volumes with  $t$ -values were corrected for multiple comparisons by thresholding voxels at  $p_{\text{voxel}} < 0.0005$  and the resulting clusters at  $k$  voxels ( $p_{\text{cluster}} = 0.05$ ). The cluster size threshold  $k$  was derived for each contrast separately based on 10,000 simulations

without a built-in math model for the spatial autocorrelation function as recommended by AFNI (for details see 3dttest++ with Clustsim option and Cox et al. (2017) as response to Eklund et al. (2016)). The rendered brain images were created with MRICron (Rorden and Brett, 2000).

### 2.10. fMRI contrast analysis in primary somatosensory cortex

Furthermore, we wanted to evaluate the BOLD signal for the near-threshold stimulation in the primary somatosensory cortex. Unlike the fMRI contrast analysis for the whole brain described above, the BOLD data was not smoothed, scaled or part of a nuisance regression. We modeled the BOLD response for all near-threshold trials and trials without stimulation (independent of the yes/no-responses). The GLMs also included one regressor for each button press. The baseline regressors were limited to (a) Friston’s 24-parameter model, (b) signal outliers and their derivatives, and (c) a constant and a linear trend separately for each block (polynomial of degree one). The estimated regression coefficients for the trials with and without near-threshold stimulation were compared with a mixed-effects meta-analysis (3dMEMA; Chen et al., 2012) that included the detection rate as a covariate. Additionally to reporting the contrast “stimulus present  $>$  absent” for the whole-brain, this analysis was limited to the right primary somatosensory cortex (Area 3b and Area 1) as defined by a multi-modal parcellation based brain atlas (Glasser et al., 2016).

### 2.11. Functional connectivity analysis

For estimating the context-dependent functional connectivity between regions of interest (ROI), we used the generalized psychophysiological interaction (gPPI; McLaren et al., 2012) without the deconvolution step, as implemented in FSL (O’Reilly et al., 2012). The deconvolution algorithm tries to estimate the underlying neural activity to match it temporally with the psychological context (Cisler et al., 2014; Gitelman et al., 2003; McLaren et al., 2012). However, it cannot be determined if this estimate is correct (Cole et al., 2013; O’Reilly et al., 2012). Furthermore, also Godwin et al. (2015) repeated their analysis without the deconvolution step. Hence, we followed the FSL implementation and convolved the psychological variable with a fixed-shaped HRF to temporally align it with the measured BOLD signal (O’Reilly et al., 2012). The gPPI model included (a) regressors for the BOLD response function for each condition, (b) a regressor for the baseline functional connectivity of a seed region of interest (ROI), and (c) regressors for the context-dependent functional connectivity of the ROI for each condition (psychophysiological interaction). For (b), the seed ROI average time series was extracted to be used as a regressor. For



(c), this baseline regressor was masked for each condition separately to generate conditional interaction regressors. The mask for each condition was equivalent to the regressor that modeled the BOLD response for the corresponding condition, hence weighting the seed time series in the post-stimulus phase with the hemodynamic response. The interaction regressors for each condition allowed the estimation of (c) the context-dependent functional connectivity by accounting for (a) the BOLD response and (b) the baseline functional connectivity (Fig. 5b). Additionally, the gPPI included baseline regressors: (a) Friston's 24-parameter model for motion, (b) signal outliers and their derivatives, and (c) a constant and a linear trend separately for each block (polynomial of degree one).

The gPPI was calculated with AFNI 3dREMLfit for a whole-brain network of 264 nodes based on a resting-state functional connectivity atlas (Power et al., 2011). The nodes were defined as 4-mm radius, spherical ROIs at the atlas' MNI coordinates. The BOLD response model was a gamma function. AFNI 3dREMLfit has the advantage of allowing for serial correlations by estimating the temporal autocorrelation structure for each voxel separately.

For each node's gPPI, the coefficients of the context-dependent functional connectivity regressors were extracted from all other nodes separately by averaging across all voxels constituting the particular node. Subsequently, the beta values were combined in a symmetric connectivity matrix for each participant and each condition. As Godwin et al. (2015), we did not assume directionality and averaged the absolute values of reciprocal connections. Subsequently, the connectivity matrices were thresholded proportionally for the strongest connections and rescaled to the range [0,1] by dividing all values by the maximum value. The figures showing nodes and edges on a glass brain (Fig. 5a,e) were created with BrainNet Viewer 1.6 (Xia et al., 2013).

After running the functional connectivity analysis as Godwin et al. (2015) for only confident trials, we repeated the analysis for all trials independent of their confidence response. Furthermore, we extended the preprocessing to include 7-mm smoothing, scaling and a nuisance regression and redid the analysis for both trial selections (confident only and all). For this analysis, the baseline regressors were (a) Friston's 24-parameter model, (b) signal outliers and their derivatives, (c) each three first principal components of core voxels in ventricle and white matter masks separately, and (d) separately for each block a constant and trends up to polynomial of degree six (~high-pass filter > 0.0046 Hz).

## 2.12. Graph-theoretical analysis

The context-dependent connectivity matrices were further processed with the Brain Connectivity Toolbox (BCT Version 2017-15-01; Rubinov and Sporns, 2010) to describe their network topologies. Across proportional thresholds (5-40%) graph metrics were calculated and normalized with the average graph metrics of 100 random networks with the same degree distribution (see BCT function `randmio_und.m` on <https://sites.google.com/site/bctnet/Home/functions>). In order to compare our results with the report for visual awareness (Godwin et al., 2015), we chose the same metrics for (a) segregation, (b) integration, and (c) centrality: (a) weighted undirected modularity (BCT function `modularity_und.m`; Newman, 2004) and weighted undirected clustering coefficient averaged over all nodes (BCT function `clustering_coef_wu.m`; Onnela et al., 2005), (b) weighted characteristic path length (BCT function `charpath.m`), and (c) weighted participation coefficient averaged over all nodes (BCT function `participation_coef.m`; Guimerà and Nunes Amaral, 2005). The participants' graph metrics were compared between each condition with the Wilcoxon's signed-rank test because the distributions of the graph metrics are unknown. The resulting 24 *p*-values for each graph metric (8 network threshold times 3 comparisons: hit vs. miss, hit vs. correct rejection, and miss vs. correct rejection) were FDR-corrected with a false discovery rate of 5% (Benjamini and Hochberg, 1995). Furthermore, we calculated the Bayes factors based

on *t*-tests with a JZS prior ( $r = \sqrt{2/2}$ ) to assess the evidence for the null hypothesis (Rouder et al., 2012).

## 3. Results

### 3.1. Behavioral data

Participants ( $N = 31$ ) detected on average 55% of the near-threshold pulses ( $SD = 13\%$ ), 88% of the supra-threshold pulses ( $SD = 12\%$ ), and correctly rejected 97% of the catch trials without stimulation ( $SD = 6.0\%$ ; Fig. 2a). Participants reported on average to be "rather confident" or "very confident" for 87% of the correct rejections ( $SD = 13\%$ ), 70% of the near-threshold misses ( $SD = 23\%$ ), 59% of the near-threshold hits ( $SD = 27\%$ ) and 89% of the supra-threshold hits ( $SD = 13\%$ ). Participants reported significantly more often "very confident" for near-threshold misses ( $M = 37.2\%$ ) than hits ( $M = 28.7\%$ , FDR-corrected  $p = 0.037$ ) and less often "very unconfident" for misses ( $M = 6.9\%$ ) than hits ( $M = 17.7\%$ , FDR-corrected  $p = 0.023$ ; Fig. 2b). The conditional probabilities for "rather unconfident" and "rather confident" did not differ between near-threshold hits and misses. Near-threshold misses and correct rejections differed in their conditional probabilities for "very unconfident", "rather unconfident" and "very confident" (Fig. 2b) indicating higher confidence for correct rejections. Also, participants were on average more confident for supra-threshold hits than near-threshold hits. Additionally, we assessed the stability of near-threshold detection and false alarms across the experiment. We used linear mixed-effects models with maximum likelihood estimation (lmer function in R) to investigate the effect of block on near-threshold hit rate (near\_yes) and false alarm rate (null\_yes). Model comparison of the model "near\_yes ~ block + (1|ID)" with the null model "near\_yes ~ 1 + (1|ID)" resulted in no significant difference ( $\chi^2 = 1.40$ ,  $p = 0.24$ ), indicating no effect of block on near-threshold hit rate. Also, for false alarms, the linear mixed-effects model "null\_yes ~ block + (1|ID)" was not significantly different compared to the null model "null\_yes ~ 1 + (1|ID)" ( $\chi^2 = 1.41$ ,  $p = 0.23$ ). Therefore, we conclude that the behavioral performance is not affected by acclimatization or mental fatigue.

### 3.2. BOLD amplitude contrasts

First, we modeled the BOLD contrast between hits and misses (Fig. 3a-c), as well as misses and correct rejections independent of the confidence rating (Fig. 3d-f). Second, we compared only confident hits and misses (Fig. 4a-c), as well as confident misses and correct rejections (Fig. 4d-f). Third, we modeled the contrast between near-threshold stimuli and trials without stimulation for the whole brain (Fig. 5) and the primary somatosensory cortex only (Fig. 6). The preprocessing for this contrast excluded smoothing, scaling or nuisance regression. For all group-level comparisons, we used the detection rate as a covariate to account for the interindividual variance (Fig. 2a).

Contrasting near-threshold hits and misses (stimulus awareness) showed a fronto-parietal network including the left inferior frontal gyrus (IIFG), the left nucleus accumbens (INAC), the left and right anterior insula (lINS1; rINS), the left and right intraparietal sulcus (lIPS1; rIPS2; rIPS) and the right precuneus (rPCUN; Fig. 3a-c, Table 1). When the statistical threshold for the family-wise error was set to  $p_{cluster} \leq 0.06$ , resulting in a decreased cluster size  $k \geq 28$ , two additional clusters were observed for hits compared to misses in the contralateral secondary somatosensory cortex (cS2) and the left precuneus (lPCUN). When comparing missed near-threshold trials with correctly rejected null trials (somatosensory processing of undetected stimuli), the contra- and ipsilateral S2 (cS2b; iS2), the left anterior insula (lINS2) and the left supplementary motor area (ISMA) showed statistically significant activations (Fig. 3d-f).

Second, we contrasted only confident hits, misses, and correct rejections. Trials were classified as confident when rated with 3 or 4 ("rather confident" or "very confident"). Since the first trial of each block was

**Table 1**

MNI coordinates for significant BOLD contrast clusters “hit > miss” and “miss > correct rejection (CR)” in Fig. 3. Correction for multiple comparisons with  $t_{\text{voxel}}(30) \geq 3.92$ ,  $p_{\text{voxel}} \leq 0.0005$  and  $p_{\text{cluster}} \leq 0.05$ , resulting in a cluster size  $k \geq 31$  for “hit > miss” and a cluster size  $k \geq 27$  for “miss > CR”. Clusters are ordered by volume (number of voxels). MNI coordinates of the maximum  $t$  value (peak) are reported in millimeters (mm) on the left-right (LR), posterior-anterior (PA) and inferior-superior (IS) axes. The mean  $t$  value is the average across all voxels of one cluster.

Contrast	Area	Label	Volume	LR	PA	IS	Mean	
Hit > miss $p_{\text{cluster}} \leq 0.05 \mid k \geq 31$ $N = 31$	Left anterior insula	lINS1	84	-35	19	-3	4.56	
	Left intraparietal sulcus	lIPS1	74	-32	-62	50	4.50	
	Right precuneus	rPCUN	64	13	-71	39	4.50	
	Left nucleus accumbens	lINAC	62	-14	10	-10	4.47	
	Left inferior frontal gyrus	lIFG	57	-44	46	4	4.54	
	Right anterior insula	rINS	54	40	19	-7	4.56	
	Right intraparietal sulcus	rIPS	42	52	-35	46	4.56	
	Left intraparietal sulcus	lIPS2	37	-50	-41	46	4.21	
	$p_{\text{cluster}} \leq 0.06 \mid k \geq 28$	Right/contralateral S2	cS2a	30	58	-20	22	4.52
		Left precuneus	lPCUN	29	-11	-71	39	4.48
Right/contralateral S2		cS2b	101	64	-20	14	4.78	
Miss > CR $p_{\text{cluster}} \leq 0.05 \mid k \geq 27$ $N = 31$	Left anterior insula	lINS2	75	-56	10	0	4.32	
	Left/ipsilateral S2	iS2	52	-68	-26	22	4.73	
	Left supplementary motor area	lISMA	32	-8	16	57	4.73	

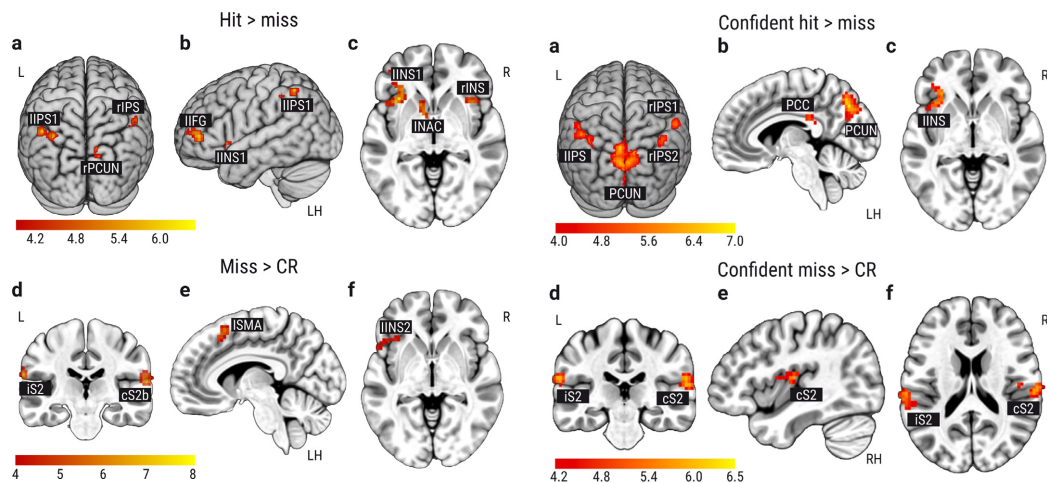


**Fig. 3.** BOLD amplitude contrasts for awareness and stimulation effect. (a–c) Contrast between near-threshold hits and misses with focus on (a) the right precuneus (rPCUN) and the left and right intraparietal sulcus (lIPS1, rIPS1), (b) the left inferior frontal gyrus (lIFG) and (c) the left nucleus accumbens (lINAC) and the left and right anterior insula (lINS1, rINS;  $z = -3$ ). Correction for multiple comparison with  $t_{\text{voxel}}(30) \geq 3.92$ ,  $p_{\text{voxel}} \leq 0.0005$  and cluster size  $k \geq 31$  ( $p_{\text{cluster}} \leq 0.05$ ). (d–f) Contrast between near-threshold misses and correct rejections (CR) of trials without stimulation. (d) Coronal view ( $y = -29$ ) with the contralateral and ipsilateral secondary somatosensory cortices (cS2, iS2). (e) Sagittal view ( $x = -7$ ) on the supplementary motor area (SMA). (f) Axial view ( $z = -3$ ) on the left anterior insula (INS). Correction for multiple comparison with  $t_{\text{voxel}}(30) \geq 3.92$ ,  $p_{\text{voxel}} \leq 0.0005$  and cluster size  $k \geq 27$  ( $p_{\text{cluster}} \leq 0.05$ ). Left (L), right (R), and the left hemisphere (LH) are indicated.

not considered for the fMRI analysis, the participants ( $N = 31$ ) had on average 28 confident hits ( $SD = 14$ ), 28 confident misses ( $SD = 15$ ), and 29 confident correct rejections ( $SD = 7$ ). For confident hits and misses, the precuneus bilaterally (PCUN), the left and the right intraparietal sulcus (lIPS, rIPS1, rIPS2), the posterior cingulate cortex (PCC) and the left anterior insula (lINS) had significant activation clusters with conscious tactile perception (Fig. 4a–c). The contralateral secondary somatosen-

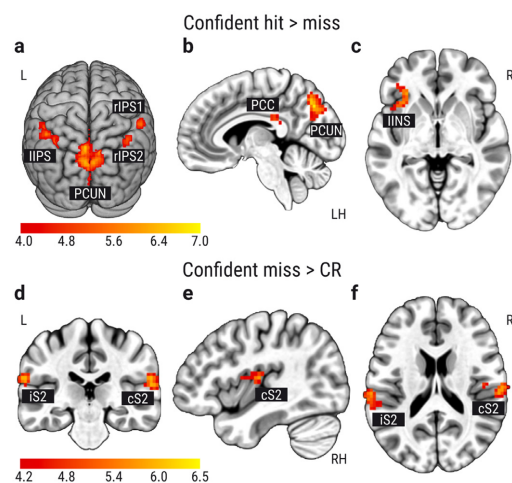


**Fig. 4.** BOLD amplitude contrasts for only confident trials. Correction for multiple comparison with  $t_{\text{voxel}}(30) \geq 3.92$ ,  $p_{\text{voxel}} \leq 0.0005$  and cluster size  $k \geq 28$  ( $p_{\text{cluster}} \leq 0.05$ ). (a–c) Contrast between confident near-threshold hits and misses with focus on (a) the precuneus (PCUN) and the intraparietal sulcus (IPS), (b) the posterior cingulate cortex (PCC;  $x = -7$ ), and (c) the left anterior insula (lINS;  $z = -3$ ). (d–f) Contrast between near-threshold misses and correct rejections (CR) of trials without stimulation. (d) Coronal view ( $y = -26$ ) with the contralateral and ipsilateral secondary somatosensory cortices (cS2; iS2). (e) Sagittal view ( $x = 41$ ) on the cS2 cluster reaching into insular cortex. (f) Axial view ( $z = 18$ ). Left (L), right (R), the left hemisphere (LH), and the right hemisphere (RH) are indicated.

sory cortex (cS2) showed activation again with the statistical threshold  $p_{\text{cluster}} \leq 0.06$  (Table 2). Confident misses showed a higher activation than confident correct rejections in the ipsilateral and contralateral secondary somatosensory cortices (iS2, cS2). The cS2 cluster was reaching into the posterior insular cortex (Fig. 4d–f).

Third, we contrasted all near-threshold and catch trials independent of their behavioral response to investigate the stimulation effect in the whole brain. In contrast to the BOLD contrast analysis above, the pre-

**Table 2**

MNI coordinates for significant BOLD contrast clusters “confident hit > miss” and “confident miss > correct rejection (CR)” in Fig. 4. Correction for multiple comparisons with  $t_{\text{voxel}}(30) \geq 3.92$ ,  $p_{\text{voxel}} \leq 0.0005$  and  $p_{\text{cluster}} \leq 0.05$ , resulting in a cluster size  $k \geq 28$ . Clusters are ordered by volume (number of voxels). MNI coordinates of the maximum  $t$  value (peak) are reported in millimeters (mm) on the left-right (LR), posterior-anterior (PA) and inferior-superior (IS) axes. The mean  $t$  value is the average across all voxels of one cluster.

Contrast	Area	Label	Volume	LR	PA	IS	Mean
Confident hit > miss	Left/right precuneus	PCUN	387	-8	-74	39	4.66
$p_{\text{cluster}} \leq 0.05 \mid k \geq 28$ $N = 31$	Left intraparietal sulcus	IIPS	137	-47	-53	50	4.43
	Left anterior insula	IINS	57	-32	28	-3	4.68
	Right intraparietal sulcus	rIIPS1	42	55	-38	50	4.46
	Posterior cingulate cortex	PCC	39	4	-35	22	4.45
	Right intraparietal sulcus	rIIPS2	34	40	-62	53	4.33
$p_{\text{cluster}} \leq 0.06 \mid k \geq 26$	Right/contralateral S2	cS2	26	61	-20	22	4.36
Confident miss > CR	Right/contralateral S2	cS2	141	64	-20	14	4.56
$p_{\text{cluster}} \leq 0.05 \mid k \geq 28$	Left/ipsilateral S2	iS2	85	-65	-26	22	4.60

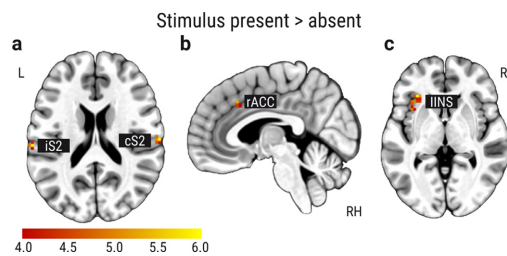


**Fig. 5.** BOLD amplitude contrast for near-threshold stimulation. Correction for multiple comparison with  $t_{\text{voxel}}(30) \geq 3.92$ ,  $p_{\text{voxel}} \leq 0.0005$  and cluster size  $k \geq 5$  ( $p_{\text{cluster}} \leq 0.05$ ). (a-c) Contrast between near-threshold stimulation trials and trials without stimulation with significant clusters in (a) the ipsilateral and contralateral secondary somatosensory cortex (iS2, cS2;  $z = 19$ ), (b) the right anterior cingulate cortex (rACC;  $x = 4$ ), and (c) the left anterior insula (lINS;  $z = 0$ ). Left (L), right (R), and the right hemisphere (RH) are indicated.

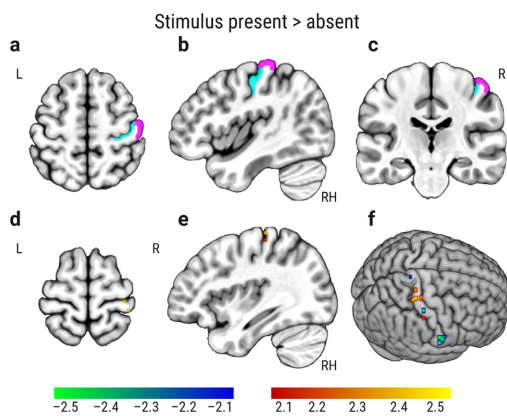


**Fig. 6.** BOLD amplitude contrast for near-threshold stimulation in the primary somatosensory cortex (Area 3b and Area 1). (a-c) Region of interest Area 3b (cyan) and Area 1 (violet,  $z = 56$ ,  $x = 43$ ,  $y = -22$ ). (d-f) Only voxels with  $t_{\text{voxel}}(30) \leq -2.045$  and  $t_{\text{voxel}}(30) \geq 2.045$ ,  $p_{\text{voxel}} \leq 0.05$  ( $z = 68$ ,  $x = 36$ ). Left (L), right (R), and the right hemisphere (RH) are indicated.

processing excluded smoothing, scaling or nuisance regression to align it with the preprocessing of the functional connectivity analysis. For the near-threshold stimulation compared to no stimulation, the ipsilateral and contralateral secondary somatosensory (iS2, cS2), the left anterior insula (lINS) and the right anterior cingulate cortex (rACC) showed significant clusters with a larger activation (Fig. 5, Table 3).

Fourth, we contrasted all near-threshold and catch trials independent of their behavioral response only within the right primary somatosensory cortex (Area 3b and Area 1). The region of interest was defined by a multi-modal brain atlas (Glasser et al., 2016). Furthermore, the preprocessing did not include smoothing, scaling, or nuisance regression. We found positive and negative significant voxels for uncorrected  $p_{\text{voxel}} \leq 0.05$  in Area 3b and Area 1. A positive voxel in the latter ( $x = 38$ ,  $y = -38$ ,  $z = 67$ ; Fig. 6) was close to previously reported peak coordinates in Area 1 ( $x = 38$ ,  $y = -40$ ,  $z = 66$ ) for electrical stimulation of the median nerve (Schröder et al., 2019). Yet, these voxels did not meet the criteria by a correction for multiple comparisons (FDR-corrected  $p \leq 0.05$  or a cluster size  $k \geq 12$  for  $p_{\text{cluster}} \leq 0.05$ ; Table 4). Additionally, a contrast of supra-threshold hits and correct rejections corrected for multiple comparisons in the whole brain ( $p_{\text{voxel}} < 0.0005$  and cluster size  $k \geq 5$ ,  $p_{\text{cluster}} \leq 0.05$ ) revealed a cluster in the contralateral primary somatosensory cortex ( $k = 6$  voxels, mean  $t = 4.27$ ) whose peak coordinates ( $x = 52$ ,  $y = -32$ ,  $z = 53$ ) were in Area 1 according to the Eickhoff-Zilles atlas (Eickhoff et al., 2005).

### 3.3. Context-Dependent Graph Measures

We assessed whether tactile conscious perception is accompanied by alterations of the brain’s functional network topology. An atlas of 264 nodes (Power et al., 2011) was used to capture the whole-brain network as in (Godwin et al., 2015), who reported decreased modularity and increased participation with visual awareness. Whole-brain functional networks were modeled for each condition with the generalized psychophysiological interaction (gPPI; McLaren et al., 2012) without the deconvolution step (O’Reilly et al., 2012); see Methods Functional Connectivity Analysis for details). The gPPI has the advantage of controlling the context-dependent functional connectivity estimates for (a) the stimulation-related BOLD response and (b) the baseline functional connectivity across the experiment (Fig. 7b). The graph-theoretical analysis of the context-dependent functional connectivity matrices was performed with the Brain Connectivity Toolbox (Rubinov and Sporns, 2010) to test for changes in the same measures of integration and segregation as in (Godwin et al., 2015). We thresholded the context-dependent connectivity matrices across a range of proportional thresholds from 5% to 40% in steps of 5% (Garrison et al., 2015) and separately calculated their normalized modularity, mean clustering coefficient, mean participation coefficient and characteristic path length (Fig. 7c-f). Since Godwin et al. (2015) analyzed the graph-theoretical

**Table 3**

MNI coordinates for significant BOLD contrast clusters “near-threshold stimulation > trials without stimulation (catch trials)” in Fig. 5. Correction for multiple comparisons with  $t_{\text{voxel}}(30) \geq 3.92$ ,  $p_{\text{voxel}} \leq 0.0005$  and  $p_{\text{cluster}} \leq 0.05$ , resulting in a cluster size  $k \geq 5$ . Clusters are ordered by volume (number of voxels). MNI coordinates of the maximum  $t$  value (peak) are reported in millimeters (mm) on the left-right (LR), posterior-anterior (PA) and inferior-superior (IS) axes. The mean  $t$  value is the average across all voxels of one cluster.

Contrast	Area	Label	Volume	LR	PA	IS	Mean
Near > catch trials	Left anterior insula	lINS	35	-35	13	4	4.64
$p_{\text{cluster}} \leq 0.05$   $k \geq 5$	Right anterior cingulate cortex	rACC	15	4	22	39	4.37
$N = 31$	Right/contralateral S2	cS2	13	64	-20	18	5.07
	Left/ipsilateral S2	iS2	6	-65	-26	18	4.62

**Table 4**

MNI coordinates for BOLD contrast clusters in the primary somatosensory cortex (Area 3b and Area 1) for “near-threshold stimulation > trials without stimulation (catch trials)” in Fig. 6. Voxel threshold  $t_{\text{voxel}}(30) \geq 2.045$  and  $t_{\text{voxel}}(30) \leq -2.045$ ,  $p_{\text{voxel}} \leq 0.05$  and cluster size  $k \geq 2$ . Clusters are ordered by displaying first the positive cluster and then the negative cluster. MNI coordinates of the maximum  $t$  value (peak) are reported in millimeters (mm) on the left-right (LR), posterior-anterior (PA) and inferior-superior (IS) axes. The mean  $t$  value is the average across all voxels of one cluster.

Contrast	Area	Label	Volume	LR	PA	IS	Mean
Near > catch trials	Right/contralateral Area 3b	A3b	2	31	-29	60	2.25
Near < catch trials	Right/contralateral Area 1	A1	7	67	-8	22	-2.63

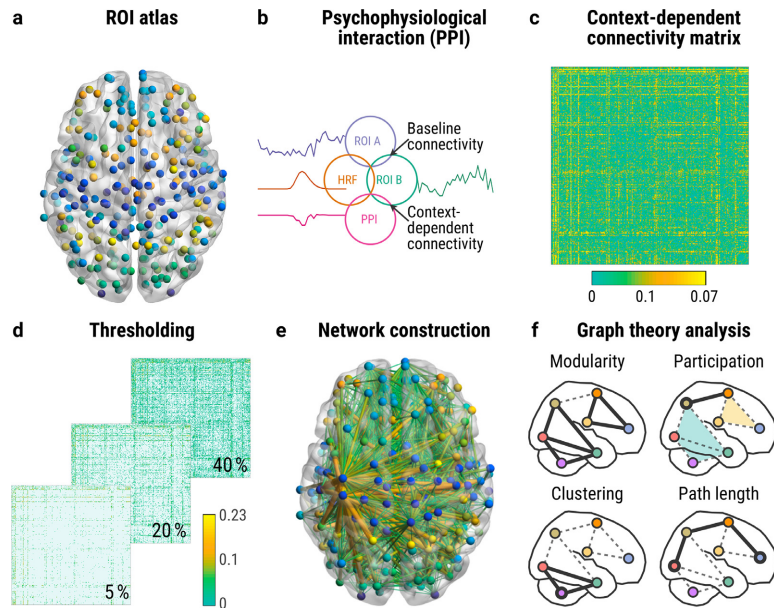


**Fig. 7.** Context-dependent functional connectivity analysis. (a) Regions of interest (ROIs) were defined as 4-mm radius spheres at the MNI coordinates of a 264-nodes atlas (Power et al., 2011). (b) We used the generalized psychophysiological interaction (gPPI; McLaren et al., 2012) to calculate the context-dependent functional connectivity between all pairs of ROIs for each condition separately (hit, miss, and correct rejection). This measure controls for baseline functional connectivity and the stimulus-evoked hemodynamic response (HRF). (c) These context-dependent functional connectivity estimates were merged into individual, normalized, symmetric functional connectivity matrices to evaluate their network topology. For the latter, the matrices were thresholded to include only the strongest edges (d), and the resulting networks (e) were analyzed with graph-theoretical measures (f). For visualization, we selected the mean context-dependent connectivity matrix for hits (e) and thresholded it proportionally with 5–40% (d) and with 5% for the visualization of the edges (e). Edge color and diameter capture the strength of functional connectivity. Fig. concept was inspired by Fig. 2 in (Uehara et al., 2014).

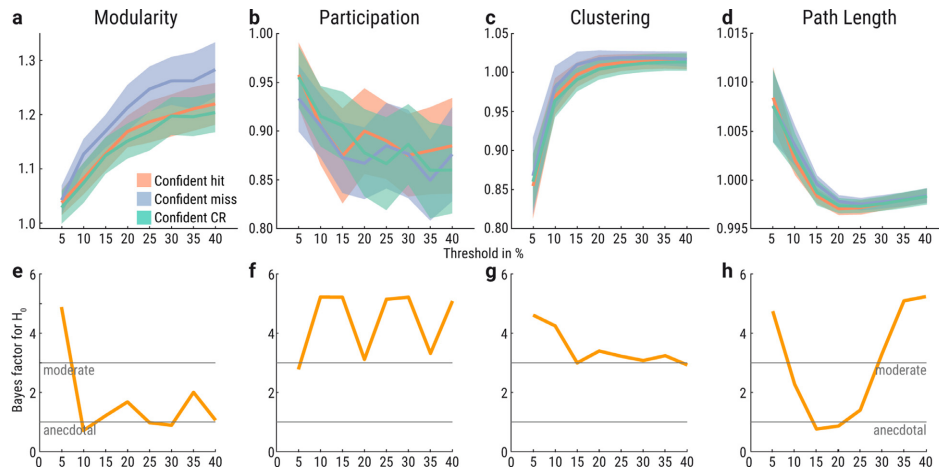


**Fig. 8.** Functional network topology of only confident hits (red), misses (purple), and correct rejections (green). (a–d) Graph measures for network thresholds from 5–40% in 5% steps (x-axes). Y-axes indicate normalized graph metric values. Confidence bands reflect within-participant 95% confidence intervals. (e–h) Bayes factors (BF<sub>01</sub>) based on paired *t*-test between confident hits and misses. Bayes factor of 2 indicates that the evidence for the null hypothesis is twice as likely compared to the alternative hypothesis given the data. Bayes factors between 1–3 are interpreted as anecdotal and between 3–10 as moderate evidence for the null hypothesis (Schönbrodt and Wagenmakers, 2018).

metrics only for confident hits and misses, we first ran the analysis for confident trials only (Fig. 8). Trials were classified as confident when the yes/no-decision was rated with 3 or 4 (“rather confident” or “very confident”). Additionally, we repeated the analysis for all trials independent of their confidence rating (Fig. 10) and with an extended preprocessing including a nuisance regression (Figs. 11, 12).

Confident hits and misses showed no significant differences in measures of global segregation into distinct networks (modularity), local segregation (clustering), integration (path length), and centrality (participation) based on paired two-sided Wilcoxon’s signed-rank tests and FDR-correction (Fig. 8a–d). Additionally, we calculated the Bayes factors based on paired *t*-tests with a JZS prior ( $r = \sqrt{2/2}$ ; Rouder et al., 2012) to evaluate the evidence for the null hypothesis ( $H_0$ : confident hits and misses do not differ). For modularity, participation, clustering, and path length, the evidence was anecdotal or moderate for the null hypothesis across the network thresholds (Fig. 8e–h). The Bayes factor for modularity was below 1 at the 10%, 25% and 30%-threshold (Fig. 8e) and hence reflecting anecdotal evidence for the alternative hypothesis. Path length had a Bayes factor below 1 at the 20%-threshold (Fig. 8h). Confident correct rejections showed no significant differences to confident misses or confident hits (Fig. 8a–d). Furthermore, we calculated the mean connectivity matrices of each condition for the 10%-network threshold to visualize the context-dependent functional connectivity estimates across all 264 nodes (Fig. 9).

Because graph metrics of the whole brain might be similar between conditions while the graph metrics of individual nodes and subnetworks differ, we normalized the averaged participation and clustering coefficients separately for each of the 14 Power et al. (2011) subnetworks. For this analysis, we chose the networks thresholded for the top 10% connections (Fig. 9). The resulting graph metrics were compared with Wilcoxon’s signed-rank tests between the three conditions while correcting for multiple comparisons with a false discovery rate of 5%. There was no significant difference in any subnetwork between confident correct rejections, misses, and hits.

We repeated the analysis for all trials independent of the confidence rating to increase the number of trials and hence the statistical power.

As in the preceding analysis (Fig. 8), we observed no significant differences in modularity, participation, clustering, and path length based on paired two-sided Wilcoxon’s signed-rank tests and FDR-correction (Fig. 10a–d). There was anecdotal to moderate evidence for the null hypothesis ( $H_0$ : hits and misses do not differ; Fig. 9e–h). Only the Bayes factors for participation at the 40%-threshold (Fig. 10f) and path length at the 20%-threshold (Fig. 10h) were below 1 and hence reflected anecdotal evidence for the alternative hypothesis. Correct rejections showed no significant differences to misses or hits (Fig. 10a–d).

In a third step, we extended the preprocessing to include smoothing, scaling and a nuisance regression as in the whole-brain BOLD contrast analysis (Figs. 3, 4). We then analyzed again the graph metrics for only confident trials (Fig. 11) and all trials independent of the confidence response (Fig. 12). For only confident trials, we observed no significant differences in modularity, participation, clustering, and path length based on paired two-sided Wilcoxon’s signed-rank tests and FDR-correction (Fig. 11a–d). There was anecdotal to moderate evidence for the null hypothesis ( $H_0$ : confident hits and misses do not differ; Fig. 8e–h). Confident correct rejections showed no significant differences to confident misses or confident hits (Fig. 11a–d).

For the extended preprocessing and all trials independent of the confidence response, hits and misses did not differ significantly in modularity, participation, clustering, and path length based on paired two-sided Wilcoxon’s signed-rank tests and FDR-correction (Fig. 12a–d). There was anecdotal or moderate evidence for the null hypothesis ( $H_0$ : hits and misses do not differ; Fig. 12e–h). Only the Bayes factors for path length at the 10% and 15%-threshold were below 1 (Fig. 12h) and hence reflected anecdotal evidence for the alternative hypothesis. The path length was higher for correct rejections than hits at the 35%-threshold (FDR-corrected  $p = 0.017$ ), and at the 40%-threshold (FDR-corrected  $p = 0.042$ ).

Furthermore, to investigate whether the atlas-based approach missed functional connectivity of subnetworks, we performed a seed-based gPPI analysis with the cS2 cluster from the contrast between near-threshold and catch trials (Fig. 5;  $x = 64$ ,  $y = -20$ ,  $z = 18$ ). We created a 4-mm radius sphere and extracted the mean BOLD time course, as in the atlas-

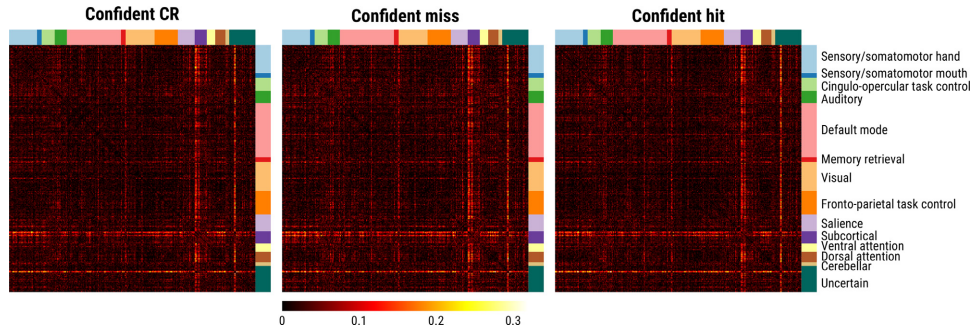


**Fig. 9.** Mean connectivity matrices of confident correct rejections (CR), misses and hits for the 10%-threshold (Fig. 8). The values represent the normalized gPPI estimates between the 264 nodes ordered by subnetworks.

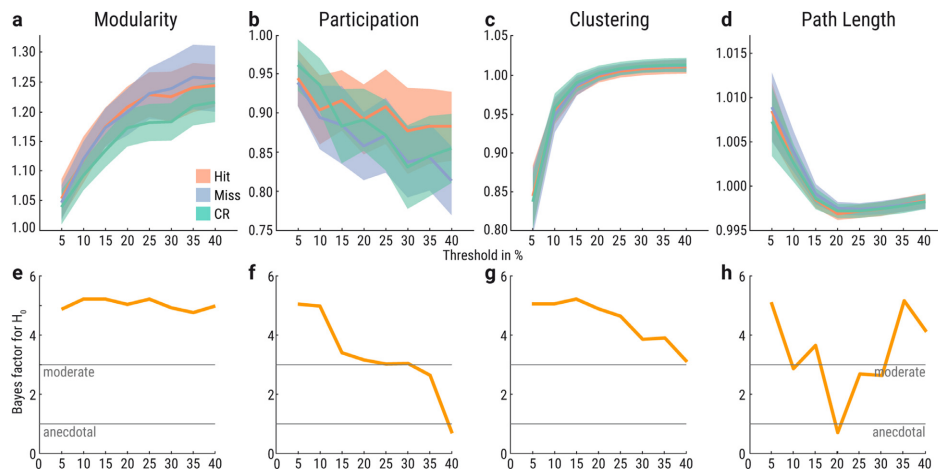


**Fig. 10.** Functional network topology of all hits (red), misses (purple), and correct rejections (green). (a-d) Graph measures for network thresholds from 5-40% in 5% steps (x-axes). Y-axes indicate normalized graph metric values. Confidence bands reflect within-participant 95% confidence intervals. (e-h) Bayes factors ( $BF_{H_0}$ ) based on paired *t*-tests between detected and undetected near-threshold trials. Bayes factors of 2 indicates that the evidence for the null hypothesis is twice as likely compared to the alternative hypothesis given the data. Bayes factors between 1-3 are interpreted as anecdotal and between 3-10 as moderate evidence for the null hypothesis (Schönbrodt and Wagenmakers, 2018).

based approach. After computing individual gPPI models, we tested the psychophysiological interaction regressors of the three conditions (confident correct rejections, misses, and hits) against each other across participants for all voxels and applied a cluster correction for multiple comparisons ( $p_{\text{voxel}} \leq 0.0005$ , cluster size  $k \geq 4$  for  $p_{\text{cluster}} \leq 0.05$ ). We did not observe any significant cluster for the cS2 functional connectivity contrast between confident hits and misses, and confident hits and correct rejections. For the contrast of confident misses and correct rejections, we found one negative significant cluster at threshold (cluster size  $k = 4$  voxels) in the right cerebellum ( $x = 7$ ,  $y = -41$ ,  $z = 17$ ). We repeated the analysis with extended preprocessing (including smoothing, scaling, and nuisance regression) and with all trials independent of their confidence response (corresponding to Fig. 11). We did not observe any significant cluster for the cS2 functional connectivity contrast between any two of the three conditions (correct rejections, misses, and hits) for  $p_{\text{voxel}} \leq 0.0005$  and  $p_{\text{cluster}} \leq 0.05$  (cluster size  $k \geq 18$  for hits vs. misses, and cluster size  $k \geq 19$  for hits vs. correct rejections, and misses vs. correct rejections). That is why we conclude that the small negative

cluster between confident misses and correct rejections is a spurious finding.

#### 4. Discussion

Using fMRI during a near-threshold somatosensory detection task, we investigated changes in local brain activity and functional brain network topology associated with conscious perception. We found that conscious somatosensory perception ('detected' compared to 'undetected' stimuli) led to higher activation in precuneus, intraparietal sulcus, insula, inferior frontal gyrus, and nucleus accumbens. The latter two showed higher activation only when all trials were included (confident and unconfident) but not with confident trials only. At a slightly looser statistical threshold ( $p = 0.06$ ) bilateral secondary somatosensory cortex also showed higher activity during conscious perception. Significant positive voxels in contralateral S1 for near-threshold stimuli were only noted in an ROI-based analysis. The graph-theoretical analysis of network topology did not provide any evidence for a difference between

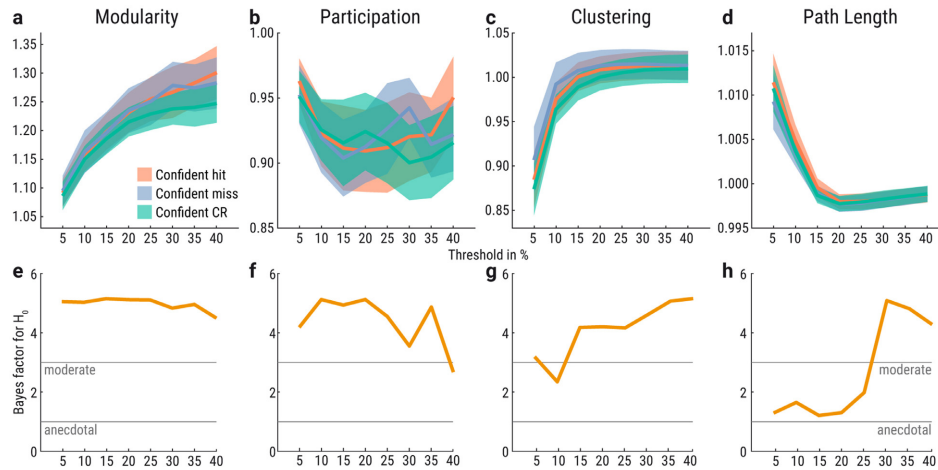


**Fig. 11.** Functional network topology of only confident hits (red), misses (purple), and correct rejections (green) with extended preprocessing. (a–d) Graph measures for network thresholds from 5–40% in 5% steps (x-axes). Y-axes indicate normalized graph metric values. Confidence bands reflect within-participant 95% confidence intervals. (e–h) Bayes factors ( $BF_{01}$ ) based on paired *t*-tests between confident detected and undetected near-threshold trials. Bayes factor of 2 indicates that the evidence for the null hypothesis is twice as likely compared to the alternative hypothesis given the data. Bayes factors between 1–3 are interpreted as anecdotal and between 3–10 as moderate evidence for the null hypothesis (Schönbrodt and Wagenmakers, 2018).

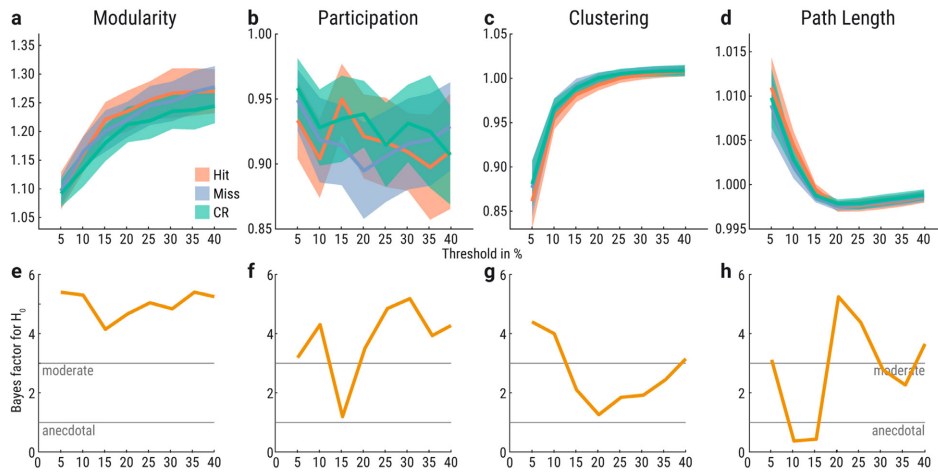


**Fig. 12.** Functional network topology of all hits (red), misses (purple), and correct rejections (green) with extended preprocessing. (a–d) Graph measures for network thresholds from 5–40% in 5% steps (x-axes). Y-axes indicate normalized graph metric values. Confidence bands reflect within-participant 95% confidence intervals. (e–h) Bayes factors ( $BF_{01}$ ) based on paired *t*-tests between detected and undetected near-threshold trials. Bayes factor of 2 indicates that the evidence for the null hypothesis is twice as likely compared to the alternative hypothesis given the data. Bayes factors between 1–3 are interpreted as anecdotal and between 3–10 as moderate evidence for the null hypothesis (Schönbrodt and Wagenmakers, 2018).

aware and unaware trials in modularity, participation, clustering, nor path length. Finally, when comparing misses with correctly rejected catch trials, we found activation of S2, insula, and supplementary area; also, in this contrast, no changes in network properties were observed. Subsequently, we first discuss the observed BOLD activity patterns and then the absent graph metric changes in comparison to the findings in the visual system using a masking paradigm by Godwin et al. (2015).

It is generally accepted, that primary and secondary somatosensory cortices (S1, S2) are necessary for somatosensory processing leading to conscious perception (Hirvonen and Palva, 2016; Moore et al., 2013). It has long been established that lesions in S1 go along with hypoesthesia (Roland, 1987). Recently, we have shown in stroke patients, that - despite intact S1 - also lesions in S2 (along with anterior and posterior insula, putamen, and subcortical white matter connections to prefrontal structures) lead to impaired tactile conscious experience (Preusser et al.,

2015). fMRI studies employing supra-threshold somatosensory stimulation - in passive or active designs - have consistently shown activation of S1 and S2 (Ruben et al., 2001). As we have previously shown, S1 and S2 are already affected by subthreshold stimuli (below the absolute detection threshold), which lead to a deactivation of these areas (Blankenburg et al., 2003). In the current study, we now show that near-threshold stimuli, which are not detected, i.e., below the response criterion (in signal detection theory terminology) for conscious detection, lead to an activation of S2 and insula (when compared to 'correct rejections' of catch trials). This leads to the interesting conclusion that non-detected stimuli lead to differential involvement of S1 and S2 depending on their intensity. Similarly, in our recent EEG study, we found that non-detected stimuli lead to a negativity 150 milliseconds after stimulation (N150) for principally detectable near-threshold stimuli but not for imperceptible stimulus intensities (Forschack et al., 2020). The N150 has been shown to originate in area S2 (Aukstulewicz et al., 2012). It will be an interesting issue for future studies whether an analysis based on objective detection paradigms (e.g., two-alternative forced-choice tasks, 2AFC) will further help to differentiate the meaning of these signal changes in S1 and S2, i.e., whether the "transition" from deactivation in S2 (and S1) to an activation is related to the "objective detection" in a criterion-free 2AFC task and the emergence of the N150. It should be noted that while others have shown that S1 represents the stimulus properties that get access to consciousness in interaction with S2 (Blankenburg et al., 2006; Moore et al., 2013; Rajaei et al., 2018; Schröder et al., 2019), we did not observe a strong stimulation effect in S1 for our near-threshold trials. This might be due to the weak stimulus intensity and stimulation "only" at the index finger in contrast to the commonly used median nerve stimulation.

For theories of consciousness, the difference between perceived versus non-perceived stimuli is most relevant. In our study, contralateral secondary somatosensory cortex (cS2) was found for both contrasts "hit > miss" and "confident hit > miss" when the statistical cluster threshold was set to  $p = 0.06$ . This finding is consistent with previous suggestions that there is additional activity in S2 with conscious detection. For example, a previous fMRI study on vibrotactile detection reported ipsilateral and contralateral S2 as the best correlate for detection success (Moore et al., 2013), and in another recent study bilateral S2 activity was best explained by a psychometric (detection) function (Schröder et al., 2019). One reason for detection-associated S2 activity might be recurrent processing (Lamme, 2006; van Gaal and Lamme, 2012). For example, in an EEG study, the detection of near-threshold electrical pulses to the finger was best explained by the recurrent processing between contralateral S1 and S2, as well as contralateral and ipsilateral S2 (Aukstulewicz et al., 2012). Another explanation might be that separate parts of the secondary somatosensory cortex might serve different functions. E.g., in a recent study, more inferior and superior parts of cS2 correlated with a binary detection function, and more posterior and anterior parts of cS2 correlated with a linear intensity function (Schröder et al., 2019).

While our data overall agree with the necessity of S1 and S2 activation for conscious perception, it is less clear whether activation of these areas is sufficient for conscious somatosensory perception: The fact that certain areas "best explain" detection in an fMRI study (Schröder et al., 2019), does not rule out that the activity of other areas is also involved in the conscious experience. Like several previous studies on conscious perception in other sensory domains (Bisenius et al., 2015; Dehaene and Changeux, 2011; Naghavi and Nyberg, 2005; Rees et al., 2002), we find fronto-parietal areas more active in the 'detected versus missed' contrast. Among these, the activations in left and right intraparietal sulcus, the bilateral posterior cingulate cortices, and the bilateral precuneus are consistent with the notion of a "posterior hot zone" for conscious experience as suggested by Koch and colleagues (Koch et al., 2016). Koch et al. (2016) argue that the increased activity that is seen with conscious perception in additional (e.g., frontal) brain areas is related to response preparation, and/or other task-related activations (confi-

dence, etc.) as they have not been found activated in a no-response paradigm (Frässle et al., 2014). For example, in our study, the nine-second period between stimulation and response most likely leads to increased activity in areas involved in working memory (see, e.g., tac-spatial sketchpad, Schmidt and Blankenburg, 2018). Recent literature has pointed out this interrelation: the default mode network (e.g., posterior cingulate cortex) supports a stronger global workspace configuration, which improves working memory performance (Vatansever et al., 2015) and might be beneficial for conscious perception. On the other hand, even if one assumes that a "pure sensory conscious experience" could arise from a "posterior hot zone" only, the increased activity in other brain areas with conscious perception - still leaves the possibility of conscious experience related to action, confidence, working memory etc. to be dependent on e.g., frontal brain areas (Frith, 2019). In this view, the "integrated conscious experience" during a task would then be related to the entire fronto-parietal network. Obviously, this notion is close to the global workspace theory (Dehaene et al., 2006; Dehaene and Changeux, 2011; Mashour et al., 2020). While our data do not allow to definitely differentiate between these major theories of consciousness, we provide new information for somatosensory conscious perception, which is consistent with the idea that domain-general areas (interacting with domain-specific areas for example via recurrent processing (Lamme, 2006; van Gaal and Lamme, 2012) play a role for conscious perception.

A major hypothesis underlying our study was that conscious perception goes along with widespread changes in graph metrics as it has recently been reported by Godwin et al. (2015) for the visual system. However, we did not observe such context-dependent functional connectivity changes that result in network topology alterations through modularity, participation, clustering and path length between hits, misses or correct rejections. This does not change when the number of trials is increased by considering all trials independent of their confidence response (Fig. 10). Also, improving the preprocessing with a nuisance regression that controls for motion and noise components derived from white matter and ventricles, does not affect this result (Figs. 11, 12). The isolated network topology differences between correct rejections and hits at the 35-40%-threshold for path length with the improved preprocessing (Fig. 12d) were not consistent across thresholds and not present in the analysis of only confident trials (Fig. 11), as well as in the analyses with the basic preprocessing (Figs. 8, 10). That is why we do not interpret these differences as a valid and reliable effect. Thus, there was neither a functional network alteration by stimulus awareness (hit > miss) nor by the detected (hit > CR) or undetected stimulation (miss > CR).

Two apparent differences between the study of Godwin et al. (2015) and our study are the somatosensory versus visual modality and the use of a masking paradigm (Godwin et al.) as opposed to near-threshold stimuli. However, assuming that the connectivity changes observed by Godwin et al. are related to the conscious experience, it is difficult to see why those differences should explain the different results. One possible reason why Godwin et al. observed whole-brain network topology alterations for visual awareness might be the unbalanced physical similarity between aware and unaware trials. Hits and misses originated from two different masking conditions: backward masking generated 83% of all hits and forward masking 84% of all misses. Additionally, their total number of trials for 24 participants was not balanced (276 confident misses vs. 486 confident hits). In contrast, our study did not rely on masking the target stimulus and resulted in a balanced total amount of 882 confident misses and 870 confident hits for 31 participants (Figs. 8, 10). Furthermore, we also present the results of 1507 hits, and 1190 misses independent of the confidence rating (Figs. 10, 11). Future studies investigating visual awareness may be able to distill conscious percepts for present stimuli without confounding masking conditions, for instance taking advantage of sub-millisecond precision of modern tachistoscopes (Sperdin et al., 2013). Awaiting such studies as well as



further studies on the somatosensory system and acknowledging – of course – that “absence of proof” is not “proof of absence” – our study cannot provide support for changes in graph metrics with awareness.

In summary (integrating our previous findings on the effect of sub-threshold stimulation (Blankenburg et al., 2003; Taskin et al., 2008), there seem to be three discernable stages of fMRI-BOLD signal changes with increasing somatosensory stimulus intensity: (i) A deactivation of S1, S2 following (trains of) subthreshold (never-detected) stimuli, (ii) activation of S1, S2, and insula following near-threshold not-detected stimuli, (iii) additional activation of S1, S2 accompanied by activation of a fronto-parietal (likely to be domain-general) network when stimuli are consciously perceived. The potentially differential contribution of the involved brain areas to the conscious experience should be subject to future investigations in which modulations of different aspects of the tasks (e.g., varying delay, way of report, design e.g., 2AFC versus yes/no task) may be employed. Our study could not confirm changes in graph metrics with awareness for the somatosensory system. Whether this is related to the specific somatosensory modality (electrical nerve stimulation) or the weak stimulation should be investigated by future studies. We think that the data of electrical finger nerve stimulation - despite its limited spatial extent - is a useful model for a range of somatosensory receptors in the fingers, because the nerve integrating the receptor signals is directly stimulated. This view is also supported by similar topographical activation patterns for passive proprioceptive stimulation compared with tactile stimulation (Nasrallah et al., 2019). The potentially differential contribution of the involved brain areas to the conscious experience of electrical stimuli is in line with global broadcasting of individual content of consciousness across the brain without substantial reconfiguration of the brain's network topology resulting in an integrative conscious experience - at least for the observed somatosensory submodality.

#### Declaration of Competing Interest

The authors declare no competing financial interest.

#### CRediT authorship contribution statement

**Martin Grund:** Conceptualization, Methodology, Investigation, Project administration, Software, Data curation, Formal analysis, Visualization, Writing - original draft, Writing - review & editing. **Norman Förschack:** Conceptualization, Methodology, Writing - review & editing. **Till Nierhaus:** Conceptualization, Methodology, Writing - review & editing. **Arno Villringer:** Conceptualization, Methodology, Supervision, Writing - review & editing, Funding acquisition.

#### Acknowledgements

The research was funded by the Max Planck Society. We thank Ramona Menger, Anke Kummer, Mandy Jochemko, and Nicole Pampus for their data acquisition support; Bettina Johst, Hendrik Grunert, and Jöran Lepsius for their technical advice; Heike Schmidt-Duderstedt and Kerstin Flake for preparing the figures for publication; and Joshua Grant for proofreading and commenting.

#### References

Aru, J., Bachmann, T., Singer, W., Melloni, L., 2012. Distilling the neural correlates of consciousness. *Neurosci. Biobehav. Rev.* 36, 737–746. doi:10.1016/j.neubiorev.2011.12.003.

Auksztulewicz, R., Spitzer, B., Blankenburg, F., 2012. Recurrent neural processing and somatosensory awareness. *J. Neurosci.* 32, 799–805. doi:10.1523/JNEUROSCI.3974-11.2012.

Baars, B.J., 1988. *A Cognitive Theory of Consciousness*. Cambridge [England]; New York: Cambridge University Press.

Bassett, D.S., Sporns, O., 2017. Network neuroscience. *Nat. Neurosci.* 20, 353–364. doi:10.1038/nm.4502.

Benjamini, Y., Hochberg, Y., 1995. Controlling the false discovery rate: a practical and powerful approach to multiple testing. *R. Stat. Soc. Series B Methodol.* 57, 289–300. doi:10.2307/2346101.

Bisenius, S., Trapp, S., Neumann, J., Schroeter, M.L., 2015. Identifying neural correlates of visual consciousness with ALE meta-analyses. *NeuroImage* 122, 177–187. doi:10.1016/j.neuroimage.2015.07.070.

Blankenburg, F., Ruff, C.C., Deichmann, R., Rees, G., Driver, J., 2006. The cutaneous rabbit illusion affects human primary sensory cortex somatotopically. *PLoS Biol.* 4, e69. doi:10.1371/journal.pbio.0040069.

Blankenburg, F., Taskin, B., Ruben, J., Moosmann, M., Ritter, P., Curio, G., Villringer, A., 2003. Imperceptible stimuli and sensory processing impediment. *Science* 299, 1864. doi:10.1126/science.1080806, -1864.

Boly, M., Massimini, M., Tsuchiya, N., Postle, B.R., Koch, C., Tononi, G., 2017. Are the neural correlates of consciousness in the front or in the back of the cerebral cortex? Clinical and neuroimaging evidence. *J. Neurosci.* 37, 9603–9613. doi:10.1523/JNEUROSCI.3218-16.2017.

Bullmore, E.T., Bassett, D.S., 2011. Brain graphs: graphical models of the human brain connectome. *Annu. Rev. Clin. Psychol.* 7, 113–140. doi:10.1146/annurev-clinpsy-040510-143934.

Casali, A.G., Gosseries, O., Rosanova, M., Boly, M., Sarasso, S., Casali, K.R., Casarotto, S., Bruno, M.-A., Laureys, S., Tononi, G., Massimini, M., 2013. A theoretically based index of consciousness independent of sensory processing and behavior. *Sci. Transl. Med.* 5, doi:10.1126/scitranslmed.3006294, 198ra105–198ra105.

Chen, G., Saad, Z.S., Nath, A.R., Beauchamp, M.S., Cox, R.W., 2012. fMRI group analysis combining effect estimates and their variances. *NeuroImage* 60, 747–765. doi:10.1016/j.neuroimage.2011.12.060.

Cisler, J.M., Bush, K., Steele, J.S., 2014. A comparison of statistical methods for detecting context-modulated functional connectivity in fMRI. *NeuroImage* 84, 1042–1052. doi:10.1016/j.neuroimage.2013.09.018.

Cole, M.W., Reynolds, J.R., Power, J.D., Repovs, G., Anticevic, A., Braver, T.S., 2013. Multi-task connectivity reveals flexible hubs for adaptive task control. *Nat. Neurosci.* 16, 1348–1355. doi:10.1038/nrn.3470.

Cox, R.W., 1996. AFNI: software for analysis and visualization of functional magnetic resonance neuroimages. *Comput. Biomed. Res.* 29, 162–173. doi:10.1006/cbmr.1996.0014.

Cox, R.W., Chen, G., Glen, D.R., Reynolds, R.C., Taylor, P.A., 2017. fMRI clustering in AFNI: false-positive rates redux. *Brain Connect.* 7, 152–171. doi:10.1089/brain.2016.0475.

Dehaene, S., Changeux, J.-P., 2011. Experimental and theoretical approaches to conscious processing. *Neuron* 70, 200–227. doi:10.1016/j.neuron.2011.03.018.

Dehaene, S., Changeux, J.-P., Naccache, L., Sackur, J., Sergent, C., 2006. Conscious, pre-conscious, and subliminal processing: a testable taxonomy. *Trends Cogn. Sci.* 10, 204–211. doi:10.1016/j.tics.2006.03.007.

De Ridder, D., Van Laere, K., Dupont, P., Menovsky, T., Van de Heyning, P., 2007. Visualizing out-of-body experience in the brain. *N. Engl. J. Med.* 357, 1829–1833. doi:10.1056/NEJMo070010.

Eickhoff, S.B., Stephan, K.E., Mohlberg, H., Grefkes, A., Fink, G.R., Amunts, K., Zilles, K., 2005. A new SPM toolbox for combining probabilistic cytoarchitectonic maps and functional imaging data. *NeuroImage* 25, 1325–1335. doi:10.1016/j.neuroimage.2004.12.034.

Eklund, A., Nichols, T.E., Knutsson, H., 2016. Cluster failure: Why fMRI inferences for spatial extent have inflated false-positive rates. *Proc. Natl. Acad. Sci. U.S.A.* 113, 7900–7905. doi:10.1073/pnas.1602413113.

Fischl, B., 2012. FreeSurfer. *NeuroImage* 62, 774–781. doi:10.1016/j.neuroimage.2012.01.021.

Förschack, N., Nierhaus, T., Müller, M.M., Villringer, A., 2020. Dissociable neural correlates of stimulation intensity and detection in somatosensation. *NeuroImage*, 116908. doi:10.1016/j.neuroimage.2020.116908.

Förschack, N., Nierhaus, T., Müller, M.M., Villringer, A., 2017. Alpha-band brain oscillations shape the processing of perceptible as well as imperceptible somatosensory stimuli during selective attention. *J. Neurosci.* 37, 6983–6994. doi:10.1523/JNEUROSCI.2582-16.2017.

Frässle, S., Sommer, J., Jansen, A., Naber, M., Einhäuser, W., 2014. Binocular rivalry: frontal activity relates to introspection and action but not to perception. *J. Neurosci.* 34, 1738–1747. doi:10.1523/JNEUROSCI.4403-13.2014.

Friston, K.J., Williams, S., Howard, R., Frackowiak, R.S., Turner, R., 1996. Movement-related effects in fMRI time-series. *Magn. Reson. Med.* 35, 346–355.

Frith, C.D., 2019. The neural basis of consciousness. *Psychol. Med.* 133, 1–13. doi:10.1017/S0033291719002204.

Garrison, K.A., Scheinost, D., Finn, E.S., Shen, X., Constable, R.T., 2015. The (in)stability of functional brain network measures across thresholds. *NeuroImage* 118, 651–661. doi:10.1016/j.neuroimage.2015.05.046.

Gitelman, D.R., Penny, W.D., Ashburner, J., Friston, K.J., 2003. Modeling regional and psychophysiological interactions in fMRI: the importance of hemodynamic deconvolution. *NeuroImage* 19, 200–207. doi:10.1016/S1053-8119(03)00058-2.

Glasser, M.F., Coalson, T.S., Robinson, E.C., Hacker, C.D., Harwell, J., Yacoub, E., Ugurbil, K., Andersson, J., Beckmann, C.F., Jenkinson, M., Smith, S.M., Van Essen, D.C., 2016. A multi-modal parcellation of human cerebral cortex. *Nature* 536, 171–178. doi:10.1038/nature18933.

Godwin, D., Barry, R.L., Marois, R., 2015. Breakdown of the brain's functional network modularity with awareness. *Proc. Natl. Acad. Sci. U.S.A.* 112, 3799–3804. doi:10.1073/pnas.1414466112.

Guimera, R., Nunes Amaral, L.A., 2005. Functional cartography of complex metabolic networks. *Nature* 433, 895–900. doi:10.1038/nature03288.

Hirvonen, J., Palva, S., 2016. Cortical localization of phase and amplitude dynamics predicting access to somatosensory awareness. *Hum. Brain Mapp.* 37, 311–326. doi:10.1002/hbm.23033.

- Ionta, S., Martuzzi, R., Salomon, R., Blanke, O., 2014. The brain network reflecting bodily self-consciousness: a functional connectivity study. *Soc. Cogn. Affect. Neurosci.* 9, 1904–1913. doi:10.1093/scan/nst185.
- Kingdom, F.A.A., Prins, N., 2009. *Psychophysics*. Academic Press Inc, London.
- Kleiner, M., Brainard, D., Pelli, D., Ingling, A., Murray, R., Broussard, C., 2007. What's new in psychtoolbox-3. *Perception* 36, 1–16.
- Koch, C., Massimini, M., Boly, M., Tononi, G., 2016. Neural correlates of consciousness: progress and problems. *Nat. Rev. Neurosci.* 17, 307–321. doi:10.1038/nrn.2016.22.
- Lamme, V.A.F., 2006. Towards a true neural stance on consciousness. *Trends Cogn. Sci.* 10, 494–501. doi:10.1016/j.tics.2006.09.001.
- Martuzzi, R., van der Zwaag, W., Dieguez, S., Serino, A., Gruetter, R., Blanke, O., 2015. Distinct contributions of Brodmann areas 1 and 2 to body ownership. *Soc. Cogn. Affect. Neurosci.* 10, 1449–1459. doi:10.1093/scan/nsv031.
- Mashour, G.A., Roelfsema, P., Changeux, J.-P., Dehaene, S., 2020. Conscious processing and the global neuronal workspace hypothesis. *Neuron* 105, 776–798. doi:10.1016/j.neuron.2020.01.026.
- McLaren, D.G., Ries, M.L., Xu, G., Johnson, S.C., 2012. A generalized form of context-dependent psychophysiological interactions (gPPI): a comparison to standard approaches. *NeuroImage* 61, 1277–1286. doi:10.1016/j.neuroimage.2012.03.068.
- Moeller, S., Yacoub, E., Olman, C.A., Auerbach, E., Strupp, J., Harel, N., Ugurbil, K., 2010. Multiband multislice GE-EPI at 7 tesla, with 16-fold acceleration using partial parallel imaging with application to high spatial and temporal whole-brain fMRI. *Magn. Reson. Med.* 63, 1144–1153. doi:10.1002/mrm.22361.
- Moore, C.J., Crosier, E., Greve, D.N., Savoy, R., Merzenich, M.M., Dale, A.M., 2013. Neurocortical correlates of vibrotactile detection in humans. *J. Cognit. Neurosci.* 25, 49–61. doi:10.1162/jocn.2012.00315.
- Morey, R.D., 2008. Confidence intervals from normalized data: a correction to Cousineau (2005). *Tutor. Quant. Methods Psychol.* 61–64.
- Naghavi, H.R., Nyberg, L., 2005. Common fronto-parietal activity in attention, memory, and consciousness: shared demands on integration? *Conscious Cogn.* 14, 390–425. doi:10.1016/j.concog.2004.10.003.
- Nasrallah, F.A., Mohamed, A.Z., Campbell, M.E., Yap, H.K., Yeow, C.-H., Lim, J.H., 2019. Functional connectivity of brain associated with passive range of motion exercise: Proprioceptive input promoting motor activation? *NeuroImage* 202, 116023. doi:10.1016/j.neuroimage.2019.116023.
- Newman, M.E.J., 2004. Analysis of weighted networks. *Phys. Rev. E* 70, 056131. doi:10.1103/PhysRevE.70.056131.
- Nierhaus, T., Forschack, N., Piper, S.K., Holtze, S., Krause, T., Taskin, B., Long, X., Stelzer, J., Margulies, D.S., Steinbrink, J., Villringer, A., 2015. Imperceptible somatosensory stimulation alters sensorimotor background rhythm and connectivity. *J. Neurosci.* 35, 5917–5925. doi:10.1523/JNEUROSCI.3806-14.2015.
- Oldfield, R.C., 1971. The assessment and analysis of handedness: the Edinburgh inventory. *Neuropsychologia* 9, 97–113. doi:10.1016/0028-3932(71)90067-4.
- Onnela, J.-P., Saramäki, J., Kertész, J., Kaski, K., 2005. Intensity and coherence of motifs in weighted complex networks. *Phys. Rev. E* 71, 065103. doi:10.1103/PhysRevE.71.065103.
- O'Reilly, J.X., Woolrich, M.W., Behrens, T.E.J., Smith, S.M., Johansen-Berg, H., 2012. Tools of the trade: psychophysiological interactions and functional connectivity. *Soc. Cogn. Affect. Neurosci.* 7, 604–609. doi:10.1093/scan/nss055.
- Park, H.-D., Blanke, O., 2019. Coupling inner and outer body for self-consciousness. *Trends Cogn. Sci.* 23, 377–388. doi:10.1016/j.tics.2019.02.002.
- Power, J.D., Barnes, K.A., Snyder, A.Z., Schlaggar, B.L., Petersen, S.E., 2012. Spurious but systematic correlations in functional connectivity MRI networks arise from subject motion. *NeuroImage* 59, 2142–2154. doi:10.1016/j.neuroimage.2011.10.018.
- Power, J.D., Cohen, A.L., Nelson, S.M., Wig, G.S., Barnes, K.A., Church, J.A., Vogel, A.C., Laumann, T.O., Miezin, F.M., Schlaggar, B.L., Petersen, S.E., 2011. Functional network organization of the human brain. *Neuron* 72, 665–678. doi:10.1016/j.neuron.2011.09.006.
- Preusser, S., Thiel, S.D., Rook, C., Roggenhofer, E., Kosatschek, A., Draganski, B., Blankenburg, F., Driver, J., Villringer, A., Pleger, B., 2015. The perception of touch and the ventral somatosensory pathway. *Brain* 138, 540–548. doi:10.1093/brain/awu370.
- Rajaei, N., Aoki, N., Takahashi, H.K., Miyaoka, T., Kochiyama, T., Ohka, M., Sadato, N., Kitada, R., 2018. Brain networks underlying conscious tactile perception of textures as revealed using the velvet hand illusion. *Hum. Brain Mapp.* 39, 4787–4801. doi:10.1002/hbm.24323.
- Rees, G., Kreiman, G., Koch, C., 2002. Neural correlates of consciousness in humans. *Nat. Rev. Neurosci.* 3, 261–270. doi:10.1038/nrn783.
- Roland, P.E., 1987. Somatosensory detection in patients with circumscribed lesions of the brain. *Exp. Brain Res.* 66, 303–317. doi:10.1007/BF00243307.
- Ronchi, R., Bello-Ruiz, J., Lukowska, M., Herbelin, B., Cabrilo, I., Schaller, K., Blanke, O., 2015. Right insular damage decreases heartbeat awareness and alters cardio-visual effects on bodily self-consciousness. *Neuropsychologia* 70, 11–20. doi:10.1016/j.neuropsychologia.2015.02.010.
- Rorden, C., Brett, M., 2000. Stereotaxic display of brain lesions. *Behav. Neurol.* 12, 191–200.
- Rouder, J.N., Morey, R.D., Speckman, P.L., Province, J.M., 2012. Default Bayes factors for ANOVA designs. *J. Math. Psychol.* 56, 356–374. doi:10.1016/j.jmp.2012.08.001.
- Ruben, J., Schwiemann, J., Deuchert, M., Meyer, R., Krause, T., Curio, G., Villringer, K., Kurth, R., Villringer, A., 2001. Somatotopic organization of human secondary somatosensory cortex. *Cereb. Cortex* 11, 463–473.
- Rubinow, M., Sporns, O., 2010. Complex network measures of brain connectivity: uses and interpretations. *NeuroImage* 52, 1059–1069. doi:10.1016/j.neuroimage.2009.10.003.
- Sadaghiani, S., Poline, J.-B., Kleinschmidt, A., D'Esposito, M., 2015. Ongoing dynamics in large-scale functional connectivity predict perception. *Proc. Natl. Acad. Sci. U.S.A.* 112, 8463–8468. doi:10.1073/pnas.1420687112.
- Schmidt, T.T., Blankenburg, F., 2018. Brain regions that retain the spatial layout of tactile stimuli during working memory - A 'tactospacial sketchpad'? *NeuroImage* 178, 531–539. doi:10.1016/j.neuroimage.2018.05.076.
- Schönbrodt, F.D., Wagenmakers, E.-J., 2018. Bayes factor design analysis: planning for compelling evidence. *Psychon. Bull. Rev.* 25, 128–142. doi:10.3758/s13423-017-1230-y.
- Schröder, P., Schmidt, T.T., Blankenburg, F., 2019. Neural basis of somatosensory target detection independent of uncertainty, relevance, and reports. *eLife* 8, 34. doi:10.7554/eLife.43410.
- Schubert, R., Blankenburg, F., Lemm, S., Villringer, A., Curio, G., 2006. Now you feel it - now you don't: ERP correlates of somatosensory awareness. *Psychophysiology* 43, 31–40. doi:10.1111/j.1469-8986.2006.00379.x.
- Setsompop, K., Gagoski, B.A., Polimeni, J.R., Witzel, T., Wedeen, V.J., Wald, L.L., 2012. Blipped-controlled aliasing in parallel imaging for simultaneous multislice echo planar imaging with reduced g-factor penalty. *Magn. Reson. Med.* 67, 1210–1224. doi:10.1002/mrm.23097.
- Smith, S.M., Jenkinson, M., Woolrich, M.W., Beckmann, C.F., Behrens, T.E.J., Johansen-Berg, H., Bannister, P.R., De Luca, M., Drobnjak, I., Flitney, D.E., Niazy, R.K., Saunders, J., Vickers, J., Zhang, Y., De Stefano, N., Brady, J.M., Matthews, P.M., 2004. Advances in functional and structural MR image analysis and implementation as FSL. *NeuroImage* 23 (Suppl 1), S208–S219. doi:10.1016/j.neuroimage.2004.07.051.
- Sperdin, H.F., Repnow, M., Herzog, M.H., Landis, T., 2013. An LCD tachistoscope with submillisecond precision. *Behav. Res. Methods* 45, 1347–1357. doi:10.3758/s13428-012-0311-0.
- Taskin, B., Holtze, S., Krause, T., Villringer, A., 2008. Inhibitory impact of subliminal electrical finger stimulation on SI representation and perceptual sensitivity of an adjacent finger. *NeuroImage* 39, 1307–1313. doi:10.1016/j.neuroimage.2007.09.039.
- van Gaal, S., Lamme, V.A.F., 2012. Unconscious high-level information processing: implication for neurobiological theories of consciousness. *Neuroscientist* 18, 287–301. doi:10.1177/1073858411404079.
- Vatanssever, D., Menon, D.K., Manktelow, A.E., Sahakian, B.J., Stamatakis, E.A., 2015. Default mode dynamics for global functional integration. *J. Neurosci.* 35, 15254–15262. doi:10.1523/JNEUROSCI.2135-15.2015.
- Weisz, N., Wühle, A., Monitola, G., Demarchi, G., Frey, J., Popov, T., Braun, C., 2014. Prestimulus oscillatory power and connectivity patterns predispose conscious somatosensory perception. *Proc. Natl. Acad. Sci. U.S.A.* 111, E417–E425. doi:10.1073/pnas.1317267111.
- Xia, M., Wang, J., He, Y., 2013. BrainNet Viewer: a network visualization tool for human brain connectomics. *PLoS ONE* 8, e68910. doi:10.1371/journal.pone.0068910.

## Chapter 5

### 5 General Discussion

Studying consciousness seems to be far away for empirical researchers at first glance. Yet, the present thesis shows that it is possible to get closer with experimental work which distills the determinants and consequences of conscious tactile perception. As the exploration of new places on earth (e.g., deep sea) is enabled by technological advancements, this thesis built upon new developments in software-based experimental control, physiological data acquisition, and statistical modeling. Thus, to our knowledge, this thesis includes the first automated studies of (a) tactile conscious perception uniformly sampled across the cardiac and respiratory cycle (*Study 1* and *Study 2*), and (b) post-stimulus brain activity data in terms of graph metrics based on functional magnetic resonance imaging (*Study 3*). All studies, presented in Chapter 2-4, went through rigorous peer review which was able to rule out errors and to improve the research quality of this thesis. In the following, first, the main research questions and hypotheses will be addressed. Second, the general conclusions for the goals of the thesis will be discussed: improving our understanding of (a) interactions between bodily signals and conscious tactile perception, and (b) neural correlates accompanying conscious tactile perception.

#### **5.1 Does conscious tactile perception vary across the cardiac cycle?**

Contrary to my original belief when we started this line of research, we found near-threshold tactile detection to be decreased during systole and increased during diastole (*Study 1*). This variation of perceptual reports was replicated in *Study 2* and by two other studies of our group (Al et al., 2020, 2021) which speaks for a reliable effect at hand for studying the mechanisms of external and internal signal integration in the human brain.

## General Discussion

Given the data of *Study 1* and *2*, we must reject *Hypothesis 1* "Conscious tactile perception does not vary across the cardiac cycle". In *Study 1*, we discussed whether the perceptual attenuation effect during systole might be explained by the visceral afferent feedback hypothesis (Edwards et al., 2009; Lacey & Lacey, 1978), which argues that baroreceptor firing associated with the pulse wave leads to general cortical inhibition of sensory processing in the brain. Baroreceptor firing was estimated to be present 90-390 ms after the R-peak, with a maximum at 250 ms (Edwards et al., 2009). In *Study 2*, we were able to pinpoint the time window of decreased detection 250-300 ms after the R-peak to the pulse wave arrival onset in the finger pad. Additional to maximum baroreceptor firing, this is the very same time window when perceived heartbeat sensations (R+200-300 ms) are temporally estimated (Brener & Kluitse, 1988; Ring & Brener, 1992; Yates et al., 1985). That is why next to general cortical inhibition (visceral afferent feedback hypothesis), baroreceptor firing starting at 90 ms after the R-peak might inform predictions about upcoming heartbeat sensations and associated bodily changes (interoceptive predictive coding), e.g., finger pulsation and modulation of afferent fibers in the finger pad (Macefield, 2003). Subsequently, these interoceptive predictive coding models lead to a perceptual suppression of tactile stimuli (signal) as expected "noise", i.e., heartbeat-related sensations or pulse wave-associated bodily changes. Furthermore, we could show in *Study 2* that the increased detection during diastole relied on an increased probability of confident hits. Perceptual confidence was shown to be an integration of both external sensory signals and embodied states (Allen et al., 2016). Taken together with our findings of unchanged early ERPs across the cardiac cycle (Al et al., 2020), we interpret our observations in *Study 1* and *2* as evidence for a cardiac modulation of cognitive processes which integrate internal and external signals into a unified conscious percept (Allen et al., 2019).

## 5.2 Does conscious tactile perception vary across the respiration cycle?

In *Study 2*, we observed that (a) expected stimulus onsets occurred more likely during late inspiration / early expiration and that (b) tactile detection rate was increased in early expiration. This observation speaks for an adapted respiration rhythm to improve detection task performance and hence confirms *Hypothesis 2* "Respiration rhythm is locked to the paradigm to optimize task performance". Interestingly this pattern matched the period of highest heart rate across the respiration cycle due to sinus arrhythmia. Also, this period is presumably the phase of highest alertness and cortical excitability (Kluger et al., 2021). While the timing of our cardiac cycle cannot be modulated intentionally, our respiration can be controlled. We can decide when to inhale, when to hold our breath, and when to exhale. This possibility seems to be deployed (also unconsciously) by the organism to tune the system for incoming information (Perl et al., 2019). That is why we think that interoceptive predictive coding models which mirror our internal states (e.g., heartbeats or respiration phase) are used to form different predictions that (a) attenuate tactile detection during systole (highest uncertainty about internal or external origin of perceived pulse) and that (b) allow to plan behavior which optimizes perceptual sampling during windows of heightened neural excitability (e.g., lower pre-stimulus alpha for conscious tactile perception).

## 5.3 Do brain network topologies in terms of graph metrics change with conscious tactile perception?

With fMRI we investigated the neural consequences of conscious tactile perception in *Study 3* and modelled brain activity in two ways: (i) stimulus-evoked BOLD response and (ii) functional connectivity in terms of graph metrics. This showed an increased brain activity in domain-general brain

## General Discussion

areas (precuneus, insula, and inferior frontal gyrus) in addition to somatosensory regions, but no network topology differences in graph metrics (modularity, clustering, path length, and participation) between detected and undetected tactile stimuli. This null effect was supported by Bayes factor statistics and hence there was no evidence for the *Hypothesis 3 "Conscious tactile perception does change the whole-brain functional network configuration in terms of graph metrics (increased global integration)".* This was contrary to a previous report of decreased modularity and increased participation with visual conscious perception (Godwin et al., 2015). However, this observation was possibly due to missing physical similarity between detected and undetected trials (different masking conditions). An explanation for the brain-wide activity differences with conscious tactile perception is that sensory information can be broadcasted without changes of the whole-brain functional network configuration.

### **5.4 Interaction of bodily signals with conscious tactile perception and its neural correlates**

Conscious tactile perception did not only correlate with brain activity in the somatosensory cortex and domain-general brain areas (*Study 3*), but it also showed a complex interaction with cardiac and respiratory activity (*Study 1 and 2*). While cardiac phase determined the likelihood of detecting somatosensory near-threshold stimuli, cardiac cycle durations showed an attenuated post-stimulus deceleration for detected compared to undetected stimuli. This effect by detection was reduced when we accounted for confidence, namely deceleration was greater for unconfident decisions. The heart slowing, a parasympathetic correlate of the orienting response to a change in the environment, was also observed for trials without stimulation and might primarily reflect uncertainty about the perceptual decision which is in line with previous reports on violation of performance-based expectations (Bury et al., 2019; Crone et al., 2003; Łukowska et al., 2018).

Furthermore, heart acceleration with confidence (attenuating the orienting response in a visual discrimination task) has been reported to be reversed by negative emotional cues, which was interpreted as confidence being a correlate of internal and external signal integration (Allen et al., 2016, 2019). The very same mechanism could underly our observation, namely that changes in the heart rate are integrated as prediction errors in the metacognitive decision process. The unexpected strength of post-stimulus heart deceleration (increased prediction errors) would hence be inversely incorporated in the decision confidence (lower confidence).

While the timing of our heartbeats cannot be controlled easily, the respiration rhythm was adapted to expected stimulus onsets to occur more likely during late inspiration / early expiration (*Study 2*). The respiration phase determined the detection probability (more likely during early expiration), and inter-individually, a more pronounced respiratory phase-locking was associated with a higher detection rate. That is why we think that the organism is indeed using the modulation of the respiration rhythm to tune the sensory system for incoming information (Perl et al., 2019). Future research is necessary to show how this timing of respiration relates to known beneficial neural oscillatory patterns for conscious tactile perception as decreased pre-stimulus alpha activity (Craddock et al., 2017; Forschack et al., 2020; Nierhaus et al., 2015; Schubert et al., 2009; Stephani et al., 2021), and whether respiration is a tool at hand to modulate these neural oscillatory patterns (Kluger et al., 2021; Kluger & Gross, 2020).

*Study 3* showed for undetected near-threshold stimuli compared to correctly rejected trials without stimulation greater brain activity in the primary and secondary somatosensory cortices (S1, S2), as well as in the insula. This was a new observation compared to previously reported deactivation in S1 and S2 for imperceptible sub-threshold somatosensory stimulation (Blankenburg et al., 2003; Taskin et al., 2008). Probably there are multiple neural stages towards conscious tactile perception, which then

## General Discussion

also involves domain-general brain areas: precuneus, insula, and inferior frontal gyrus (Grund et al., 2021). One possible interpretation together with the results of *Study 1* and *2*: This indicates the integration of internal and external signals to a unified percept of the world (including the state of the organism). On the perceptual level, it is a demanding negotiation for the organism and thus requires the involvement of multiple brain areas to decide whether a very weak pulse was (a) an *external* electrical stimulus or (b) an *internal* heartbeat-related sensation. It has been argued that uncertainty due to cardiac-related inferences is not uniformly distributed across the cardiac cycle but peaks during systole around the heartbeat sensation (Allen et al., 2019). In *Study 2*, we did not observe a cardiac cycle effect on confidence or metacognition, but the increase of hits in the end of the cardiac cycle was solely based on confident hits. Uncertainty in a tactile detection task has been shown to be correlated with activity in the insula and the anterior cingulate cortex (Schröder et al., 2019), the very same brain areas which were associated (next to amygdala and somatosensory cortex) with the processing of visceral signals (e.g., heartbeat-evoked potentials) and hence discussed as central hub for the integration of interoceptive and exteroceptive signals (Critchley et al., 2003; Park & Blanke, 2019a; Park & Tallon-Baudry, 2014; Ronchi et al., 2015; Seth et al., 2011). Recently, it has been shown that the anterior insula codes respiratory predictions and prediction errors (Harrison et al., 2021).

What did we learn about consciousness? Bodily signals are represented in the brain and form together an interoceptive model of the body state which influences cognition and behavior (Azzalini et al., 2019; Critchley & Harrison, 2013; Seth & Friston, 2016). Some even argue these bodily signals are a neural reference frame for subjective experiences as self-consciousness (Babo-Rebelo et al., 2016; Park & Tallon-Baudry, 2014). This notion is in so far of high interest because in psychology the theory develop-



ment of consciousness favors a "self" as a necessary component for consciousness (Damasio, 2010; Graziano et al., 2019; Graziano & Kastner, 2011; Prinz, 2017, 2020). For instance, Damasio (2010) argued that it needs a "protoself" which unconsciously monitors changes in body states and can detect changes that are caused by external signals. The reflection about these changes then creates a "core consciousness", i.e., the subjective sensory experience (Damasio, 2010). Following this line of thinking, being conscious of an external somatosensory stimulus is not possible without integrating the body state. Furthermore, interoceptive predictive coding models which represent the uncertainty about heartbeat-related sensations might be also the ones that initiate perceptual sampling (Galvez-Pol et al., 2020; Kundendorf et al., 2019; Ohl et al., 2016) and tune respiration (Grund et al., 2022) to serve the task by reducing prediction errors about internal states and thus also improve external signal precision (Allen et al., 2019; Seth, 2013). Studying the mechanisms which integrate internal and external signals, particularly in an active interoceptive inference approach (Allen et al., 2019; Corcoran et al., 2018; Seth & Friston, 2016), will bring us closer to the underpinnings of consciousness which have been dominated too long by a brain-centric perspective.

## **5.5 Outlook and future research**

For future research, it would be of high interest to investigate the neural correlates of the tuned respiration for tactile detection. It is known that respiration has a strong effect on the BOLD signal in fMRI (Birn et al., 2009; Tort et al., 2018). For instance, the negative BOLD contrast in the posterior midline region (including precuneus and posterior cingulate cortex) between remembered and forgotten items in a memory task was decreased when participants were instructed to hold their breath and correlated with the respiratory amplitude difference between remembered and forgotten

## General Discussion

items (Huijbers et al., 2014). While *Study 2* shows that respiration and conscious tactile perception are correlated, it is very likely that *Study 3* entailed respiration-related effects in the BOLD contrast for conscious tactile perception. For instance, the positive cluster in the precuneus for detected compared to undetected near-threshold trials might be partially explained by respiration-related changes in the BOLD signal. Very recent research with EEG has shown that the respiratory cycle modulates alpha power and facilitates visual discrimination sensitivity during late inspiration (Kluger et al., 2021). Alpha power is known to be inversely related with the BOLD signal (Becker et al., 2011) and was shown to be decreased pre-stimulus for tactile detection (Craddock et al., 2017; Forschack et al., 2020; Nierhaus et al., 2015; Schubert et al., 2009; Stephani et al., 2021). This means respiration affects neuroimaging in at least two ways. One effect serves the task, because respiration can tune neural excitability (alpha power) which leads to increased evoked responses in fMRI and EEG (Becker et al., 2011; Kluger et al., 2021). The second effect causes artifacts in fMRI, because magnetic properties close to brain tissue change over the course of respiration, e.g., due to chest movement or cerebral blood flow / oxygenation changes in large blood vessels (Birn et al., 2008).

The very same applies for the cardiac-related BOLD signal changes, when conscious tactile perception is correlated with cardiac activity, as shown in *Study 1* and *2*. For instance, the heart-evoked potential was reported to rely on neural structures as the insula, the anterior cingulate cortex, the amygdala, and the somatosensory cortex (Park & Blanke, 2019a), which partially overlap with the brain areas reported for conscious tactile perception in *Study 3* (somatosensory cortex, insula, precuneus, and inferior frontal gyrus). Recent work in our group has shown that late somatosensory evoked potentials were attenuated for near-threshold stimuli applied in systole compared to diastole (Al et al., 2020). That is why it is im-

portant to control for cardiac activity when imaging neural activity of conscious tactile perception. This will also help to better understand the role of the insula for perceptual consciousness.

Generally, we have very limited knowledge about the mechanisms underlying the integration of external and internal signals, and how internal signals motivate perceptual sampling and actions. The somatosensory cortex plays a central role for the processing of visceral signals, as intracranial EEG has shown for the heart-evoked potential (Kern et al., 2013), which makes it even more important to consider interoceptive processes for the study of exteroceptive somatosensory perception.

## Curriculum Vitae

# Curriculum Vitae

## **Martin Grund**

[www.linktr.ee/MartinGrund](http://www.linktr.ee/MartinGrund)

### **Education**

since 2014     **Doctoral Candidate in Psychology (Dr. rer. nat.)**

Universität Leipzig

2012            **Exchange Program**

New York University, USA

2008 - 2014   **Diploma in Psychology (Dipl.-Psych.)**

Humboldt-Universität zu Berlin

### **Experience**

since 2014     **Doctoral Researcher**

Max Planck Institute for Human Cognitive and Brain  
Sciences

2013 - 2014   **User Experience Design Consultant**

akquinet tech@spree GmbH

2012 - 2013   **Student Research Assistant**

Technische Universität Berlin,  
Center of Human-Machine Systems

2009 - 2012   **Student Research Assistant**

Humboldt-Universität zu Berlin, Experimental Psychology

### **Science Policy**

since 2020     **Working Group Member**

#FactoryWisskomm - Think tank by Federal Ministry for  
Education and Research

## Curriculum Vitae

- since 2020      **Management Committee Member**  
European COST Action "Researcher Mental Health"
- since 2019      **Advisory Board Member**  
wissenschaftskommunikation.de
- 2017 - 2021    **Co-Founder, Advisory Board Member**  
N<sup>2</sup> - Network of Networks
- 2016            **President/Spokesperson**  
Max Planck PhDnet
- 2015            **Deputy Spokesperson & Section Representative**  
**Humanities**  
Max Planck PhDnet

### **Grants**

- 2019            Travel grant "Revisiting Doctoral Education"  
by VolkswagenStiftung
- 2016            Funding for "Science & Society Session 2017"  
by Schering Foundation
- 2012            Exchange grant "PROMOS"  
by German Academic Exchange Service (DAAD)
- 2011 - 2013    Scholarship "Deutschlandstipendium"

### **Reviewer for International Journals and Conferences**

Biological Psychology, Cognitive Neuroscience, Cortex, NeuroImage, Neuro-  
psychologia

MindBrainBody Symposium 2017-2022

## Research Publications

### Peer-reviewed Journal Articles

Grund, M., Al, E., Pabst, M., Dabbagh, A., Stephani, T., Nierhaus, T., Gaebler, M., & Villringer, A. (2022). Respiration, Heartbeat, and Conscious Tactile Perception. *The Journal of Neuroscience*, 42(4), 643–656. <https://doi.org/10.1523/jneurosci.0592-21.2021>

Grund, M., Forschack, N., Nierhaus, T., & Villringer, A. (2021). Neural correlates of conscious tactile perception: An analysis of BOLD activation patterns and graph metrics. *NeuroImage*, 224, 117384. <http://doi.org/10.1016/j.neuroimage.2020.117384>

Al, E., Iliopoulos, F., Forschack, N., Nierhaus, T., Grund, M., Motyka, P., Gaebler, M., Vikulin, V. V., Villringer, A. (2020). Heart-Brain Interactions Shape Somatosensory Perception and Evoked Potentials. *Proceedings of the National Academy of Sciences of the United States of America*, 117(19), 10575-10584. <https://doi.org/10.1073/pnas.1915629117>

Motyka, P., Grund, M., Forschack, N., Al, E., Villringer, A., & Gaebler, M. (2019). Interactions between cardiac activity and conscious somatosensory perception. *Psychophysiology*, 56(10), 469-13. <https://doi.org/10.1111/psyp.13424>

### Invited Research and Conference Talks

Grund, M., Nierhaus, T., Forschack, N., Breuer, E., Ott, D., Holtkamp, M., Villringer, A. (2019). Intracranial recordings of unconscious somatosensory processing. *7th MindBrainBody Symposium, Berlin, Germany*

Grund, M. (2018). Conscious tactile perception - brain networks, cardiac interactions, and intracranial recordings. *Curtis Lab Meeting, New York University, New York, USA*

## Research Publications

- Al, E., Iliopoulos, F., Forschack, N., Nierhaus, T., Grund, M., Gaebler, M., Motyka, P., Nikulin, V. V., & Villringer, A. (2018). Somatosensory Perception Varies across the Cardiac Cycle. *21st Annual Meeting of the Association for Scientific Study of Consciousness (ASSC 22), Krakow, Poland*
- Grund, M., Forschack, N., Nierhaus, T., & Villringer, A. (2017). Brain's functional network correlates of conscious somatosensory perception. *21st Annual Meeting of the Association for Scientific Study of Consciousness (ASSC 21), Beijing, China*
- Grund, M. (2017). Conscious somatosensory perception and its neural network correlates. *Center for Cognitive Neuroscience Berlin Seminar Series, Freie Universität Berlin, Berlin, Germany*



## Selbstständigkeitserklärung

Hiermit versichere ich, Martin Grund, geboren am 25.09.1989 in Hoyerswerda,

1. dass die vorliegende Arbeit ohne unzulässige Hilfe und ohne Benutzung anderer als der angegebenen Hilfsmittel angefertigt wurde und dass die aus fremden Quellen direkt oder indirekt übernommenen Gedanken in der Arbeit als solche kenntlich gemacht worden sind;
2. die Personen genannt zu haben, von denen ich bei der Auswahl und Auswertung des Materials sowie bei der Herstellung des Manuskripts Unterstützungsleistungen erhalten habe;
3. Nachweise beigefügt zu haben, die Art und Umfang des Anteils von Co-Autor\*innen an der wissenschaftlichen Leistung der vorgelegten Publikationen darlegen;
4. dass außer den in 2. Genannten weitere Personen bei der geistigen Herstellung der vorliegenden Arbeit nicht beteiligt waren, insbesondere auch nicht die Hilfe eines Promotionsberaters in Anspruch genommen wurde und dass Dritte von dem Antragsteller weder unmittelbar noch mittelbar geldwerte Leistungen für Arbeiten erhalten haben, die im Zusammenhang mit dem Inhalt der vorgelegten Dissertation stehen;
5. dass die vorgelegte Arbeit in gleicher oder in ähnlicher Form keiner anderen wissenschaftlichen Einrichtung zum Zwecke einer Promotion oder eines anderen Prüfungsverfahrens vorgelegt und auch veröffentlicht wurde;
6. dass keine früheren, erfolglosen Promotionsversuche stattgefunden haben;
7. dass mir die Promotionsordnung der Fakultät für Lebenswissenschaft der Universität Leipzig vom 30. September 2019 bekannt ist und ich diese anerkenne.

## Selbstständigkeitserklärung

Leipzig, den 19.02.2022

Martin Grund

# Nachweise über Anteile der Co-Autor\*innen

## Nachweis über Anteile der Co-Autor\*innen

**Nachweis über Anteile der Co-Autor:innen, Martin Grund**  
**Neural correlates of conscious and unconscious somatosensory processing**

---

**NACHWEIS ÜBER ANTEILE DER CO-AUTOR:INNEN:**

**Titel:** Interactions between cardiac activity and conscious somatosensory perception  
**Journal:** Psychophysiology  
**Autor:innen:** Pawel Motyka, Martin Grund, Norman Forschack, Esra Al, Arno Villringer, Michael Gaebler

---

**Pawel Motyka (Erstautor):**

- Projektidee
- **Konzeption der Studie und Experimentaldesign**
- Durchführung und Datenerhebung der Studie
- Analyse und Verarbeitung der Daten
- Visualisierung der Daten
- Schreiben des ersten Manuskripts für die Publikation
- Finalisieren der Publikation

**Martin Grund (Autor 2):**

- Projektidee
- **Konzeption der Studie und Experimentaldesign**
- Versuchsprogrammierung
- Durchführung und Datenerhebung der Studie
- Analyse und Verarbeitung der Daten
- Schreiben und Editieren des Manuskripts
- Finalisieren der Publikation

**Norman Forschack (Autor 3):**

- **Projektidee**
- **Konzeption der Studie und Experimentaldesign**
- Finalisieren der Publikation

**Esra Al (Autor 4):**

- Analyse und Verarbeitung der Daten
- Schreiben und Editieren des Manuskripts
- Finalisieren der Publikation

**Arno Villringer (Autor 5):**

- **Konzeption der Studie und Experimentaldesign**
- Finalisieren der Publikation

**Michael Gaebler (Senior-Autor):**

- Projektidee
- Konzeption der Studie und Experimentaldesign
- Analyse und Verarbeitung der Daten
- Schreiben und Editieren des Manuskripts
- Finalisieren der Publikation



Martin Grund



Dr. Michael Gaebler

**Nachweis über Anteile der Co-Autor:innen, Martin Grund**  
**Neural Correlates of conscious and unconscious somatosensory processing**

---

**NACHWEIS ÜBER ANTEILE DER CO-AUTOR:INNEN:**

**Titel:** Respiration, heartbeat, and conscious tactile perception  
**Journal:** Journal of Neuroscience  
**Autor:innen:** Martin Grund, Esra Al, Marc Pabst, Alice Dabbagh, Tilman Stephani, Till Nierhaus, Michael Gaebler, Arno Villringer

---

**Martin Grund (Erstautor):**

- Projektidee
- Konzeption der Studie und Experimentaldesign
- Versuchsprogrammierung
- Durchführung und Datenerhebung der Studie
- Analyse und Verarbeitung der Daten
- Visualisierung der Daten
- Schreiben des ersten Manuskripts für die Publikation
- Finalisieren der Publikation

**Esra Al (Autor 2):**

- Projektidee
- Konzeption der Studie und Experimentaldesign
- Analyse und Verarbeitung der Daten
- Finalisieren der Publikation

**Marc Pabst (Autor 3):**

- Analyse und Verarbeitung der Daten
- Schreiben des ersten Manuskripts für die Publikation
- Finalisieren der Publikation

**Alice Dabbagh (Autor 4):**

- Durchführung und Datenerhebung der Studie
- Analyse und Verarbeitung der Daten
- Finalisieren der Publikation

**Tilman Stephani (Autor 5):**

- Durchführung und Datenerhebung der Studie
- Analyse und Verarbeitung der Daten
- Finalisieren der Publikation

Till Nierhaus (Autor 6):

- Konzeption der Studie und Experimentaldesign
- Finalisieren der Publikation

Michael Gaebler (Autor 7):

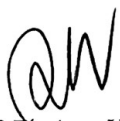
- Analyse und Verarbeitung der Daten
- Schreiben und Editieren des Manuskripts
- Finalisieren der Publikation

Arno Villringer (Senior-Autor):

- Projektidee
- Konzeption der Studie und Experimentaldesign
- Schreiben und Editieren des Manuskripts
- Finalisieren der Publikation



Martin Grund



Prof. Dr. Arno Villringer



**Nachweis über Anteile der Co-Autor:innen, Martin Grund**  
**Neural correlates of conscious and unconscious somatosensory processing**

---

**NACHWEIS ÜBER ANTEILE DER CO-AUTOR:INNEN:**

Titel: Neural correlates of conscious tactile perception: An analysis of BOLD activation patterns and graph metrics  
Journal: NeuroImage  
Autoren: Martin Grund, Norman Forschack, Till Nierhaus, Arno Villringer

---

Martin Grund (Erstautor):

- Projektidee
- Konzeption der Studie und Experimentaldesign
- Versuchsprogrammierung
- Durchführung und Datenerhebung der Studie
- Analyse und Verarbeitung der Daten
- Visualisierung der Daten
- Schreiben des ersten Manuskripts für die Publikation
- Finalisieren der Publikation

Norman Forschack (Autor 2):

- Konzeption der Studie und Experimentaldesign
- Schreiben und Editieren des Manuskripts
- Finalisieren der Publikation

Till Nierhaus (Autor 3):

- Konzeption der Studie und Experimentaldesign
- Schreiben und Editieren des Manuskripts
- Finalisieren der Publikation

Arno Villringer (Senior-Autor):

- Konzeption der Studie und Experimentaldesign
- Schreiben und Editieren des Manuskripts
- Finalisieren der Publikation
- Supervision

  
Martin Grund

  
Prof. Dr. Arno Villringer

## References

## References

- Al, E., Iliopoulos, F., Forschack, N., Nierhaus, T., Grund, M., Motyka, P., Gaebler, M., Nikulin, V. V., & Villringer, A. (2020). Heart–brain interactions shape somatosensory perception and evoked potentials. *Proceedings of the National Academy of Sciences of the United States of America*, *117*(19), 10575–10584. <https://doi.org/10.1073/pnas.1915629117>
- Al, E., Iliopoulos, F., Nikulin, V. V., & Villringer, A. (2021). Heartbeat and somatosensory perception. *NeuroImage*, *238*, 118247. <https://doi.org/10.1016/j.neuroimage.2021.118247>
- Allen, M., Frank, D., Schwarzkopf, D. S., Fardo, F., Winston, J. S., Hauser, T. U., Rees, G., & Shan, H. (2016). Unexpected arousal modulates the influence of sensory noise on confidence. *ELife*, *5*, e18103. <https://doi.org/10.7554/elife.18103>
- Allen, M., Levy, A., Parr, T., & Friston, K. J. (2019). In the body’s eye: the computational anatomy of interoceptive inference. *BioRxiv*, 603928. <https://doi.org/10.1101/603928>
- Aru, J., Bachmann, T., Singer, W., & Melloni, L. (2012). Distilling the neural correlates of consciousness. *Neuroscience and Biobehavioral Reviews*, *36*(2), 737–746. <https://doi.org/10.1016/j.neubiorev.2011.12.003>
- Arzi, A., Rozenkrantz, L., Gorodisky, L., Rozenkrantz, D., Holtzman, Y., Ravia, A., Bekinshtein, T. A., Galperin, T., Krimchansky, B.-Z., Cohen, G., Oksamitni, A., Aidinoff, E., Sacher, Y., & Sobel, N. (2020). Olfactory sniffing signals consciousness in unresponsive patients with brain injuries. *Nature*, *581*(7809), 428–433. <https://doi.org/10.1038/s41586-020-2245-5>
- Auksztulewicz, R., Spitzer, B., & Blankenburg, F. (2012). Recurrent neural processing and somatosensory awareness. *Journal of Neuroscience*, *32*(3), 799–805. <https://doi.org/10.1523/jneurosci.3974-11.2012>

## References

- Azzalini, D., Rebollo, I., & Tallon-Baudry, C. (2019). Visceral Signals Shape Brain Dynamics and Cognition. *Trends in Cognitive Sciences*, 23(6), 488–509. <https://doi.org/10.1016/j.tics.2019.03.007>
- Baars, B. J. (1988). *A cognitive theory of consciousness*. Cambridge [England] ; New York : Cambridge University Press.
- Babo-Rebelo, M., Buot, A., & Tallon-Baudry, C. (2019). Neural responses to heartbeats distinguish self from other during imagination. *NeuroImage*, 191, 10–20. <https://doi.org/10.1016/j.neuroimage.2019.02.012>
- Babo-Rebelo, M., Richter, C. G., & Tallon-Baudry, C. (2016). Neural Responses to Heartbeats in the Default Network Encode the Self in Spontaneous Thoughts. *Journal of Neuroscience*, 36(30), 7829–7840. <https://doi.org/10.1523/jneurosci.0262-16.2016>
- Baumgarten, T. J., Schnitzler, A., & Lange, J. (2016). Prestimulus Alpha Power Influences Tactile Temporal Perceptual Discrimination and Confidence in Decisions. *Cerebral Cortex*, 26(3), 891–903. <https://doi.org/10.1093/cercor/bhu247>
- Becker, R., Reinacher, M., Freyer, F., Villringer, A., & Ritter, P. (2011). How ongoing neuronal oscillations account for evoked fMRI variability. *Journal of Neuroscience*, 31(30), 11016–11027. <https://doi.org/10.1523/jneurosci.0210-11.2011>
- Birn, R. M., Murphy, K., Handwerker, D. A., & Bandettini, P. A. (2009). fMRI in the presence of task-correlated breathing variations. *NeuroImage*, 47(3), 1092–1104. <https://doi.org/10.1016/j.neuroimage.2009.05.030>
- Birn, R. M., Smith, M. A., Jones, T. B., & Bandettini, P. A. (2008). The respiration response function: the temporal dynamics of fMRI signal fluctuations related to changes in respiration. *NeuroImage*, 40(2), 644–654. <https://doi.org/10.1016/j.neuroimage.2007.11.059>

- Blankenburg, F., Taskin, B., Ruben, J., Moosmann, M., Ritter, P., Curio, G., & Villringer, A. (2003). Imperceptible stimuli and sensory processing impediment. *Science*, *299*(5614), 1864–1864. <https://doi.org/10.1126/science.1080806>
- Boly, M., Massimini, M., Tsuchiya, N., Postle, B. R., Koch, C., & Tononi, G. (2017). Are the Neural Correlates of Consciousness in the Front or in the Back of the Cerebral Cortex? Clinical and Neuroimaging Evidence. *Journal of Neuroscience*, *37*(40), 9603–9613. <https://doi.org/10.1523/jneurosci.3218-16.2017>
- Brener, J., & Kluitse, C. (1988). Heartbeat detection: judgments of the simultaneity of external stimuli and heartbeats. *Psychophysiology*, *25*(5), 554–561. <https://doi.org/https://doi.org/10.1111/j.1469-8986.1988.tb01891.x>
- Bury, G., García-Huésca, M., Bhattacharya, J., & Ruiz, M. H. (2019). Cardiac afferent activity modulates early neural signature of error detection during skilled performance. *NeuroImage*, *199*, 704–717. <https://doi.org/10.1016/j.neuroimage.2019.04.043>
- Corcoran, A. W., Pezzulo, G., & Hohwy, J. (2018). Commentary: Respiration-Entrained Brain Rhythms Are Global but Often Overlooked. *Frontiers in Systems Neuroscience*, *12*, 25. <https://doi.org/10.3389/fnsys.2018.00025>
- Craddock, M., Poliakoff, E., El-dereby, W., Klepousniotou, E., & Lloyd, D. M. (2017). Pre-stimulus alpha oscillations over somatosensory cortex predict tactile misperceptions. *Neuropsychologia*, *96*, 9–18. <https://doi.org/10.1016/j.neuropsychologia.2016.12.030>
- Crick, F., & Koch, C. (1990). Towards a neurobiological theory of consciousness. *Seminars in the Neurosciences*, *2*, 263–275. <https://authors.library.caltech.edu/40352/1/148.pdf>

## References

- Critchley, H. D., & Harrison, N. A. (2013). Visceral influences on brain and behavior. *Neuron*, 77(4), 624–638. <https://doi.org/10.1016/j.neuron.2013.02.008>
- Critchley, H. D., Mathias, C. J., Josephs, O., O’Doherty, J., Zanini, S., Dewar, B., Cipolotti, L., Shallice, T., & Dolan, R. J. (2003). Human cingulate cortex and autonomic control: converging neuroimaging and clinical evidence. *Brain*, 126(10), 2139–2152. <https://doi.org/10.1093/brain/awg216>
- Crone, E. A., Veen, F. M. van der, Molen, M. W. van der, Somsen, R. J. M., Beek, B. van, & Jennings, J. R. (2003). Cardiac concomitants of feedback processing. *Biological Psychology*, 64(1–2), 143–156. [https://doi.org/10.1016/s0301-0511\(03\)00106-6](https://doi.org/10.1016/s0301-0511(03)00106-6)
- Damasio, A. (2010). *Self Comes to Mind. Constructing the Conscious Brain*. Pantheon Books.
- Dehaene, S., Changeux, J.-P., Naccache, L., Sackur, J., & Sergent, C. (2006). Conscious, preconscious, and subliminal processing: a testable taxonomy. *Trends in Cognitive Sciences*, 10(5), 204–211. <https://doi.org/10.1016/j.tics.2006.03.007>
- Dehaene, S., Sergent, C., & Changeux, J.-P. (2003). A neuronal network model linking subjective reports and objective physiological data during conscious perception. *Proceedings of the National Academy of Sciences*, 100(14), 8520–8525. <https://doi.org/10.1073/pnas.1332574100>
- Edwards, L., Ring, C., McIntyre, D., Winer, J. B., & Martin, U. (2009). Sensory detection thresholds are modulated across the cardiac cycle: evidence that cutaneous sensibility is greatest for systolic stimulation. *Psychophysiology*, 46(2), 252–256. <https://doi.org/10.1111/j.1469-8986.2008.00769.x>
- Faugeras, F., Rohaut, B., Weiss, N., Bekinschtein, T. A., Galanaud, D., Puybasset, L., Bolgert, F., Sergent, C., Cohen, L., Dehaene, S., & Naccache, L. (2011). Probing consciousness with event-related potentials in the

- vegetative state. *Neurology*, 77(3), 264–268.  
<https://doi.org/10.1212/wnl.0b013e3182217ee8>
- Forschack, N., Nierhaus, T., Müller, M. M., & Villringer, A. (2017). Alpha-Band Brain Oscillations Shape the Processing of Perceptible as well as Imperceptible Somatosensory Stimuli during Selective Attention. *Journal of Neuroscience*, 37(29), 6983–6994. <https://doi.org/10.1523/jneurosci.2582-16.2017>
- Forschack, N., Nierhaus, T., Müller, M. M., & Villringer, A. (2020). Dissociable neural correlates of stimulation intensity and detection in somatosensation. *NeuroImage*, 116908. <https://doi.org/10.1016/j.neuroimage.2020.116908>
- Galvez-Pol, A., McConnell, R., & Kilner, J. M. (2020). Active sampling in visual search is coupled to the cardiac cycle. *Cognition*, 196, 104149. <https://doi.org/10.1016/j.cognition.2019.104149>
- Gardner, E. P., & Johnson, K. O. (2012). *Touch* (E. Kandel, J H Schwartz, T M Jessell, S A Siegelbaum, & A. J. Hudspeth, Eds.; 5th ed., pp. 498–529). McGraw-Hill.
- Gardner, E. P., Johnson, K. O., & Siegelbaum, S. A. (2012). *The Somatosensory System: Receptors and Central Pathways* (E. Kandel, J H Schwartz, T M Jessell, S A Siegelbaum, & A. J. Hudspeth, Eds.; 5th ed., pp. 475–497). McGraw-Hill. <http://www.worldcat.org/title/principles-of-neural-science/oclc/879421693>
- Garfinkel, S. N., & Critchley, H. D. (2016). Threat and the Body: How the Heart Supports Fear Processing. *Trends in Cognitive Sciences*, 20(1), 34–46. <https://doi.org/10.1016/j.tics.2015.10.005>
- Godwin, D., Barry, R. L., & Marois, R. (2015). Breakdown of the brain’s functional network modularity with awareness. *Proceedings of the National Academy of Sciences of the United States of America*, 112(12), 3799–3804. <https://doi.org/10.1073/pnas.1414466112>

## References

- Gray, M. A., Rylander, K., Harrison, N. A., Wallin, B. G., & Critchley, H. D. (2009). Following one's heart: cardiac rhythms gate central initiation of sympathetic reflexes. *Journal of Neuroscience*, *29*(6), 1817–1825. <https://doi.org/10.1523/jneurosci.3363-08.2009>
- Graziano, M. S. A., Guterstam, A., Bio, B. J., & Wilterson, A. I. (2019). Toward a standard model of consciousness: Reconciling the attention schema, global workspace, higher-order thought, and illusionist theories. *Cognitive Neuropsychology*, *37*(3–4), 155–172. <https://doi.org/10.1080/02643294.2019.1670630>
- Graziano, M. S. A., & Kastner, S. (2011). Human consciousness and its relationship to social neuroscience: A novel hypothesis. *Cognitive Neuroscience*, *2*(2), 98–113. <https://doi.org/10.1080/17588928.2011.565121>
- Grund, M., Al, E., Pabst, M., Dabbagh, A., Stephani, T., Nierhaus, T., Gaebler, M., & Villringer, A. (2022). Respiration, Heartbeat, and Conscious Tactile Perception. *The Journal of Neuroscience*, *42*(4), 643–656. <https://doi.org/10.1523/jneurosci.0592-21.2021>
- Grund, M., Förschack, N., Nierhaus, T., & Villringer, A. (2021). Neural correlates of conscious tactile perception: An analysis of BOLD activation patterns and graph metrics. *NeuroImage*, *224*, 117384. <https://doi.org/10.1016/j.neuroimage.2020.117384>
- Harrison, O. K., Köchli, L., Marino, S., Luechinger, R., Hennel, F., Brand, K., Hess, A. J., Frässle, S., Iglesias, S., Vinckier, F., Petzschner, F. H., Harrison, S. J., & Stephan, K. E. (2021). Interoception of breathing and its relationship with anxiety. *Neuron*, *109*(24), 4080–4093.e8. <https://doi.org/10.1016/j.neuron.2021.09.045>
- Hassanpour, M. S., Yan, L., Wang, D. J. J., Lapidus, R. C., Arevian, A. C., Simmons, W. K., Feusner, J. D., & Khalsa, S. S. (2016). How the heart speaks to the brain: neural activity during cardiorespiratory interoceptive stimulation. *Philosophical Transactions of the Royal Society of London. Series*



- B, Biological Sciences*, 371(1708).  
<https://doi.org/10.1098/rstb.2016.0017>
- Huijbers, W., Pennartz, C. M. A., Beldzik, E., Domagalik, A., Vinck, M., Hofman, W. F., Cabeza, R., & Daselaar, S. M. (2014). Respiration phase-locks to fast stimulus presentations: implications for the interpretation of posterior midline “deactivations”. *Human Brain Mapping*, 35(9), 4932–4943. <https://doi.org/10.1002/hbm.22523>
- Jones, S. R., Kerr, C. E., Wan, Q., Pritchett, D. L., Hamalainen, M., & Moore, C. I. (2010). Cued Spatial Attention Drives Functionally Relevant Modulation of the Mu Rhythm in Primary Somatosensory Cortex. *Journal of Neuroscience*, 30(41), 13760–13765. <https://doi.org/10.1523/jneurosci.2969-10.2010>
- Kern, M., Aertsen, A., Schulze-Bonhage, A., & Ball, T. (2013). Heart cycle-related effects on event-related potentials, spectral power changes, and connectivity patterns in the human ECoG. *NeuroImage*, 81, 178–190. <https://doi.org/10.1016/j.neuroimage.2013.05.042>
- Khalsa, S. S., Rudrauf, D., Feinstein, J. S., & Tranel, D. (2009). The pathways of interoceptive awareness. *Nature Neuroscience*, 12(12), 1494–1496. <https://doi.org/10.1038/nn.2411>
- Kluger, D. S., Balestrieri, E., Busch, N. A., & Gross, J. (2021). Respiration aligns perception with neural excitability. *ELife*, 10. <https://doi.org/10.7554/elife.70907>
- Kluger, D. S., & Gross, J. (2020). Depth and phase of respiration modulate cortico-muscular communication. *NeuroImage*, 222, 117272. <https://doi.org/10.1016/j.neuroimage.2020.117272>
- Koch, C., Massimini, M., Boly, M., & Tononi, G. (2016). Neural correlates of consciousness: progress and problems. *Nature Reviews Neuroscience*, 17(5), 307–321. <https://doi.org/10.1038/nrn.2016.22>
- Kondziella, D., Bender, A., Diserens, K., Erp, W. van, Estraneo, A., Formisano, R., Laureys, S., Naccache, L., Ozturk, S., Rohaut, B., Sitt, J. D., Stender, J.,

## References

- Tiainen, M., Rossetti, A. O., Gosseries, O., Chatelle, C., & Consciousness, the E. P. on C., Disorders of. (2020). European Academy of Neurology guideline on the diagnosis of coma and other disorders of consciousness. *European Journal of Neurology*, 27(5), 741–756. <https://doi.org/10.1111/ene.14151>
- Kunzendorf, S., Klotzsche, F., Akbal, M., Villringer, A., Ohl, S., & Gaebler, M. (2019). Active information sampling varies across the cardiac cycle. *Psychophysiology*, 56(5), e13322. <https://doi.org/10.1111/psyp.13322>
- Lacey, B. C., & Lacey, J. I. (1978). Two-way communication between the heart and the brain: Significance of time within the cardiac cycle. *American Psychologist*, 33(2), 99–113. <https://doi.org/10.1037/0003-066x.33.2.99>
- Lamme, V. A. F. (2006). Towards a true neural stance on consciousness. *Trends in Cognitive Sciences*, 10(11), 494–501. <https://doi.org/10.1016/j.tics.2006.09.001>
- Lau, H., & Rosenthal, D. (2011). Empirical support for higher-order theories of conscious awareness. *Trends in Cognitive Sciences*, 15(8), 365–373. <https://doi.org/10.1016/j.tics.2011.05.009>
- Laureys, S. (2005). The neural correlate of (un)awareness: lessons from the vegetative state. *Trends in Cognitive Sciences*, 9(12), 556–559. <https://doi.org/10.1016/j.tics.2005.10.010>
- Linkenkaer-Hansen, K., Nikulin, V. V., Palva, S., Ilmoniemi, R. J., & Palva, J. M. (2004). Prestimulus Oscillations Enhance Psychophysical Performance in Humans. *Journal of Neuroscience*, 24(45), 10186–10190. <https://doi.org/10.1523/jneurosci.2584-04.2004>
- Lollo, V. D., Clark, C. D., & Hogben, J. H. (1988). Separating visible persistence from retinal afterimages. *Perception & Psychophysics*, 44(4), 363–368. <https://doi.org/10.3758/bf03210418>

- Łukowska, M., Sznajder, M., & Wierzchoń, M. (2018). Error-related cardiac response as information for visibility judgements. *Scientific Reports*, *8*(1), 1131. <https://doi.org/10.1038/s41598-018-19144-0>
- Macefield, V. G. (2003). Cardiovascular and Respiratory Modulation of Tactile Afferents in the Human Finger Pad. *Experimental Physiology*, *88*(5), 617–625. <https://doi.org/10.1113/eph8802548>
- Martuzzi, R., Zwaag, W. van der, Dieguez, S., Serino, A., Gruetter, R., & Blanke, O. (2015). Distinct contributions of Brodmann areas 1 and 2 to body ownership. *Social Cognitive and Affective Neuroscience*, *10*(11), 1449–1459. <https://doi.org/10.1093/scan/nsv031>
- McLaren, D. G., Ries, M. L., Xu, G., & Johnson, S. C. (2012). A generalized form of context-dependent psychophysiological interactions (gPPI): a comparison to standard approaches. *NeuroImage*, *61*(4), 1277–1286. <https://doi.org/10.1016/j.neuroimage.2012.03.068>
- Moore, C. I., Crosier, E., Greve, D. N., Savoy, R., Merzenich, M. M., & Dale, A. M. (2013). Neocortical correlates of vibrotactile detection in humans. *Journal of Cognitive Neuroscience*, *25*(1), 49–61. [https://doi.org/10.1162/jocn\\_a\\_00315](https://doi.org/10.1162/jocn_a_00315)
- Motyka, P., Grund, M., Forschack, N., Al, E., Villringer, A., & Gaebler, M. (2019). Interactions between cardiac activity and conscious somatosensory perception. *Psychophysiology*, *56*(10), 469–13. <https://doi.org/10.1111/psyp.13424>
- Naghavi, H. R., & Nyberg, L. (2005). Common fronto-parietal activity in attention, memory, and consciousness: Shared demands on integration? *Consciousness and Cognition*, *14*(2), 390–425. <https://doi.org/10.1016/j.concog.2004.10.003>
- Nierhaus, T., Forschack, N., Piper, S. K., Holtze, S., Krause, T., Taskin, B., Long, X., Stelzer, J., Margulies, D. S., Steinbrink, J., & Villringer, A. (2015). Imperceptible somatosensory stimulation alters sensorimotor background

## References

- rhythm and connectivity. *Journal of Neuroscience*, 35(15), 5917–5925. <https://doi.org/10.1523/jneurosci.3806-14.2015>
- Odegaard, B., Knight, R. T., & Lau, H. (2017). Should a Few Null Findings Falsify Prefrontal Theories of Conscious Perception? *Journal of Neuroscience*, 37(40), 9593–9602. <https://doi.org/10.1523/jneurosci.3217-16.2017>
- Ohl, S., Wohltat, C., Kliegl, R., Pollatos, O., & Engbert, R. (2016). Microsaccades Are Coupled to Heartbeat. *Journal of Neuroscience*, 36(4), 1237–1241. <https://doi.org/10.1523/jneurosci.2211-15.2016>
- Owen, A. M., Coleman, M. R., Boly, M., Davis, M. H., Laureys, S., & Pickard, J. D. (2006). Detecting awareness in the vegetative state. *Science*, 313(5792), 1402. <https://doi.org/10.1126/science.1130197>
- Palva, S., Linkenkaer-Hansen, K., Näätänen, R., & Palva, J. M. (2005). Early neural correlates of conscious somatosensory perception. *Journal of Neuroscience*, 25(21), 5248–5258. <https://doi.org/10.1523/jneurosci.0141-05.2005>
- Park, H.-D., Bernasconi, F., Salomon, R., Tallon-Baudry, C., Spinelli, L., Seeck, M., Schaller, K., & Blanke, O. (2017). Neural Sources and Underlying Mechanisms of Neural Responses to Heartbeats, and their Role in Bodily Self-consciousness: An Intracranial EEG Study. *Cerebral Cortex*, 1–14. <https://doi.org/10.1093/cercor/bhx136>
- Park, H.-D., & Blanke, O. (2019a). Heartbeat-evoked cortical responses: Underlying mechanisms, functional roles, and methodological considerations. *NeuroImage*, 197, 502–511. <https://doi.org/10.1016/j.neuroimage.2019.04.081>
- Park, H.-D., & Blanke, O. (2019b). Coupling Inner and Outer Body for Self-Consciousness. *Trends in Cognitive Sciences*, 23(5), 377–388. <https://doi.org/10.1016/j.tics.2019.02.002>

- Park, H.-D., Correia, S., Ducorps, A., & Tallon-Baudry, C. (2014). Spontaneous fluctuations in neural responses to heartbeats predict visual detection. *Nature Neuroscience*, *17*(4), 612–618. <https://doi.org/10.1038/nn.3671>
- Park, H.-D., & Tallon-Baudry, C. (2014). The neural subjective frame: from bodily signals to perceptual consciousness. *Philosophical Transactions of the Royal Society of London. Series B, Biological Sciences*, *369*(1641), 20130208. <https://doi.org/10.1098/rstb.2013.0208>
- Perl, O., Ravia, A., Rubinson, M., Eisen, A., Soroka, T., Mor, N., Secundo, L., & Sobel, N. (2019). Human non-olfactory cognition phase-locked with inhalation. *Nature Human Behaviour*, *3*(5), 501–512. <https://doi.org/10.1038/s41562-019-0556-z>
- Petzschner, F. H., Weber, L. A., Wellstein, K. V., Paolini, G., Do, C. T., & Stephan, K. E. (2019). Focus of attention modulates the heartbeat evoked potential. *NeuroImage*, *186*, 595–606. <https://doi.org/10.1016/j.neuroimage.2018.11.037>
- Pollatos, O., Kirsch, W., & Schandry, R. (2005). Brain structures involved in interoceptive awareness and cardioafferent signal processing: A dipole source localization study. *Human Brain Mapping*, *26*(1), 54–64. <https://doi.org/10.1002/hbm.20121>
- Preusser, S., Thiel, S. D., Rook, C., Roggenhofer, E., Kosatschek, A., Draganski, B., Blankenburg, F., Driver, J., Villringer, A., & Pleger, B. (2015). The perception of touch and the ventral somatosensory pathway. *Brain*, *138*(3), 540–548. <https://doi.org/10.1093/brain/awu370>
- Prinz, W. (2017). Modeling self on others: An import theory of subjectivity and selfhood. *Consciousness and Cognition*, *49*, 347–362. <https://doi.org/10.1016/j.concog.2017.01.020>
- Prinz, W. (2020). The social roots of consciousness. *Cognitive Neuropsychology*, *37*(3–4), 1–3. <https://doi.org/10.1080/02643294.2020.1730312>

## References

- Raimondo, F., Rohaut, B., Demertzi, A., Valente, M., Engemann, D. A., Salti, M., Slezak, D. F., Naccache, L., & Sitt, J. D. (2017). Brain-heart interactions reveal consciousness in noncommunicating patients. *Annals of Neurology*, *82*(4), 578–591. <https://doi.org/10.1002/ana.25045>
- Rees, G., Kreiman, G., & Koch, C. (2002). Neural correlates of consciousness in humans. *Nature Reviews Neuroscience*, *3*(4), 261–270. <https://doi.org/10.1038/nrn783>
- Reinacher, M., Becker, R., Villringer, A., & Ritter, P. (2009). Oscillatory brain states interact with late cognitive components of the somatosensory evoked potential. *Journal of Neuroscience Methods*, *183*(1), 49–56. <https://doi.org/10.1016/j.jneumeth.2009.06.036>
- Ring, C., & Brener, J. (1992). The temporal locations of heartbeat sensations. *Psychophysiology*, *29*(5), 535–545. <https://doi.org/10.1111/j.1469-8986.1992.tb02027.x>
- Ronchi, R., Bello-Ruiz, J., Lukowska, M., Herbelin, B., Cabrilo, I., Schaller, K., & Blanke, O. (2015). Right insular damage decreases heartbeat awareness and alters cardio-visual effects on bodily self-consciousness. *Neuropsychologia*, *70*, 11–20. <https://doi.org/10.1016/j.neuropsychologia.2015.02.010>
- Rubinov, M., & Sporns, O. (2010). Complex network measures of brain connectivity: uses and interpretations. *NeuroImage*, *52*(3), 1059–1069. <https://doi.org/10.1016/j.neuroimage.2009.10.003>
- Sadaghiani, S., Poline, J.-B., Kleinschmidt, A., & D'Esposito, M. (2015). Ongoing dynamics in large-scale functional connectivity predict perception. *Proceedings of the National Academy of Sciences of the United States of America*, *112*(27), 8463–8468. <https://doi.org/10.1073/pnas.1420687112>
- Schröder, P., Nierhaus, T., & Blankenburg, F. (2021). Dissociating Perceptual Awareness and Postperceptual Processing: The P300 Is Not a Reliable

- Marker of Somatosensory Target Detection. *The Journal of Neuroscience*, 41(21), 4686–4696. <https://doi.org/10.1523/jneurosci.2950-20.2021>
- Schröder, P., Schmidt, T. T., & Blankenburg, F. (2019). Neural basis of somatosensory target detection independent of uncertainty, relevance, and reports. *ELife*, 8, 34. <https://doi.org/10.7554/elife.43410>
- Schubert, R., Blankenburg, F., Lemm, S., Villringer, A., & Curio, G. (2006). Now you feel it-now you don't: ERP correlates of somatosensory awareness. *Psychophysiology*, 43(1), 31–40. <https://doi.org/10.1111/j.1469-8986.2006.00379.x>
- Schubert, R., Haufe, S., Blankenburg, F., Villringer, A., & Curio, G. (2009). Now you'll feel it, now you won't: EEG rhythms predict the effectiveness of perceptual masking. *Journal of Cognitive Neuroscience*, 21(12), 2407–2419. <https://doi.org/10.1162/jocn.2008.21174>
- Seth, A. K. (2013). Interoceptive inference, emotion, and the embodied self. *Trends in Cognitive Sciences*, 17(11), 565–573. <https://doi.org/10.1016/j.tics.2013.09.007>
- Seth, A. K., & Friston, K. J. (2016). Active interoceptive inference and the emotional brain. *Philosophical Transactions of the Royal Society of London. Series B, Biological Sciences*, 371(1708). <https://doi.org/10.1098/rstb.2016.0007>
- Seth, A. K., Suzuki, K., & Critchley, H. D. (2011). An interoceptive predictive coding model of conscious presence. *Frontiers in Psychology*, 2, 395. <https://doi.org/10.3389/fpsyg.2011.00395>
- Sperdin, H. F., Repnow, M., Herzog, M. H., & Landis, T. (2013). An LCD tachistoscope with submillisecond precision. *Behavior Research Methods*, 45(4), 1347–1357. <https://doi.org/10.3758/s13428-012-0311-0>
- Stephani, T., Hodapp, A., Idaji, M. J., Villringer, A., & Nikulin, V. V. (2021). Neural excitability and sensory input determine intensity perception with opposing directions in initial cortical responses. *ELife*, 10, e67838. <https://doi.org/10.7554/elife.67838>

## References

- Taskin, B., Holtze, S., Krause, T., & Villringer, A. (2008). Inhibitory impact of subliminal electrical finger stimulation on SI representation and perceptual sensitivity of an adjacent finger. *NeuroImage*, *39*(3), 1307–1313. <https://doi.org/10.1016/j.neuroimage.2007.09.039>
- Tort, A. B. L., Brankačk, J., & Draguhn, A. (2018). Respiration-Entrained Brain Rhythms Are Global but Often Overlooked. *Trends in Neurosciences*, *41*(4), 186–197. <https://doi.org/10.1016/j.tins.2018.01.007>
- Weisz, N., Wühle, A., Monittola, G., Demarchi, G., Frey, J., Popov, T., & Braun, C. (2014). Prestimulus oscillatory power and connectivity patterns predispose conscious somatosensory perception. *Proceedings of the National Academy of Sciences of the United States of America*, *111*(4), E417–25. <https://doi.org/10.1073/pnas.1317267111>
- Yates, A. J., Jones, K. E., Marie, G. V., & Hogben, J. H. (1985). Detection of the heartbeat and events in the cardiac cycle. *Psychophysiology*, *22*(5), 561–567. <https://doi.org/10.1111/j.1469-8986.1985.tb01651.x>
- Zelano, C., Jiang, H., Zhou, G., Arora, N., Schuele, S., Rosenow, J., & Gottfried, J. A. (2016). Nasal Respiration Entrained Human Limbic Oscillations and Modulates Cognitive Function. *Journal of Neuroscience*, *36*(49), 12448–12467. <https://doi.org/10.1523/jneurosci.2586-16.2016>